TÉCNICO LISBOA

Cultivation of Mycobacteria in Submerged Fermentation: Towards a Reproducible Method for Vaccine Production

Carolina Viana da Costa Araújo

Thesis to obtain the Master of Science Degree in

Biotechnology

Supervisors: Prof. Dr. Carla da Conceição Caramujo Rocha de Carvalho and Prof. Dr. Pedro Carlos de Barros Fernandes

Examination Committee

Chairperson: Prof. Dr. Ana Cristina Anjinho Madeira Viegas

Supervisor: Prof. Dr. Carla da Conceição Caramujo Rocha de Carvalho

Member of the Committee: Dr. Pedro Nuno Sousa Sampaio

October 2021

Preface

The work presented in this thesis was performed at the iBB – Institute for Bioengineering and Biosciences of Instituto Superior Técnico (Lisbon, Portugal), during the period of March-July 2021, under the supervision of Prof. Dr. Carla da Conceição Caramujo Rocha de Carvalho and Prof. Dr. Pedro Carlos de Barros Fernandes.

Declaration

I declare that this document is an original work of my own authorship and that it fulfils all the requirements of the Code of Conduct and Good Practices of the Universidade de Lisboa.

Acknowledgements

Finda aqui uma das etapas mais desafiantes da minha vida. Este percurso não teria sido possível sem todo o apoio, orientação, ajuda e amizade de todos aqueles que fizeram parte do meu percurso.

Em primeiro lugar, quero expressar o meu grande agradecimento aos meus orientadores, Drª. Carla de Carvalho e Dr. Pedro Fernandes, por toda a ajuda, disponibilidade e simpatia para comigo ao longo deste projeto. Desempenharam um papel importantíssimo no meu desenvolvimento por tudo o que me ensinaram, e por isso, não poderia ter tido melhor orientação. Agradeço também ao iBB (Instituto de Bioengenharia e Biociências) do Instituto Superior Técnico, onde desenvolvi esta tese.

Quero também agradecer aos meus colegas e alunos de doutoramento Carlos e Ricardo, sem vocês nada disto teria sido possível. Obrigada pelos conselhos, pela ajuda, pela paciência, pelas gargalhadas e sobretudo pelo grande companheirismo. Foi um enorme prazer partilhar o laboratório com vocês. Obrigada, Carlos, por teres aquecido tantas vezes o meu almoço quando me encontrava tão focada no trabalho laboratorial.

A todos os meus amigos da FCUL e do IST um grande obrigada por todos os momentos e por terem feito todo este percurso mais especial. Em particular, quero agradecer à Mariana, Catarina, Raquel, Sara e Vítor por terem sido as pessoas que tornaram tudo isto melhor. Pela vossa amizade e por todo o apoio, sobretudo neste último ano. Não tenho palavras para descrever o que significam para mim. Mariana, obrigada por teres estado do meu lado quando precisei e pela tua força.

À Carolina Almeida, a minha grande amiga, o meu enorme agradecimento por aturares os meus devaneios e dúvidas existenciais durante a realização desta tese. Para além disso, obrigada por seres quem és. Sou muito grata por te ter a ti e à tua família na minha vida.

Por fim, e não menos importante, agradeço do fundo do meu coração aos meus pais Fernando e Maria da Conceição por todo o apoio ao longo da minha vida. Foram vocês que me deram a força que precisava para perseverar. Obrigada ao meu irmão Rodrigo por todo o apoio, és o melhor irmão que podia ter. Um agradecimento também à minha avó Aurora por tudo. Meu querido avô Fernando, esta tese é dedicada a ti. Sei o quão orgulhoso estarias por tudo o que conquistei até agora.

Abstract

Tuberculosis (TB) is an infectious disease caused by *Mycobacterium tuberculosis* that to this day continues to affect millions of people. The only vaccine available to prevent the development of the disease is the Bacille Calmette-Guérin (BCG) vaccine, which is made from a live attenuated *M. bovis*, the causing agent of bovine TB. However, BCG has ranging efficacies, with one of the reasons being the cell aggregates formed, resulting in a defective quantification and quality control of the vaccine. In this study, the aggregative phenotype was studied to find conditions allowing smaller cell clusters and to obtain cells in planktonic state, using *M. smegmatis* as model organism. To this end, the effect of culture media composition and growth temperature were evaluated. Cells exposed to either 0.25% (v/v) ethanol, methanol, or DMSO presented a decrease in aggregation velocity, meaning that the cell aggregates formed were smaller. Cell aggregation also decreased after seven 15-min temperature shocks without agitation were executed. Moreover, carbon starvation led to a decrease in the size of the cell aggregates. The effect of nitrogen supplementation of the culture medium via ammonium-containing compounds in cell aggregation was studied, with cells in planktonic state being obtained during supplementation with 50 mM ammonium acetate, 50 mM ammonium chloride, or 100 mM ammonium sulphate. The fatty acid composition of the phospholipids of the membrane was assessed for every experiment, with mycobacteria responding accordingly, either by increasing or decreasing the fluidity of the membrane. Surprisingly, increased fluidity was obtained through the introduction of polyunsaturated fatty acids in the cellular membrane.

Keywords: Tuberculosis; BCG vaccine; cell aggregation; *Mycobacterium smegmatis*; culture media composition

Resumo

A tuberculose (TB) é uma doença infeciosa causada por *Mycobacterium tuberculosis* e que atualmente continua a afetar milhões de pessoas. A única vacina disponível para a prevenção de desenvolvimento da doença é a vacina Bacille Calmette-Guérin (BCG), que é feita através de uma versão viva, mas atenuada de *M. bovis*, que por sua vez é o agente causador da TB bovina. Contudo, a eficácia da BCG é variável, sendo que uma das razões para tal é a formação de agregados celulares, o que leva a uma defeituosa quantificação e controlo de qualidade da vacina. Neste estudo, o fenótipo agregativo foi estudado de modo a encontrar condições que permitissem agregados celulares menores e para obter células planctónicas, através do uso de *M. smegmatis* como organismo-modelo. Para tal, o efeito da composição do meio de cultura e temperatura de crescimento foram avaliados. Células expostas a 0.25% (v/v) etanol, metanol ou DMSO apresentaram um decréscimo na velocidade de agregação, o que por sua vez significa que os agregados celulares formados eram menores. A agregação celular também foi diminuída após a execução de sete choques térmicos sem agitação de 15 min. Adicionalmente, privação de fonte de carbono levou a um decréscimo no tamanho dos agregados celulares. O efeito da suplementação de nitrogénio através de compostos com amónio na agregação celular foi estudado, e células planctónicas foram obtidas aquando da suplementação com 50 mM acetato de amónio, 50 mM cloreto de amónio, ou 100 mM sulfato de amónio. A composição em ácidos gordos dos fosfolípidos da membrana foi avaliada em cada experiência, sendo que a mycobactéria respondeu conformemente, aumentando ou diminuindo a fluidez da membrana. Surpreendentemente, o aumento da fluidez foi obtido através da introdução de ácidos gordos polinsaturados na membrana celular.

Palavras-chave: Tuberculose; vacina BCG; agregação celular; *Mycobacterium smegmatis*; composição do meio de cultura

Table of Contents

List of Figures

List of Tables

List of Abbreviations

10Me-BFAs – 10-Methyl Branched Fatty Acids

ADC – Albumin, dextrose, and catalase

BCG – Bacille Calmette-Guérin

DMF – Dimethylformamide

DMSO – Dimethyl sulfoxide

FAMEs – Fatty Acid Methyl Esters

GlcNac – N-acetylglucosamine

Hly – Listeriolysin

LAM – Lipoarabinomannan

LM – Lipomannan

MDR-TB – Multidrug-resistant tuberculosis

MM – Mineral Medium

MTBC – *Mycobacterium tuberculosis* complex

MUFAs – Monounsaturated Fatty Acids

MurNac – N-acetylmuramic acid

MurNGlyc – N-glycolylmuramic acid

NTM – Non-tuberculous mycobacteria

OADC – Oleic acid, albumin, dextrose, and catalase

OD – Optical Density

PAA – Polyacrylic acid

PDIM - Phthiocerol dimycocerosates

PIMs – Phosphatidyl-*myo*-inositol mannosides

PUFAs – Polyunsaturated Fatty Acids

SMBFAs – Saturated Mono-Branched Fatty Acids

SSFAs – Saturated Straight Fatty Acids

TB – Tuberculosis

TCA – Tricarboxylic acid

TDM – Trehalose dimycolate

TSA – Tryptic Soy Agar

TSB – Tryptic Soy Broth

WHO – World Health Organization

XDR-TB – Extensively drug-resistant tuberculosis

1. Introduction

1.1. Tuberculosis

Tuberculosis (TB) is a disease caused by the infectious agent *Mycobacterium tuberculosis* and is currently the leading cause of death from a single infectious agent, according to the World Health Organization (WHO). In 2019, it was estimated that 10 million people contracted the disease, with 1.4 million deaths registered [1].

Being a communicable disease, TB is transmitted through the inhalation of droplet nuclei containing infectious bacilli that an infected patient exhales when coughing. Upon infection of the lung, the tissue suffers remodelling induced by bacterial and host factors, forming a granuloma [2, 3]. These inflammatory lesions are composed of aggregates containing a core of infected macrophages, which in turn are surrounded by foamy and epithelioid macrophages, monocytes, and multinucleated giant cells. Afterwards, a fibrous capsule is formed around the innate immune cells that constitute the centre of the granuloma, leading to the formation of a capsule [2]. When adaptative immunity is formed, the granulomas become surrounded by T cells and B cells and at this stage the capsule is stable and maintains a relatively constant bacterial load [3]. This constant bacterial load is what characterizes latent TB, which occurs when there is an absence of symptoms in the infected individual. The progression to an active form of TB is consistent with the formation of necrotic material resulting from the death of macrophages (caseum). Its accumulation leads to liquefaction and rupture into the lung airway, causing the bacilli to be exhaled into the air and facilitating the spread of the infection [2, 3]. However, it is still unclear whether granulomas are used as a strategy for bacterial control, for structures that facilitate bacterial transmission, or both [3].

Active TB can be defined as being pulmonary TB, if it infects only the lungs, or as extrapulmonary, when *M. tuberculosis* spreads to other sites that include the skeleton, genitourinary tract, and the central nervous system [4]. Nevertheless, pulmonary TB is predominant, as it occurs in around 70% of the patients, with symptoms that include fever, cough, night sweats and weight loss [5]. The development of active TB upon infection is further increased when there are risk factors present such as undernutrition, HIV infection, diabetes, smoking, alcohol disorders, and poverty [1, 5]. In contrast, latent TB renders the infected patients asymptomatic and is estimated to affect one third of the world population, with the ability to further develop to active TB in around 5 to 10% of the cases [5].

1.1.1. Treatment of active pulmonary TB and drug-resistant strains

The treatment regimen utilized nowadays for the treatment of active pulmonary TB was introduced in the 1990s and has a length of 6 months, in which four first-line drugs are used: isoniazid, rifampicin, ethambutol and pyrazinamide [6]. In the first two months, the treatment includes the four drugs, while during the remaining four months only isoniazid and rifampicin are used [1, 6]. This treatment has a high efficiency for drug-susceptible TB. However, the extensive length of the treatment and the amount of drugs required

causes noncompliance and lack of adherence to medication, which in turn can lead to treatment failure, infection relapse, and increase in proliferation of drug-resistant strains [7, 8]. These strains can be multidrug-resistant (MDR-TB), being resistant to both isoniazid and rifampicin, or extensively drug-resistant (XDR-TB) when they present multidrug-resistance in addition to resistance to fluoroquinolones and any second-line injectable antibiotics (amikacin, kanamycin and capreomycin) [6]. In order to treat MDR-TB, typically four to six drugs must be used, in which a fluoroquinolone and one injectable agent must be present, with a treatment regimen of at least 18 months, being less efficient and far more toxic than the treatment used for drug-susceptible strains [7].

According to the WHO, it is estimated that 465 000 of the cases of TB in 2019 were caused by MDR strains, accounting for 3.3% of the total cases reported [1]. Additionally, in 2017 the treatment success rate for this type of cases was only 54%, which is low when compared to the 85% treatment success rate for drug-susceptible TB [1].

Despite lack of treatment adherence by patients being the main reason for the increasing evolution of drug resistant variants, the differences in the quality of public health systems also contribute to this major problem [6]. As a consequence, incidence of such variants is unequally distributed throughout the world [6]. Therefore, the development of efficient vaccines is of extreme importance as a new strategy to control MDR-TB and XDR-TB, given that resistance to new mycobacterial drugs has been reported [9, 10].

1.2. The BCG vaccines

Nowadays, the only vaccine that is approved for the prevention of TB is the Bacille Calmette-Guérin (BCG), which consists of a live attenuated form of *M. bovis*, the main cause of bovine TB [10]. The primary BCG strain was developed by Calmette and Guérin at Institute Pasteur between 1908 and 1919 by making 230 passages over glycerinated bile potato medium [11]. Since then, more than 4 billion of doses have been administered, with BCG being given to infants few days after birth, or upon their first interaction with health services [10]. However, according to *Direção Geral de Saúde,* BCG is not administered in Portugal since 2017 as part of the vaccination plan, being only used in infants that present risk factors or that live in a community with a high incidence rate of TB [12, 13].

The first BCG vaccination in humans occurred in 1921 in France [14]. Afterwards, from 1924 to the early 1950s, several cultures of BCG were distributed worldwide and their repeated subculture in different laboratories led to the appearance of phenotypically different strains, given that the subculture methods varied from potato or Sauton media and the bacteria were harvested after several passages [11, 14]. Upon the introduction of master cell seeds by freeze-drying in the 1960s, more than 50 BCG sub-strains exist, which can cause impacts in virulence, immunogenicity, viability, colony counts and heterologous effects [11, 15]. Presently, around 14 BCG strains are globally used, UNICEF being the largest distributor, with the vaccines being supplied by the Statens Serum Institute (Denmark), Bulbio (Bulgaria), Serum Institute (India), and by the Japan BCG Laboratory [16]. However, these remaining strains still present variabilities that can

be dependent on the original seed strain, mutations developed before freeze-drying, genome predominance and/or epigenetic and structural differences due to different culture conditions [15]. Among the strains currently used, the most common ones are the Brazilian (Moreau/Rio de Janeiro), Danish (Copenhagen – 1331), Japanese (Tokyo – 172-1), Russian (Moscow – 368) and the Bulgarian (Sofia – SL222) strains [17].

1.2.1. Vaccines Currently in Use

1.2.1.1. BCG-Moreau

Around 1925, a doctor from Montevideo named Moreau received a BCG strain, which upon its passing in 1931 to Brazil, was named BCG Moreau. This strain was freeze-dried in 1950, having been propagated in different media until then [11].

1.2.1.2. BCG-Danish

Denmark received its first strain directly from Calmette at the beginning of 1927. However, after noticing that it originated large abscesses at the site of vaccination, it was deemed too potent and so the country was provided with a new one in 1931 [11]. In 1960, the batch 1331, which meant that the strain had been serially passed 1331 times, was freeze-dried and adopted as primary seed-lot in 1966. It is noteworthy that the current strain maintained its characteristics since 1931 [11].

1.2.1.3. BCG-Japan

Tokyo received a seed culture in 1925 from Institute Pasteur. Unlike other producers, lyophilization was first attempted in 1943 and achieved in 1950, which may have resulted in a vaccine with different phenotypical characteristics, such as resistance to high temperatures [11]. In 1960, the 172^{th} passage in potato-bile medium was freeze-dried and adopted as the primary seed-lot, hence the name Tokyo 172-1 [11].

1.2.1.4. BCG-Russia

The BCG strain was received in Russia in 1924, being named *M. bovis* BCG-I since 1925. It was freeze-dried in the 1940s and in 1963 the seed-lot 352 was the first to be used for vaccine production. However, since 2006 the seed-lot 368 is used for the vaccine manufacturing in Russia [18].

1.2.1.5. BCG-Bulgaria

Samples of the seed-lot 374a of the Russian BCG strain were sent to Bulgaria in 1971 and the primary seed-lot of the Sofia – SL222 strain was obtained in 1972 directly from the seed-lot received [19].

1.2.2. BCG Vaccine Production Problems

It is known that a single dose of a given BCG vaccine confers significant protection against the development of severe forms of childhood TB in infants [20, 21]. However, the same cannot be said for adults. Protection against pulmonary active TB in adults has efficacy ranging from 0 to 80% [20 - 22]. Such variable efficacy can be explained by several hypothesis, including acquired mutations through the years of

passaging, reducing its ability to stimulate protective immunity; genetic variability of vaccine recipients; exposure to environmental mycobacteria leading to tolerance; different doses of BCG administered; rapid clearance of the vaccine by the vaccinated individuals, not providing exposure long enough for the development of long-term immunological memory; and lack of vaccine production standardization [20, 23].

The problem of BCG vaccine standardization is of extreme importance. Most of the production is based on the growth of *M. bovis* BCG as surface pellicles on Sauton medium in culture flasks and harvested after 6-9 days [20, 24, 25]. This method, coupled with the slow growth of the bacilli, requires long culture periods. Additionally, due to the formation of aggregates, the quantification and quality control of the product is made difficult, leading to nonviable portions of the harvested bacteria [20]. Therefore, the drawbacks of this method may contribute to the variable levels of efficacy of the vaccines, as previously mentioned.

1.3. Vaccine Development Against TB for Adults

The development of new vaccines against TB has become the main approach to overcome the limitations in efficacy derived from the different BCG strains. The design of new vaccines involves three main strategies, namely prevention of infection, prevention of disease and therapy [26]. Vaccines that prevent the infection are administered pre-exposure, to induce a more robust response in terms of immunity or to produce a faster response, when compared to BCG, which can also be categorized as a pre-exposure vaccine [26]. Therefore, this strategy can prevent the disease or even the establishment of the infection. Regarding vaccines that prevent disease, its target is the induction of a response that is robust and long-lasting so that disease reactivation can be prevented. In addition, its aim also includes the induction of sterilizing immunity to eliminate latent TB, given that bacteria cannot be reactivated and lead to active TB [26]. Lastly, therapeutic vaccines are used to accelerate the treatment and shorten the duration of drug therapy, while improving treatment completion rates. Such vaccines are administered together with the conventional drugs used in TB treatment [27]. An example of a therapeutic vaccine is “Vaccae”, that was approved for administration with conventional TB treatment in China [27].

Vaccines can be further divided according to its biochemical forms and grouped into two main categories: mycobacterial whole cell-derived vaccines and subunit vaccines [10, 26]. The former can be sub-divided into live attenuated and inactivated/killed or fractionated whole cells, while the latter can be further divided into adjuvanted protein subunit and recombinant, which can be even further grouped according to the organism used to express the recombinant antigen – live mycobacterial, live bacterial, and live viral [10], [26]. Presently, at least 23 vaccines are being tested, with all groups being represented [26].

1.3.1. Whole-cell Vaccines

1.3.1.1. Live Attenuated Vaccines

Live attenuated vaccines against TB that are currently in clinical trials consist of strains of *M. tuberculosis* or *M. bovis* BCG that are either altered or weakened [26]. For this approach, the two vaccines are MTBVAC and VPM1002.

MTBVAC is based on the attenuation of the clinical isolate *M. tuberculosis* Mt103, which belongs to the *Mtb* Lineage 4, which together with the Lineage 2 accounts for the most widespread lineages of the *M. tuberculosis* complex (MTBC) that are transmitted between humans through air droplets [28]. The rationale between the usage of a clinical strain is that it becomes possible to obtain an antigen repertoire representative of the clinical strains transmitted and simultaneously avoid the effects caused by the repeated sub-cultivation *in vitro* of laboratory strains, which is the case of *M. tuberculosis* H37Rv [28]. The attenuation itself was achieved by two deletions in the genes *phoP* and *fadD26*, which encode, respectively, for the transcription factor of the two-component virulence system PhoPR and for one of the 13 genes responsible for the biosynthesis of phthiocerol dimycocerosates (PDIM), the main cell-wall lipids of *M. tuberculosis* that are associated with virulence [28]. The biggest advantage of this specific live attenuated approach is that several genetic regions that are absent in BCG due to the several passages, are still present in the attenuated *M. tuberculosis*, namely the ones that encode for important antigens [29]. Nevertheless, the safety and genetic stability is still assured due to the deletion of the virulence genes [29]. In preclinical studies it was demonstrated that MTBVAC conferred similar or higher protection when compared with BCG in immunocompetent mice [26].

VPM1002 was developed in the 1990s and is a recombinant BCG Prague vaccine that has the urease C gene replaced by the *hly* gene, which encodes for listeriolysin (Hly) from *Listeria monocytogenes* [30]–[32]. This organism secretes Hly, a pore-forming protein, to escape from the phagosome and evade into the cytosol of the cell of the host [31]. However, the activity of Hly is only optimum in the acidic pH range and given that BCG modifies the phagosomal pH to neutral values, it renders the activity of the protein suboptimal. Therefore, it was important to delete the urease C encoding gene, which is known to play a role in the pH neutralization of the phagosomes that contain mycobacteria through the production of ammonia, leading to the survival of the bacteria inside the macrophage [32]. With the replacement of the *ureC* by *hly*, the obtained mutant (rBCG Δ*ureC::hly*) was able to provide the acidic pH necessary for the optimal activity of listeriolysin [31, 32]. As a consequence, Hly is efficiently secreted and perforates the phagosomal membrane, allowing the release of mycobacterial antigens and DNA into the cytosol, resulting in a better antigen presentation and triggering autophagy, inflammasome activation and apoptosis [31 - 33]. Interestingly, *M. tuberculosis* has a similar mode of action to evade the defence of the host. However, BCG does not possess such capacities and is therefore limited to the phagosome of the infected host cells, where it is eliminated [31]. In phase 2 clinical trials, new-borns were immunized with VPM1002 and BCG, and the

immune responses were similar overall, with VPM1002 inducing increased CD8 T cells that produce IL-17, which may aid in protection [30].

1.3.1.2. Inactivated/Killed or Fractioned Whole-Cell vaccines

The vaccines under clinical trials that fall into this sub-category include “Vaccae”, MIP and DAR-901, which are made from non-tuberculous mycobacteria (NTM), and RUTI, that contains fragmented cells of *M. tuberculosis.* The main advantage of inactivated/killed or fractioned whole-cell vaccines when comparing to live attenuated vaccines is that the former is safer given that infectious particles are not present. Nevertheless, its immunogenicity is substantially weaker and may require multiple doses [26].

“Vaccae” is a vaccine prepared with heat-killed *M. vaccae*, an environmental NTM usually found in soil and first described in 1964 [34]. This vaccine is targeted for therapy and is the most advanced candidate in its category, being already approved for administration in China together with the drug therapy regimen for patients with active TB [27]. Several studies have shown that “Vaccae” is safe, well tolerated and was associated with a better clinical outcome when administered after the start of drug therapy. Additionally, in cases of MDR-TB the vaccine demonstrated enhanced cell-mediated immune response, as well as improved cure rates [35]. One of the most worrying cases of TB are of patients co-infected with HIV, given that BCG and other live vaccines cannot be administered to them. Heat-killed *M. vaccae* was proved to be safe and well tolerated in HIV-co-infected patients with pulmonary TB [35].

Another vaccine based on non-tuberculous mycobacteria is MIP, which stands for *M. indicus pranii*, a fast-growing mycobacterium that was initially used in its heat-killed form as immunotherapy for leprosy [27]. However, it was discovered that it shares antigens with both *M. leprae* and *M. tuberculosis* and so further investigation was made to use MIP also for the treatment of TB [27, 36]. Moreover, it was found that MIP has greater immunogenicity and efficacy when compared to BCG [36]. A phase 2 trial demonstrated that when MIP was administered together with drug therapy led to the enhancement of bacterial clearance, and showed improvements in patients with pulmonary MDR-TB [27].

It is known that prior encounters with either NTM or *M. tuberculosis* leads to protection against exposure to TB. Therefore, the DAR-901 booster vaccine was constructed under the hypothesis that to protect against TB, it was necessary a whole-cell vaccine that conferred several antigens [37]. Initially, the studies were made with SRL172, a heat inactivated *M. obuense* that was intended to be used as a whole-cell BCG booster [37]. In phase 1 and 2 of clinical trials, it was demonstrated that SRL172 was safe and immunogenic and a phase 3 trial showed that five injections were safe, immunogenic, and led to a reduction by 39% of culture-confirmed tuberculosis in HIV-coinfected patients [37]. However, given that this booster vaccine was cultured in an agar-based method, it was not scalable. Therefore, a scalable broth-based culture method was developed, leading to the production of the DAR-901 booster vaccine [37]. As expected, the DAR-901 booster conferred superior protection when compared to a BCG booster, in murine studies, while a phase 1 trial showed its safety and immunogenicity [38].

Lastly, RUTI was developed with two main objectives. Firstly, to boost immunity post-infection and, secondly, to trigger an immune response against antigens of latent bacilli [39]. The latter is of utmost importance given that normally protective immunity arises against antigens of active bacilli, while latent bacilli remain imperceptible to the immune system of the host [39]. This vaccine is formulated by growing a given virulent *M. tuberculosis* strain under stressful conditions, namely starvation, low pO_2 and low pH, conditions that are thought to be found inside of the granuloma of patients with active TB [39]. The bacilli are then fragmented so that cell wall antigens can be successfully presented, being consequently detoxified to remove endotoxin-like molecules, so as to prevent the development of a skin reaction upon therapeutic vaccination against latent TB [39]. Finally, the fragments are inserted in liposomes [39]. In clinical trials, RUTI exhibited "significant humoral and cellular immune responses against antigens expressed in actively growing and latent bacilli" [26].

1.3.2. Subunit Vaccines

1.3.2.1. Adjuvanted Protein Subunit Vaccines

Adjuvanted protein subunit vaccines are composed of one or several linked antigenic proteins that are administered with an adjuvant, which is designed to enhance the immune system so that the immunological impact of the antigens is maximized [10]. An adjuvant is used because, even though subunit vaccines are safer than whole-cell vaccines, the fact that these contain selected antigens leads to a less robust immune response [26]. There are currently 7 adjuvanted subunit vaccines in clinical trials, and M72/$AS01_E$, H56:IC31, ID93/GLA-SE and *GamTBvac* are among them [26].

The M72/$AS01_E$ vaccine is composed of a recombinant fusion protein that contains two *M. tuberculosis* antigens – Mtb32A and Mtb39A, together with the $AS01_E$ adjuvant, which is also used in malaria vaccines [30, 40]. With the goal of being used to prevent active TB, in a phase 2b clinical trial it was proved that it indeed prevented active pulmonary TB in adults infected with TB, with an efficacy of 54% [26].

Another vaccine targeted to prevent disease is H56:IC31, containing a fusion protein of three antigens: Ag85B, ESAT-6 and Rv2660c administered with IC31, which is a two-component adjuvant [41]. The antigens present in this vaccine were chosen because they are thought to be important for the intracellular survival of *M. tuberculosis* [41]. Both Ag85B and ESAT-6 are associated with pathogenicity, while the antigen Rv2660c is associated with latency and so, H56:IC31 was created with the goal of obtaining immunity against both active and latent bacilli [27]. In recent clinical trials it has shown safety and immunogenicity and is also being assessed as a therapeutic vaccine to prevent disease reoccurrence [27].

ID93/GLA-SE is obtained by the same mechanisms, consisting of a fusion protein comprising three antigens associated with pathogenicity (Rv2608, Rv3619 and Rv3620) and one associated with latency (Rv1913), combined with a glucopyranosyl lipid A (GLA) adjuvant formulated in a stable oil-water emulsion (SE) [27, 42]. Studies in pre-clinical animal models have shown that ID93/GLA-SE significantly improved

protection against active TB in infected animals [27]. In addition, its assessment as a therapeutic vaccine in a phase 1 clinical trial showed that it is safe and immunogenic, while in non-human primate models it was revealed that ID93/GLA-SE reduced significantly pulmonary mycobacterial burden and improved survival [27].

Lastly, GamTBvac is composed of the *M. tuberculosis* antigens Ag85a, ESAT-6 and CFP10, being the last two fused [43]. Subsequently, the three antigens were fused with a dextrose-binding domain from *Leuconostoc mesenteroides* so that they could be immobilized non-covalently on dextran, which is immunogenic and known to mediate humoral and cell immunity [43]. The adjuvant consisted of a mixture of DEAE-dextran and CpG oligodeoxynucleotides, being the latter known to improve antigen presentation and induction of vaccine-specific responses [43]. This mechanism of vaccine construction results in a constant and slow release of the vaccine components given that the antigens are only bound covalently [43]. Therefore, the interaction between said components and the immune system is prolonged and so it is sufficient to produce a strong immune response [43]. In a phase 1 clinical trial, its safety and immunogenicity were verified through vaccination of BCG-primed healthy volunteers and all the antigens present in the vaccine induced immune responses [26].

1.3.2.2. Recombinant Subunit Vaccines

Recombinant vaccines are based on the introduction of DNA encoding for a specific antigen, or set of antigens, into a given vector, which can be either mycobacteria/bacteria or a virus [26]. In terms of live mycobacterial, the main example is the vaccine VPM1002. However, this vaccine was mentioned in the whole-cell section (section 1.3.1) given that even though it is recombinant, DNA encoding for antigens was not introduced. Instead, DNA that conferred better performance to the BCG strain of choice was introduced. Therefore, this section will only be focused on vaccines with viral vectors.

Live viral recombinant vaccines can be considered similar to the subunit protein vaccines in the sense that both use only selected antigens known to contribute to infection by *M. tuberculosis*. However, in the case of live viral vaccines, an adjuvant is not needed due to the viral vector already triggering a robust and long-lasting immune response [10]. Nevertheless, vaccines that are based on viral vectors face a few challenges. Firstly, the chosen vector needs to be safe to prevent disease derived by it, specifically to those who are coinfected with HIV [44]. Secondly, pre-exposure to the virus chosen might render it less efficient [44]. This can happen when the vaccine requires the administration of two doses, and/or when people have been previously infected or exposed to the virus [10]. To overcome the latter challenge, a heterologous prime-boost vaccination can be approached, in which both the priming and the boosting vaccines contain the same antigens, but the viral vector is different in each one [10]. In this category, at least 7 vaccines are in clinical trials, including Ad5Ag85A, ChAdOx1.85A + MVA85A, and TB/FLU-04L [26].

Commonly used viral vectors include adenoviruses and Modified Vaccinia Ankara (MVA) [27]. The former exists in more than 50 subtypes, with the subtype 5 being the most used and studied as a gene

transfer vector [45]. This subtype (Ad5) was used to construct the vaccine Ad5Ag85A, a non-replicative vector expressing Ag85A, an antigen common in all mycobacteria that is immunodominant. In animal studies using a murine model, intramuscular injection of the vaccine did not confer protection against pulmonary TB [45]. In contrast, upon its administration via respiratory mucosa, T-cell responses were elevated in the lung, which corresponds to improved protection following pulmonary challenge. Therefore, this led to believe that the route of immunization was associated with the distribution of T cells [45]. However, in larger animal models, vaccination via intramuscular injection conferred a robust lung protection [46 - 48], suggesting that the efficacy obtained by this vaccination route differs between animal species [49]. In a phase 1 clinical trial, the safety and immunogenicity was proven in BCG-primed and BCG-naïve individuals, with BCG-primed having the higher boost in T cell immunity, supporting the development of Ad5Ag85A as a booster vaccine [45].

An example of a heterologous prime-boost vaccine regime is the ChAdOx1.85A boosted with the MVA85A vaccine. The former was constructed using a chimpanzee adenovirus vector replication-deficient developed in Oxford, hence the name ChAdOx1, that expressed antigen Ag85A [50]. Using this vector in detriment of human adenoviral vectors has several advantages, such as its robust immunogenicity and low seroprevalence [27]. Adenovirus subtype 5 vectors can have a reduced efficacy due to pre-existing immunity due to natural infection [45]. In contrast, the vector used in this vaccine does not have this limitation due to its low seroprevalence in humans [27]. The MVA85A vaccine, which in this case was used as the booster, was developed using a modified Vaccinia Ankara virus expressing the antigen Ag85A. In a phase 2b clinical trial, upon vaccination of BCG-primed infants, MVA85A unfortunately did not confer additional protection against TB infection and/or disease [51]. However, when used as a boost with prime ChAdOx1.85A, the prime-boost vaccine is safe and well-tolerated, with ChAdOx1.85A inducing robust T cell responses that are further boosted with MVA85A [52].

TB/FLU-04L is a recombinant vaccine that uses the strain A/Puerto Rico/8/34 H1N1 of the influenza virus to express two of the antigens of *M. tuberculosis* – Ag85A and ESAT-6. In a phase 1 trial, this vaccine was safe and showed immunogenicity [53].

1.4. *Mycobacterium* spp. and the Difficulty of Growing these Cells

The genus *Mycobacterium* is included in the *Actinobacteria* phylum and is characterized by Gram-positive rod-shaped microorganisms, with more than 220 species and subspecies recognized [54], [55]. A striking feature of mycobacteria is the presence of long-chain mycolic acids in the cell wall, which makes it difficult to stain the cells by the Gram method. However, besides these limitations, mycobacteria are considered to be Gram-positive [55]. The most notorious members of the genus are *M. tuberculosis* and *M. leprae*, pathogens responsible for TB and leprosy, respectively [54]. Interestingly, they were also the first mycobacteria to be discovered [55, 56]. This led to a division of the species, rendering the bacteria that do not cause TB or leprosy, to be called non-tuberculous mycobacteria (NTM) [55, 56].

Mycobacteria can also be divided according to their growth rate, resulting in slow growers and fast growers. The former one includes microorganisms that require more than 7 days to develop visible colonies on solid medium, while the latter includes mycobacteria that require between 3 to 7 days to do so [55].

1.4.1. Influence of Culture Conditions on Mycobacterial Growth

As previously mentioned, the culture of BCG occurs in surface pellicles grown in liquid Sauton medium under static conditions. Specifically, a given strain of *M. bovis* BCG is grown on this medium and, after a maximum of 21 days of growth, the bacilli are harvested through filtration and centrifugation, followed by cell dispersion by stainless steel ball milling, resuspension in a solution containing 0.5% glucose, transferred to ampoules and, lastly, freeze-dried. Sauton medium is typically composed of L-asparagine, citric acid, magnesium sulphate, dipotassium hydrogen phosphate, ferric ammonium citrate, zinc sulphate, and glycerol as carbon source [20]. Nevertheless, there are different formulations that can vary in the source of amino acids, which can be either L-asparagine or L-glutamate, the glycerol concentration and the presence or absence of zinc sulphate [57].

Regarding the whole-cell vaccines currently in clinical trials, several similarities can be noted. Namely, in terms of live attenuated vaccines, the medium used is Middlebrook 7H9 supplemented with albumin, dextrose, and catalase (ADC) and 0.05% (v/v) Tween-80 [58, 59]. The main difference is that the culture medium used for the production of VPM1002 is also supplemented with glycerol [58, 59]. However, culture conditions for inactivated or fractioned vaccines are diverse in terms of carbon sources. To produce “Vaccae”, the mycobacterium is grown in solidified Sauton medium, while the production of MIP is achieved by culturing *M. indicus pranii* in Middlebrook 7H9 supplemented with ADC, glycerol, and Tween-80 [36, 60]. Lastly, the *M. tuberculosis* H37Rv used to produce the RUTI vaccine is grown for three weeks in Middlebrook 7H11, a solid medium [61]. The specifications regarding the manufacture of DAR-901 were not found.

When comparing the different culture media used to produce the vast catalogue of whole-cell vaccines currently in clinical trials, the carbon sources that are the most common, except for RUTI, are glucose (in the form of the ADC supplement) and glycerol. The former is used to produce MTBVAC, VPM1002 and MIP, while the latter is used as a carbon source in the production of VPM1002, “Vaccae” and MIP. Therefore, glucose is absent in the production of “Vaccae”, and glycerol is absent in the culture medium used to produce MTBVAC. Regarding Tween-80, its presence is noticed in the production of MTBVAC, VPM1002, and MIP [36, 58 - 61].

Interestingly, these culture conditions are also used with other *Mycobacterium* sp., namely *M. smegmatis*, whose culture medium contains a supplement of oleic acid, albumin, dextrose and catalase (OADC) and Tween 80, also containing glycerol [62]. OADC is a carbon source in the form of fatty acids and sugars. Additionally, the production of *M. bovis* BCG in bioreactors was evaluated with Sauton medium, a known source of glycerol [20]. In contrast, another bioreactor cultivation of *M. bovis* BCG took advantage of a Middlebrook 7H9 medium supplemented with OADC, glycerol, and Tween 80 [63].

Tween 80 is usually required in the culture medium of mycobacteria so that an optimal growth is achieved. In *M. smegmatis* it was confirmed that Tween 80 improves oxygen transfer, with a consequent reduction in the extent of bacilli aggregation. In addition, it was also proved that Tween 80 can be hydrolysed to oleic acid by the mycobacterial phospholipase A of *M. smegmatis* [64]. Oleic acid is further broken down in the fatty acid β-oxidation to yield acetyl-CoA (Figure 1) [65, 66]. Moreover, even though acetyl-CoA is usually a substrate of the TCA cycle, it was proven that it can be shifted to the glyoxylate cycle by *M. tuberculosis* upon growth on fatty acids as carbon source, for example OADC [66]. The same outcome was also shown in *M. smegmatis*, with the acetyl-CoA obtained from Tween 80 not entering the TCA cycle, glycolysis and the pentose phosphate pathway [65]. As a consequence, the increased levels of acetyl-CoA may lead to an increase in the levels of saturated and unsaturated fatty acids, as well as an increase in the synthesis of triacylglycerols (TAG) [66].

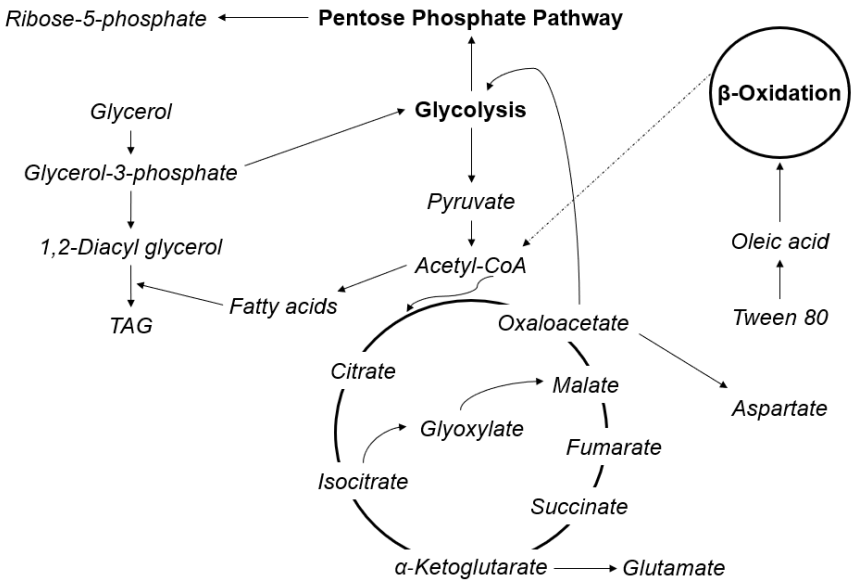

Figure 1 - Metabolic pathways influenced by mycobacterial growth on glycerol, ADC supplement, and Tween 80.

Glucose, or dextrose, was also added to most of the culture media reported, in the form of an ADC supplement. When used together with Tween 80, there is an abundant acetyl-CoA, that also leads to the production of glucose, and so this sugar is not used for energy production. Instead, it is shifted towards the pentose phosphate pathway, generating ribose-5-phosphate, which is an important precursor in nucleotide biosynthesis [66].

1.4.2. Mycobacterial Cell Envelope

The cell envelope of mycobacteria is comprised of an inner membrane, a cell wall, and an outer layer (Figure 2) [67, 68]. The inner membrane, also known as the plasma membrane, is composed of a phospholipid bilayer containing glycolipids that extend into the periplasmic space [69]. In turn, the cell wall

contains three major components: a cross-linked polymer of peptidoglycan, and an arabinogalactan polysaccharide, which are covalently linked to long-chain mycolic acids. This complex is referred to as the mAGP complex. The outer layer also presents solvent-extractable lipids, such as glycophospholipids and inert waxes, that are intercalated with the mycolic acids. Additionally, its outermost layer, the capsule, contains polysaccharides and proteins [70].

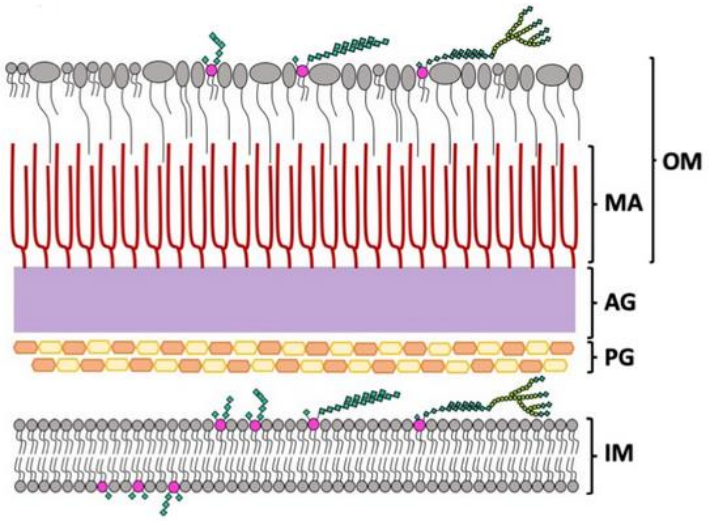

Figure 2 – Representation of the cell envelope of mycobacteria, composed of an inner membrane (IM), a cell wall with a cross-linked network of peptidoglycan (PG) and an arabinogalactan polysaccharide (AG), and an outer layer (OM) containing mycolic acids (MA), and solvent-extractable lipids. From "Structural and Functional Characterization of Phosphatidylinositol-Phosphate Biosynthesis in Mycobacteria", by M. Belcher Dufrisne et al., *J. Mol. Biol.*, vol. 432, pp. 5137–5151, 2020 (doi: 10.1016/j.jmb.2020.04.028). Copyright 2020 by Elsevier.

The peptidoglycan is present in almost all bacteria and provides shape and stability. Normally, its structure is composed of a backbone of N-acetylglucosamine (GlcNac) and N-acetylmuramic acid (MurNac), linked together by peptide side chains. However, in mycobacteria the N-acetylmuramic acid is oxidized to N-glycolylmuramic acid (MurNGlyc) [70]. Such modification is important given that it increases the strength of the peptidoglycan due to hydrogen bonding and decreases susceptibility to lysozyme [70]. It also provides a region for the covalent linkage of the arabinogalactan, a heteropolysaccharide containing sugar residues of galactose and arabinose in the furanose ring form [67, 70]. This branched macromolecule has the galactan portion in the form of a linear chain, with approximately 30 galactose residues, and two arabinan chains being composed of the same number of residues bound to a single galactan unit [70]. The arabinogalactan forms ester bonds at its non-reducing termini with mycolic acids, being also able to bind succinyl and galactosamine moieties [69].

Another important aspect of the cell envelope is the presence of non-covalently linked glycophospholipids in the inner and outer membrane, including phosphatidyl-*myo*-inositol mannosides

(PIMs), lipomannan (LM), and lipoarabinomannan (LAM), which play a role in modulating the immune response of the host upon infection [70].

Members of the *Mycobacterium* sp. are known to have cell walls composed of long chain mycolic acids. The mycolic acids are long chain α-alkyl-β-hydroxy fatty acids (C_{70}-C_{90}), composed of a meromycolate chain (C_{42}-C_{62}) and a long saturated α-chain (C_{24}-C_{26}) [69, 70]. These lipids have an important role in the permeability of the cell wall, as well as in the viability and virulence of the cell, being also present in the outer layer as trehalose mono/di-mycolates and glucose monomycolate [69]. Furthermore, they can be divided into three classes: the α-mycolic acids, which are the most abundant, contain a cyclopropane ring in a *cis*- configuration, the methoxy mycolic acids and keto mycolic acids, contain both cyclopropane rings in a *cis*- or *trans*- configuration, with methoxy or ketone groups, respectively [69, 70].

Even though long chain mycolic acids are a characteristic of mycobacteria, this class of fatty acids is also present in other genera belonging to the *Actinobacteria* phylum. Actinomycetes that contain mycolic acids belong to a phylogenetic line named mycolata and include the genera *Mycobacterium, Corynebacterium, Dietzia, Nocardia, Rhodococcus,* and *Tsukamurella* [68]. For example, corynebacteria contain corynomycolic acids (C_{30}-C_{36}), with an α-chain ranging from 16-18 carbons, with the genus *Dietzia* also producing mycolic acids with the same size [68]. The mycolic acids produced by the *Nocardia* genus are larger than the ones of the *Corynebacterium* and *Dietzia* genera, having lengths of around 50 carbons with 0-3 double bonds. Regarding the *Rhodococcus* genus, the mycolic acids can have up to 40 carbons, with α-chains containing 12-18 carbons [68]. The mycolic acids produced in the *Gordona* and *Tsukamurella* genera are larger than the ones produced in the genera *Corynebacteriu, Dietzia,* and *Rhodococcus*. The *Gordona* genus contains mycolates of 60 carbons with 1-4 double bonds, and the *Tsukamurella* genus produces mycolates of 62-78 carbons with up to six double bonds [68].

Due to the presence of long chain mycolic acids, the cell wall of mycobacteria presents a high thickness, and is permeable to hydrophobic antibiotic substances, while being impermeable to hydrophilic substances through the lipid domain [67, 71]. Hydrophilic compounds cross the cell wall through porin channels [71]. Even though several antibiotics against *M. tuberculosis* target the cell wall assembly, such as isoniazid that inhibits the synthesis of mycolic acids, this structure remains the core of pathogenicity and resistance to several anti-TB drugs [67, 72].

1.4.3. Cell Aggregation and Biofilm Formation

Members of the *Mycobacterium tuberculosis* complex (MTC), which include *M. tuberculosis* and *M. bovis*, as well as some non-tuberculous mycobacteria, have the ability to form aggregates in liquid cultures. Namely, when *M. tuberculosis* was discovered as the cause of TB by Robert Koch in 1882, its description of the bacilli included the formation of large clumps that were densely bunched and braided [73]. This phenomenon is named cording and is characterized by an organized multicellular aggregation, in which the orientation of the long axis of each cell is parallel to the long axis of the whole cord [73].

Hydrophobicity of the cell surface is known to have great importance in cell aggregation. Notoriously, the cell envelope of mycobacteria is mostly composed of lipids, such as the mycolic acids present in the cell wall [74]. Moreover, *M. smegmatis* can regulate the chain length of mycolic acids in response to environmental factors, proving that surface hydrophobicity can be regulated [75, 76]. Since aggregation is a characteristic shared among mycobacteria, Tween 80 is usually added to the culture medium to disperse the cells [76].

Several mycobacteria, such as *M. ulcerans*, *M. avium* and *M. smegmatis*, have also been reported to form biofilms, with the latter producing biofilms with high amounts of extracellular free mycolic acids [77]. It is noteworthy that given that *M. tuberculosis* can grow as pellicles in the air-liquid interface, it has been proposed that this species can also form biofilms rich in free mycolic acids and containing drug-tolerant cells [78].

1.4.4. Mechanisms of Bacterial Adaptation

Prokaryotes are known to modulate their membrane properties upon changes in environmental conditions, to maintain biological functions. This regulation is mainly achieved through changes in the cell membrane composition, namely in its lipid composition [79]. The process by which bacteria regulate the lipid composition in order to maintain membrane fluidity despite the different environmental conditions is called “homeoviscous adaptation” [80]. This process modulates barrier functions, as well as biochemical process that occur at the membrane level, such as energy transduction and transport [79, 81]. Specifically, at the fatty acid composition, bacteria can change it through a plethora of strategies that include changing the chain length, the degree of saturation, *cis-trans* isomerization, *iso*- or *anteiso*- branching, and cyclopropanation [79]. Mechanisms to do so consist of a *de novo* synthesis of the fatty acids of the cellular membrane or through the modification of the fatty acid chains [79]. For example, in response to changes in temperature, bacteria may adjust the membrane fluidity by changing the saturation degree. Increased content of saturated fatty acids lessen the membrane fluidity, while increased content of unsaturated fatty acids increase the membrane fluidity, given that the former present higher melting points than the latter [79]. Moreover, the fatty acyl chain lengths also influence the membrane fluidity, with longer chains decreasing fluidity and shorter chains leading to its increase [79]. Another mechanism used to maintain membrane fluidity across different temperatures is the methyl branching of fatty acids in the *iso*- and *anteiso*- positions, with the methyl group being positioned in the penultimate or antepenultimate carbon, respectively [82].

Cyclopropanation is the process by which fatty acid chains acquire a cyclopropane ring, rendering the membrane less fluid [79]. Moreover, cyclopropane rings introduced in the α-mycolic acids in *M. tuberculosis* are essential for its virulence and the persistence of the infection in the cells of the host [83]. Additionally, *M. smegmatis* also introduces cyclopropane rings in α-mycolic acids in response to decreasing temperatures below 37 ^{o}C [83]. This species in particular is also able to changing the proportion of mycolic acids in the *trans* configuration in response to different temperatures [83]. It is noteworthy that, even though

alterations in lipid composition are usually performed at the cellular membrane level, in mycobacteria the alterations may also be done in the mycolic acids, which are present in the cell wall [83].

Even though the main alterations in response to environmental conditions are done regarding fatty acid composition of phospholipids and mycolic acids, other macromolecules, such as proteins can be changed [79]. An example of this is the adaptation of *M. tuberculosis* to changes in pH, by the hydrolysis of asparagine catalyzed by asparaginase AnsA, which allows it to resist acid stress in the phagosome through the release of ammonia and incorporation of the nitrogen from the hydrolysis [84].

1.5. Motivation for the Present Study

Given the difficulties inherent to mycobacterial cultivation in laboratory and industrial environments, such as the development of cell aggregates, an improved cell cultivation method is necessary. Moreover, a standardization of the culture methods used for the different strains of *M. bovis* BCG is of extreme importance. Therefore, the effect of culture media composition and of growth conditions on *Mycobacterium* cell aggregation will be studied. The development of a submerged fermentation technique that is reproducible is sought after, allowing for cell cultivation in planktonic state.

1.5.1. *Mycobacterium smegmatis* as Model Organism for BCG

Since *M. bovis* is a risk group 3 microorganism, the species *M. smegmatis* will be used as model organism. *M. smegmatis* is a fast-growing saprophytic mycobacterium that is normally used as a model to investigate the cellular processes of pathogenic mycobacteria, such as *M. tuberculosis* and *M. leprae* [85]. Its fast-growing ability is the main advantage, given that *M. tuberculosis* can take up to four weeks to yield colonies on solid medium [86]. However, since it is not pathogenic, the pathogenic features of *M. tuberculosis* cannot be studied using this model organism [86]. It is important to mention that *M. smegmatis* has recently been reclassified, and now belongs to the *Mycolicibacterium* genus, which is comprised of environmental species [54]. Nevertheless, human pathogens continue to belong to the genus *Mycobacterium* [54].

M. smegmatis is well studied for its ability to form surface pellicles, a type of growth present in aerobic mycobacteria in the air-liquid interface, in which the mycolic acids produced are shorter (C_{56}-C_{68}) than the ones naturally present in the cell envelope during planktonic growth (C_{70}-C_{90}) [55, 87]. This process is thought to be regulated by the chaperone GroEL1 [87]. Moreover, the cells are surrounded by free mycolic acids, produced by the hydrolysis of trehalose dimycolate (TDM) – a glycolipid present in the outer membrane - by a serine esterase, resulting in the consideration of this process as being a biofilm formation [75]. However, the TDM used as a precursor of the free mycolic acids is newly synthesized, being its synthesis catalysed by the Ag85 complex [77]. Surprisingly, these mechanisms are similar between *M. smegmatis* and *M. tuberculosis*, constituting another advantage of the use of this non-tuberculous mycobacteria as a model organism for the study of aggregation [77].

1.6. Objectives

The main objective of this master thesis is the development of a reproducible fermentation method to prevent the formation of aggregates and allow the cultivation of *M. smegmatis* in planktonic state. The effect of media composition, as well as temperature and other culture conditions, will be assessed in order to reach the best growth rates and lowest extent of cell aggregation. Such study will help providing a standard cultivation method for mycobacterial cells, namely the ones used in vaccine production.

2. Materials and Methods

2.1. Bacterial strain and culture media

Mycobacterium smegmatis ATCC 10143 was used in this study.

The culture media used was BBL™ Trypticase™ Soy Broth (TSB) from BD (France). The medium was autoclaved at 121°C for 20 minutes and stored at 4°C.

The agar plates (Tryptic Soy Agar) used to store the bacteria at 4°C were prepared by adding 30 g of TSB and 15 g of Difco™ Agar from BD per litre of distilled water.

2.2. Chemicals

The chemicals used in this work were methanol (Fisher Scientific), ethanol (Panreac), isopropanol (Fisher Chemical, Fisher Scientific), glycerol (Sigma-Aldrich), DMSO (Fisher Bioreagents, Fisher Scientific), DMF (Fluka Analytical), Tween 80 (Merck-Schuchardt), and Polyacrylic Acid (Aldrich Chemistry). The ammonium-containing compounds used in this study were ammonium acetate (Sigma-Aldrich), ammonium chloride (Merck), ammonium nitrate (Riedel-de Haën), ammonium sulphate (Panreac), and ammonium bicarbonate (Sigma-Aldrich). All other chemicals were of analytical grade and were purchased from various suppliers unless stated otherwise.

2.3. Growth conditions

M. smegmatis ATCC 10143 was plated in Tryptic Soy Agar (TSA) and the inoculum for every experiment was prepared by adding a loopful of the plated bacteria into 20 mL of TSB. The inoculum was grown for at least 48 h at 30°C and 180 rpm in an Agitorb 200 incubator (Aralab).

2.3.1. Solvent exposure

To study the effect of different solvents on cell aggregation, methanol, ethanol, isopropanol, glycerol, DMSO, DMF, Tween 80, or PAA, were supplemented to TSB at a concentration of 0.25% (v/v), up to a total volume of 20 mL. The volume of cell suspension added as inoculum was determined so that the initial optical density at 600 nm ($OD_{600\ nm}$) was between 0.1-0.2. The cell cultures were grown for 24 hours at 30°C and 180 rpm. The experiment was done in duplicate.

The effect of an increased concentration of DMSO on cell aggregation was also studied. To do so, TSB was supplemented with either 0.25%, 0.50% or 1% (v/v) of DMSO and a given volume of cell suspension was added so that the initial $OD_{600\ nm}$ was ca. 0.1-0.2. The experiment was done in duplicate.

2.3.2. Effect of growth temperature on cell aggregation

To assess the effect of growth temperature on the cell aggregation extent, cells were cultured in TSB supplemented with 0.25% (v/v) DMSO with an initial $OD_{600\ nm}$ between 0.1-0.2, at either room temperature (23°C), 30°C, or 37°C, and 180 rpm for 24 hours. The experiment was done in duplicate.

2.3.3. Cold shocks and oxygen stress

To study the response to different stresses, a cell suspension was added to 20 mL of TSB supplemented with 0.25% (v/v) of DMSO to obtain an initial $OD_{600\ nm}$ between 0.8-0.9, so that the cell culture reached the exponential phase as fast as possible. Cell cultures were grown in 45- or 55-min intervals at 30ºC and 180 rpm, followed by a 15- or 5-min stress, respectively. The stresses applied to the cells included: cold shock (0°C) without agitation (TS-NS), cold shock (0°C) with agitation (180 rpm) (TS-S), room temperature without agitation (NS), or 30°C without agitation (30°C-NS). During the first 8 h of growth, the cell cultures suffered 5 stress shocks, with another 2 shocks being applied after 22 h of growth. The experiment was done in duplicate.

The adaptation of *M. smegmatis* to 15-min cold shocks (0°C) without agitation was also assessed, with 5 shocks being performed in the period of 8 h, followed by 2 shocks after 22 h of growth. Before and after each shock, samples were taken to analyse the fatty acid composition and the zeta potential of the cells. The adaptation experiment was done in quadruplicate.

2.3.4. Cell aggregation under carbon-starvation conditions

The effect of carbon-depleted conditions in the extent of cell aggregation was studied as follows: briefly, 3-day old cultures as well as cultures harvested during exponential phase ($OD_{600\ nm}$ between 2.2 and 2.3) were centrifuged at 10405 *g* for 5 min (Centrifuge 5810 R, Eppendorf). The supernatant of the exponential growing cells was discarded and replaced with the supernatant from the old cells and incubated at 30°C and 180 rpm for 16 h in an Agitorb 200 incubator (Aralab). The experiment was done in duplicate. Samples for the fatty acid composition analysis and zeta potential were taken before the exchange of the medium, immediately after, 1 h, and 16 h later.

After 16 h, samples for microscopy were also taken. To 1 mL of cell suspension collected from each culture, 1 µL of Rhodamin B (C.I. 45170 for microscopy from Carl Roth GmbH+Co, Germany) was added. The samples were observed by fluorescence microscopy using an Olympus CX40 microscope, with an Olympus U-RFL-T burner and an U-MWG mirror cube unit (excitation filter: BP510-550; barrier filter: BA590). Images were captured by an Evolution™ MP5.1 CCD color camera using the software Image-Pro Plus, both from Media Cybernetics, Inc. (USA). Image analysis was performed using ImageJ (National Institutes of Health, Bethesda, Maryland, USA).

2.3.5. Ammonium-containing compounds as nitrogen source supplements

The influence of ammonium-containing compounds and their role as nitrogen supplement was also assessed, based on a previous study, but with some modifications [76]. To this end, sterilized solutions of ammonium acetate, ammonium chloride, ammonium nitrate, ammonium sulphate, or ammonium bicarbonate were added at a concentration of 50, 75, or 100 mM to TSB, up to a total volume of 20 mL. Cell suspension was added to obtain an initial $OD_{600\ nm}$ between 0.1-0.2. The experiment was done in duplicate. At the 24^{th} and 42^{nd} h of growth, samples were taken for fatty acid composition and zeta potential

measurements. After 42 h of growth, samples were also taken for microscopy. Intracellular storage lipids were stained using Nile Red (Molecular Probes, Life Technologies, USA), as previously described [88]. Briefly, a stock solution of 1.3 mg/mL of Nile Red in acetone was prepared, added to suspended cells to achieve a 1:100 dilution, and the mixture was incubated for 5 min. The samples were observed by fluorescence microscopy using the previously mentioned Olympus CX40 microscope, with an Olympus U-RFL-T burner and an U-MWB mirror cube unit (excitation filter: BP450-480; barrier filter:BA515). Images were captured by the previously described CCD camera and software. Image analysis was performed using ImageJ (National Institutes of Health, Bethesda, Maryland, USA).

2.4. Cell aggregation assay

The extent of cell aggregation was assessed by the following assay: briefly, after 24 hours of growth, 16 mL of each culture were divided into four test tubes and the $OD_{600\ nm}$ was measured over time, under static conditions. Cells that are aggregated deposit at the bottom of the tubes and the values of $OD_{600\ nm}$ decrease over time. The percentage of cells remaining in suspension is then calculated from the quotient between the $OD_{600\ nm}$ at each time point and the initial $OD_{600\ nm}$. Therefore, the velocity of aggregation is estimated by the slope of the linear regression of the percentage of cells in suspension over time, i.e., during the sedimentation of the aggregates. When the sedimentation of aggregates is slowed down, the $OD_{600\ nm}$ remains constant. After said stabilization, it is possible to distinguish cells in up to three different cell locations, which are characterized below (Table 1). The time at which the cell sedimentation is slowed down is given by the interception between the linear regression of the decreasing percentage of cells in suspension over time and the linear regression of the constant values over time after the stabilization.

Table 1 – Cell populations obtained after the completion of the cell aggregation assay.

Cell population	Description
Mix	All types of cells that compose the culture
Top	Light aggregates at the air-liquid interface
Middle	Cells that remain in suspension
Bottom	Heavy aggregates deposited at the bottom

2.5. Fatty acid analysis

Samples of 1 mL of cell suspension were collected and centrifuged at 8161 *g* for 2 min (µSpeedFuge SFA12K, Savant Instruments, Inc) and washed at least once with milli-Q water. The fatty acids of the phospholipids of the cellular membrane were extracted and methylated to fatty acid methyl esters (FAMEs) with the instant-FAME method from MIDI, Inc, as previously described [89]. The FAMEs were analysed by gas chromatography using a 6890N gas chromatograph (Agilent Technologies), with a flame ionization detector, an automatic injector 7683B, and an Agilent J&W Ultra 2 capillary column. Each FAME was identified using the PLFAD1 method of the Sherlock software (MIDI, Inc). The saturation degree was defined

as the ratio between the sum of all the percentages of saturated fatty acids and the sum of the percentages of monounsaturated fatty acids. The unsaturation index was defined as the sum of the percentages of unsaturated fatty acids multiplied by their respective number of double bonds and divided by 100, as previously described [90].

2.6. Zeta potential

To determine the zeta potential of the cells, 1 mL of cell suspension in each population was collected, centrifuged at 8161 *g* for 2 min and washed at least 2 times with milli-Q water. The washed cells were then resuspended in 1 mL of a 10 mM KNO_3 solution and 40 µL of this suspension was then diluted in 2 mL of 10 mM KNO_3. From the electrophoretic mobility of the mycobacterial cells at 25 ^{o}C, the zeta potential was determined, according to the method of Helmholtz-Smoluchowski, by the Zeta Software version 7.11 (Malvern Instruments Ltd.) using a Zetasizer Nano ZS (Malvern Instruments Ltd.).

3. Results

3.1. Growth and aggregation of cells exposed to solvents

The effect of solvent exposure in cell aggregation of *M. smegmatis* was studied. The cells were firstly exposed during the lag phase ($OD_{600\ nm}$ between 0.1 and 0.2) to a concentration of 0.25% (v/v) of either methanol, ethanol, isopropanol, glycerol, dimethyl sulfoxide (DMSO), dimethyl formamide (DMF), Tween 80 or polyacrylic acid (PAA). After an exposure time of ca. 24 h, the cells were collected in test tubes, and an aggregation assay was performed (Figure 3). During the aggregation assay, the culture was not shaken for at least 2 h and so three different cell populations appeared in the test tube, being composed of cell aggregates that sedimented (Bottom), cells in suspension (Middle) and cells at the air-liquid interface (Top). At the end of the assay, cells from the three populations were collected and their fatty acid composition of the phospholipids of the cellular membrane, biomass dry weight and zeta potential were analysed.

In the assay, the $OD_{600\ nm}$ decrease over time was measured, being a slower decrease associated with the formation of fewer cell aggregates, with the slope of the percentage of cells in suspension over time corresponding to the velocity of aggregation. Furthermore, the time at which a stabilization occurred was determined. The linear regression for the velocity of aggregation and the stabilization period is of the following type:

$$y = mx + b \tag{1}$$

Therefore, considering Equation 1 represented above, the velocity of aggregation was given by the slope m, while the time of stabilization was given by the x value where both equations intercept. Both the velocities of aggregation and stabilization times obtained for all the conditions are summarized in Table 2.

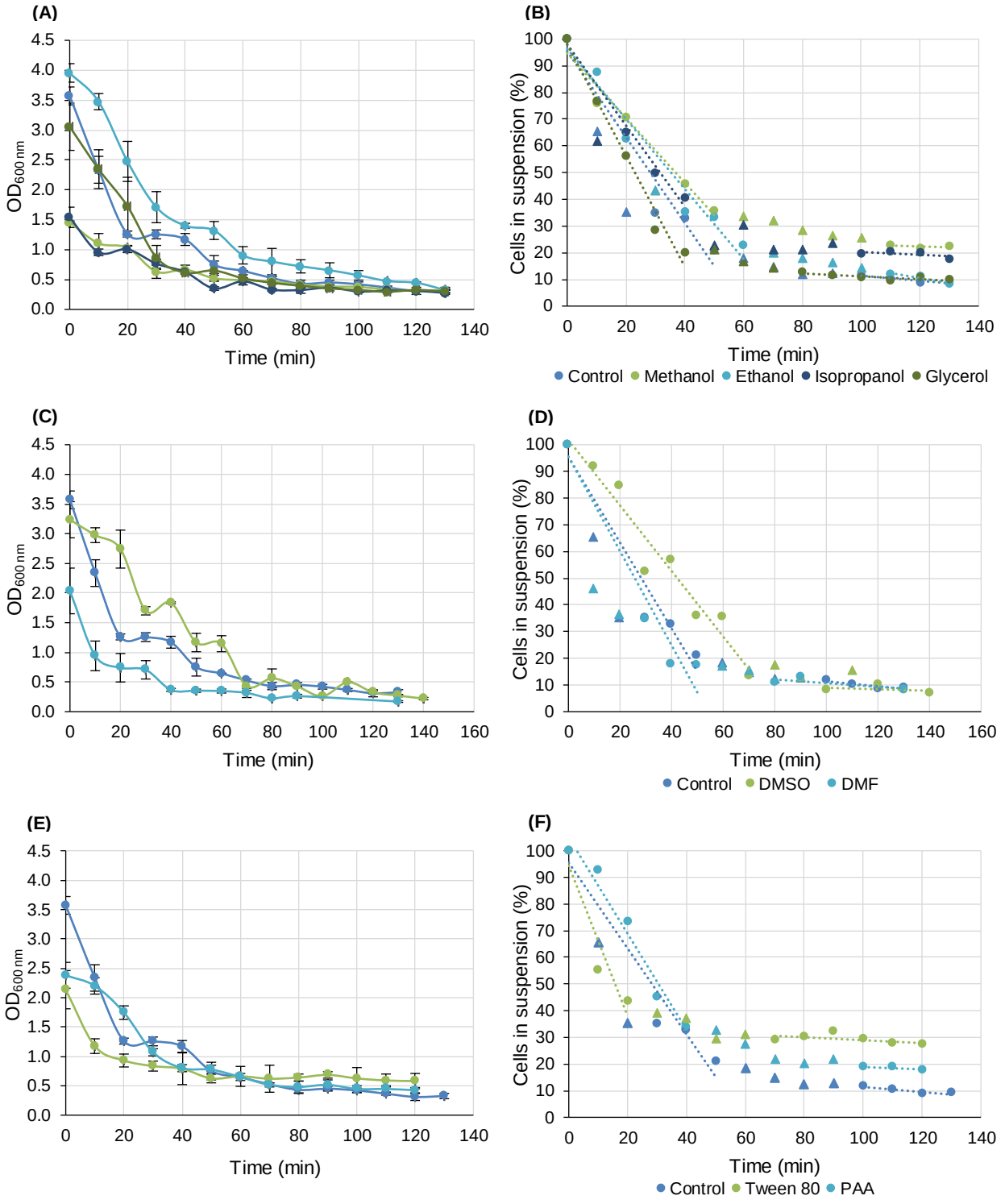

Figure 3 – Optical density ($OD_{600\ nm}$) (A, C, E) and percentage of cells in suspension (B, D, F) over time for cells exposed for 24 h to 0.25% (v/v) of methanol, ethanol, isopropanol, or glycerol (A, B); 0.25% (v/v) of DMSO, or DMF (C, D); and 0.25% (v/v) of Tween 80, or PAA (E, F). Values considered for the equations of aggregation and stabilization (closed dots); outliers (closed triangles); linear regression (dotted lines).

Table 2 – Parameters obtained in the linear equations for the period of sedimentation of aggregates and stabilization for the different solvents tested.

	Aggregation equation parameters		Stabilization equation parameters		Stabilization time (min)
	m (% cells in suspension/min)	b (% cells in suspension)	m (% cells in suspension/min)	b (% cells in suspension)	
Control	-1.6086	95.5	-0.0952	20.9	49.29
Methanol	-1.2127	94.7	-0.0344	26.5	57.95
Ethanol	-1.3125	96.4	-0.1896	33.2	56.23
Isopropanol	-1.5204	98.1	-0.0519	25.5	49.46
Glycerol	-2.0802	98.0	-0.0542	16.6	40.19
DMSO	-1.2282	101.8	-0.0278	11.7	75.06
DMF	-1.7666	95.5	-0.0681	17.5	45.92
Tween 80	-2.8220	94.4	-0.0549	34.4	21.69
PAA	-1.8025	104.9	-0.0420	23.0	46.51

The exposure of the bacterial cells to 0.25% (v/v) of either methanol, ethanol, isopropanol, or glycerol rendered different outcomes in terms of velocity of aggregation and stabilization times (Figure 3A; Figure 3B; Table 2). Regarding the velocity of aggregation, when compared to control conditions, its values were lower during growth on methanol, ethanol, and isopropanol, with a higher value being obtained during exposure to glycerol. The stabilization time is the period at which the $OD_{600\ nm}$ values stop decreasing and only free cells or very small aggregates remain in suspension. Therefore, the smaller the cell aggregates, the longer it takes for them to deposit, and so a less cell aggregation extent is observed. The time of stabilization was larger for cells exposed to methanol, and ethanol than for those observed for cells grown on TSB alone. Contrastingly, this parameter was lower for cells exposed to glycerol and similar to control conditions for cells exposed to isopropanol. In turn, exposure to DMF (Figure 3C; Figure 3D; Table 2), PAA and Tween 80 (Figure 3E; Figure 3F; Table 2) did not reduce cell aggregation, and consequently the velocity of aggregation was higher, coupled with a faster stabilization time. These results could indicate that during exposure to each of the latter three solvents the cell aggregates were larger and, therefore, deposited quickly at the bottom of the test tubes. During exposure to 0.25% DMSO, the cells presented a decrease in $OD_{600\ nm}$ that was only stabilized after 75 minutes, coupled with the lowest aggregation velocity observed amongst all conditions (Figure 3C; Figure 3D; Table 2). This result could indicate that the cells were either clustered in smaller aggregates or the number of cells in planktonic form was far superior to the cells in aggregates. Both hypotheses account for the slower velocity of aggregation.

All prokaryotes are known to modulate the composition of their cellular membrane as response to changes in environmental conditions to maintain its fluidity [79]. For example, increased content of saturated fatty acids in the cellular membrane decreases membrane fluidity, while increased content of unsaturated fatty acids leads to increased fluidity. Moreover, shorter fatty acyl chains and methyl branching also contribute to an increase in the fluidity of the membrane [79]. Therefore, the fatty acid composition of the

cellular membrane presented variations according to the exposure to each solvent and each cell population analysed (Figure 4).

In general, the composition varied according to the cell population in the following manner: when compared to the Bottom population, cells in the Top population presented phospholipids with the highest increased content in 18:3 ω6c, followed by the Middle population. Consequently, both populations presented phospholipids with a decreased content in 18:1 ω9c and 18:0 10-methyl. The increase in polyunsaturated fatty acids could be associated with a decrease in cell density – cells in the Top population have a lower density when compared to the cells present in the Middle population. Furthermore, the appearance of shorter saturated fatty acids such as 12:0 was noticeable in the Top and Middle populations, thus contributing to an increase in membrane fluidity. The Bottom population presented phospholipids with a decreased content in 18:3 ω6c, with the fatty acids 18:1 ω9c and 18:0 10-methyl having a larger presence in the membrane.

The fatty acids present in the phospholipids of the membrane could be grouped according to their classes: SSFAs (Saturated Straight Fatty Acids), MUFAs (Monounsaturated Fatty Acids), PUFAs (Polyunsaturated Fatty Acids), 10Me-BFA (10-Methyl Branched Fatty Acids), and SMBFAs (Saturated Mono-Branched Fatty Acids). Furthermore, the saturation degree and the unsaturation index were also determined (Figure 5). It was noticeable that the unsaturation index followed a population-dependent pattern, due to the highest value being obtained for cells at the Top (except for those exposed to DMF), followed by the unsaturation index for the Middle populations, and the lowest value for the Mix and the Bottom populations. The higher unsaturation index observed for the Top and Middle populations could be explained by the presence of phospholipids with an increased content in polyunsaturated fatty acids, which in turn may be associated to a decrease in density, resulting in a subsequent growth as light cell aggregates or planktonic cells, respectively. In turn, the saturation degree did not follow a population-dependent pattern, being different with each exposure experiment.

The biomass dry weight obtained from each cell population constituted an important parameter to evaluate the extent of cell aggregation during exposure to the different solvents (Figure 6).

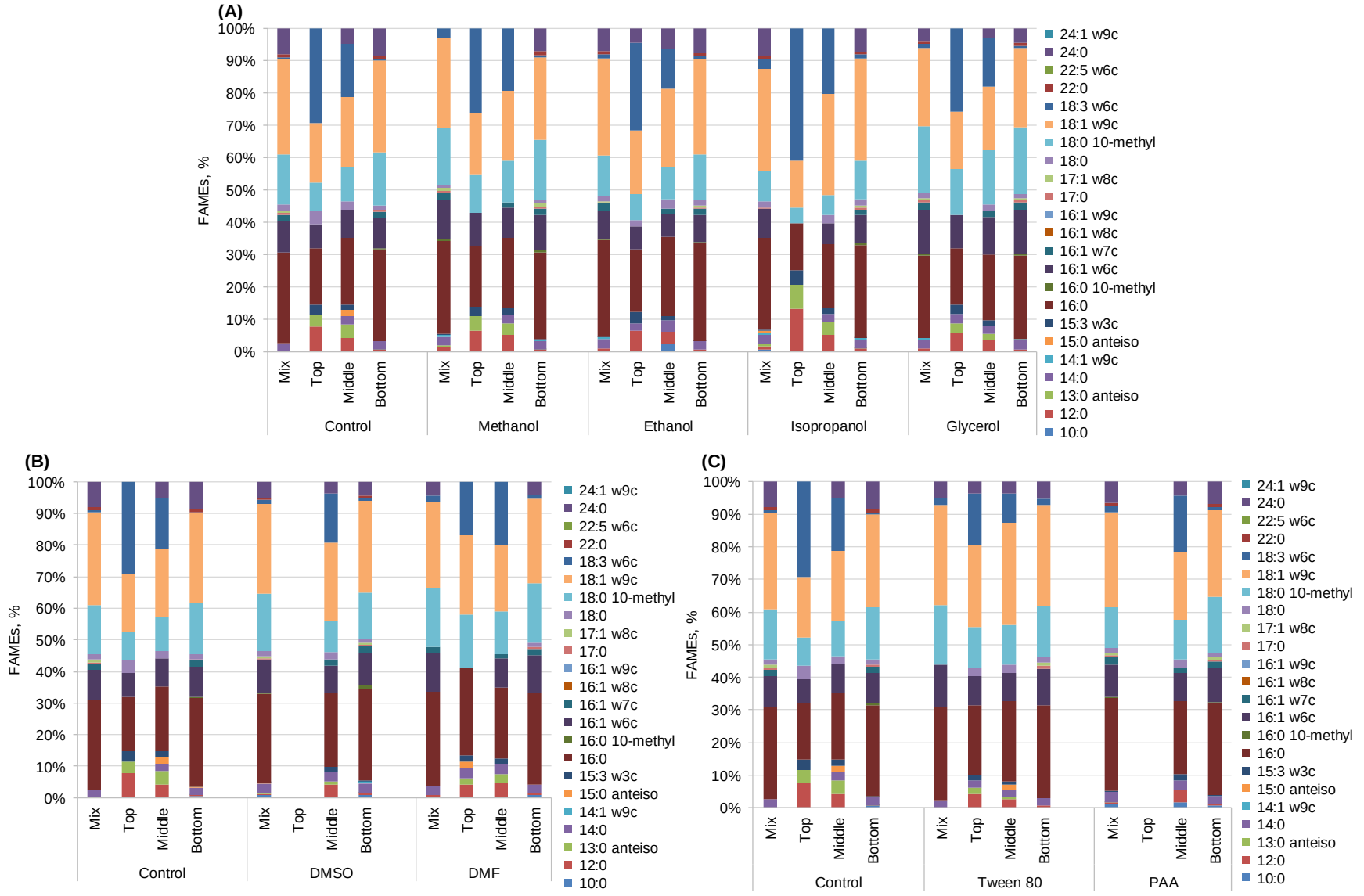

Figure 4 - Fatty acid composition of cells grown on TSB alone or exposed to 0.25% (v/v) methanol, ethanol, isopropanol, or glycerol (A); 0.25% (v/v) DMSO, or DMF (B); 0.25% (v/v) Tween 80, or PAA (C) before (Mix sample) and after the cell aggregation assay (Top, Middle, and Bottom samples).

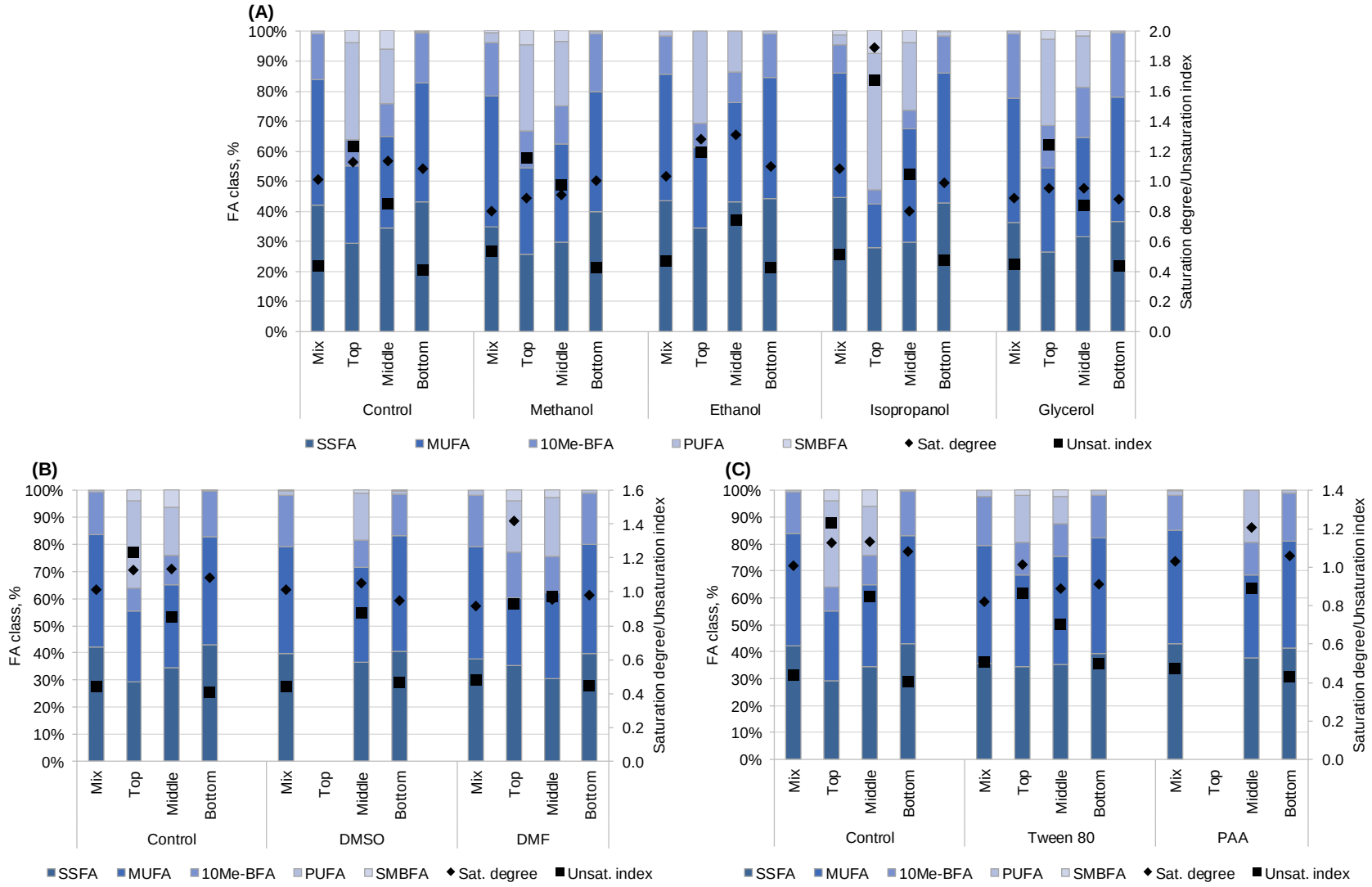

Figure 5 - Fatty acid composition and the corresponding saturation degree and unsaturation index of cells grown on TSB alone or exposed to 0.25% (v/v) methanol, ethanol, isopropanol, or glycerol (A); 0.25% (v/v) DMSO, or DMF (B); 0.25% (v/v) Tween 80, or PAA (C) before (Mix sample) and after the cell aggregation assay (Top, Middle, and Bottom samples). SSFAs – saturated straight fatty acids; MUFAs – monounsaturated fatty acids; 10Me-BFAs – 10-methyl branched fatty acids; PUFAs – polyunsaturated fatty acids; SMBFAs – saturated mono-branched fatty acids; Sat. degree – saturation degree; Unsat. Index – unsaturation index.

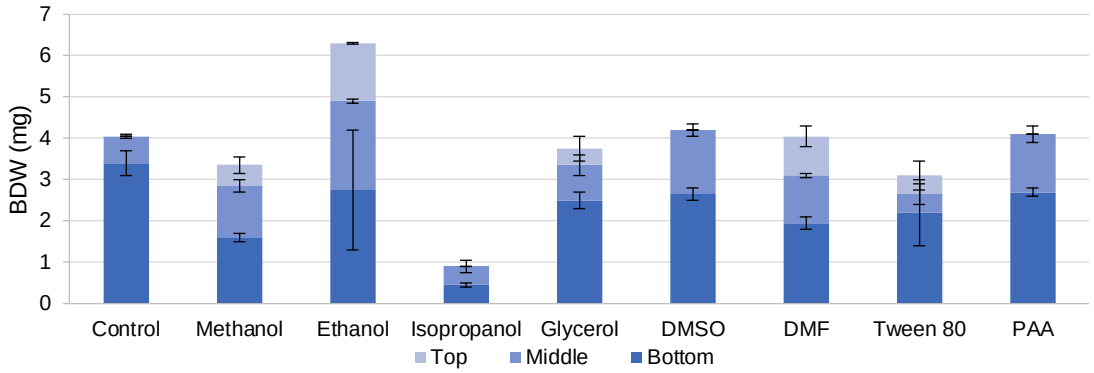

Figure 6 - Biomass dry weight (BDW) of deposited cells (Bottom), in suspension (Middle) and of light aggregates (Top) grown on TSB alone (Control) or exposed to 0.25% (v/v) methanol, ethanol, isopropanol, glycerol, DMSO, DMF, Tween 80, or PAA.

Exposure to methanol, ethanol, or DMSO returned the lowest aggregation velocities, coupled with a longer period up to stabilization (Figure 3B; Figure 3D; Table 2). Therefore, the fatty acid composition of the membrane of cells exposed to these solvents will be further analysed.

Regarding the control conditions, after 24 hours of growth on TSB, the cellular membrane was mainly composed of 16:0, 16:1 ω6c, 18:0 10-methyl, 18:1 ω9c, and 24:0 fatty acids (Figure 4). Therefore, *M. smegmatis* cells grown on TSB alone for 24 h contained a cellular membrane mainly composed of SSFAs (42%) and MUFAs (41%), with a smaller percentage of 10Me-BFA (15.5%) (Figure 5). The composition of the cellular membrane in PUFAs was residual, accounting for only 0.75% of the lipids. However, the three populations obtained after the aggregation assay had distinct patterns of lipids. Namely, the Top population was mainly characterized by the prevalence of PUFAs (32%), followed by SSFAs (29%), MUFAs (26%), and 10Me-BFAs (8.7%), with the appearance of 3.8% of SMBFAs. In the Middle population, the fatty acids in the form of SSFAs constituted most of the cellular membrane (34.5%), followed by MUFAs (30.6%). Furthermore, PUFAs comprised 18% of the membrane, while 10Me-BFAs and SMBFAs corresponded to 10.8% and 6%, respectively. Lastly, the Bottom population had a lipid profile similar to the Mix population. By analysing the biomass dry weight for the control condition, it was noticeable that Bottom cells made up 84% of the culture (Figure 6). Therefore, it was expected that the Mix and Bottom populations presented similar fatty acid profiles.

After a 24-hour exposure to methanol, the cells presented a membrane mainly composed by MUFAs, with 43.5% of the fatty acids belonging to this class, followed by 34.6% of SSFAs (Figure 5A). This was mainly achieved through the increase in the 16:1 ω6c content by 2.3% and the disappearance of 24:0 (Figure 4A). After the cell aggregation assay, the cell populations were distinguished, with differences being observed in each population. In the Top population, cells presented phospholipids with an increased content in 10Me-BFAs of 3.3% and of 3.0% in MUFAs, and a decreased content in PUFAs of 3.4% and of 3.6% in SSFAs, which could be mainly attributed to the decrease of 3.0% in 18:3 ω6c, the increase of 3.3% in 18:0 10-methyl and of 2.6% in 16:1 ω6c, and the disappearance of 18:0. Cells in the Middle population adapted

their membrane by increasing the content in PUFAs by 3.4%, in MUFAs by 2.0%, and in 10Me-BFAs by 2.0% while decreasing the composition in SSFAs by 4.9% and in SBMFAs by 2.6%, when compared to the Middle population in control conditions. These rearrangements suggest that the planktonic cells increased their membrane fluidity in response to methanol through the increase in 18:3 ω6c by 3.1% and 18:0 10-methyl by 2.1%, the production of 16:1 ω7c, with 24:0 and 15:0 anteiso no longer being produced. The Bottom population presented a cellular membrane with a decreased content in SSFAs by 3.0%, and a consequent increase in 10Me-BFAs of 2.6%, mainly due to the decrease of 24:0 and 16:0 fatty acids, and the increase of 18:0 10-methyl, respectively, when compared to the Bottom population in control conditions. Altogether, and comparing with the cell populations in control conditions, these results show that *M. smegmatis* produced alterations at the membrane level when exposed to methanol that were characterized by an increase in membrane fluidity for all cell populations analysed. This can be further shown by the saturation degree of the cellular membrane of the Mix, Top, Middle, and Bottom populations, which decreased 1.27-, 1.27-, 1.24-, and 1.07-fold, for respectively, when compared to the corresponding cell populations in control conditions.

The exposure of Mix population cells to 0.25% ethanol for 24 h also reduced the velocity of aggregation, with changes being observed in the fatty acid composition of the cellular membrane (Figure 4A; Figure 5A). Similar to what was observed in control conditions, the Mix population presented a cellular membrane mainly composed of SSFAs, with its percentage being further increased by 1.4% during ethanol exposure, due to the increase in the 16:0 fatty acid. Such increase was coupled with the decrease of 2.5% in 10Me-BFAs, attributed to the decrease in 18:0 10-methyl by 2.9%. In turn, the Top population was characterized by an increase in SSFAs of 5.1% and a decrease in PUFAs of 1.6%, when compared to the Top population in control conditions, with the cease in production of SMBFAs, which resulted from the production of 14:0, the increase of 1.9% in 16:0, the decrease in 18:3 ω6c by 2.0%, and the disappearance of 13:0 anteiso. When compared to the Middle population in control conditions, the Middle population of cells exposed to ethanol did not produce any SMBFAs, with SSFAs and MUFAs increasing by 8.6%, and 2.4%, respectively, due to the increase in 16:0, 24:0, and 18:1 ω9c, with a concomitant decrease in PUFAs by 4.3% attributed to a decrease in 18:3 ω6c. Similar to the Mix population, the Bottom cell population also presented an increase in SSFAs by 1.2% and a decrease in 10Me-BFAs of 1.9%, thanks to the increase in the 16:0 fatty acid and a decrease in the 18:1 ω9c fatty acid, when compared to the Bottom population in control conditions. As opposed to what was observed in cells exposed to methanol, cells exposed to ethanol presented an increase in saturation degree in all the cell populations, when compared to the cell populations in control conditions. Namely, the Mix, Top, Middle, and Bottom populations presented a saturation degree increased by 1.03-, 1.13-, 1.16-, and 1.02-fold, respectively.

During exposure to DMSO the membrane of cells in the Mix population presented a decrease in SSFAs and MUFAs by 2.0%, and 2.3%, respectively, with a consequent increase by 3.4% in 10Me-BFAs, when compared to the Mix population in control conditions (Figure 5B). This was mainly achieved through the decrease in 24:0, 18:1 ω9c, and the increase in 18:0 10-methyl (Figure 4B). Surprisingly, no cell aggregates

at the air-liquid interface were formed during exposure to DMSO. Furthermore, when compared to the Middle population in control conditions, the Middle population of cells exposed to DMSO suffered a decrease of 5.1% in SMBFAs, due to the decrease in 13:0 anteiso, as well as an increase in MUFAs and SSFAs of 4.4% and 2.1%, respectively, possibly due to the increase in 18:1 ω9c, and 16:0, and the appearance of 16:1 ω7c. The Bottom population was characterized by an increase of 2.7% in MUFAs, with a consequent decrease of 2.8% in the content of SSFAs and 1.5% in 10Me-BFAs, when compared to the Bottom population in control conditions. Such composition could be mainly due to the decrease in 24:0 and 18:0 10-methyl. Therefore, the saturation degree remained constant in the Mix population, while decreasing by 1.08- and 1.14-fold in the Middle and Bottom populations, respectively, when compared to the respective populations in control conditions.

Despite the exposure to either methanol, ethanol, or DMSO, the Mix population continued to present a fatty acid composition of the phospholipids of the cellular membrane similar to the cells at the Bottom population. In fact, cells from the Bottom population continued to have the highest percentage of biomass dry weight (Figure 6). Therefore, it was expected that the cellular membrane of both Bottom and Mix populations presented similar fatty acid compositions. In particular, the percentage biomass dry weight of cells at the Bottom population was the highest for cells in control conditions (84.0%) and lowest for cells exposed to ethanol (43.6%). However, it is also important to mention that the cells in the latter condition formed light cell aggregates, which accounted for 22.2% of the biomass dry weight. Also, the error bar is significant, which could be due to the distribution of sizes of aggregates. The percentage of cells in suspension was the highest for the culture exposed to methanol, followed by exposure to DMSO, with 37.3% and 36.9% of the cells being in planktonic state, respectively. Exposure to ethanol led to 34.1% of cells being in the Middle population, compared to the 16% obtained under control conditions. Therefore, the decrease in cell aggregation during exposure to either methanol, ethanol or DMSO can also be verified by the increase of the percentage of cells in suspension.

The zeta potential of cells from the different populations was also measured (Figure 7).

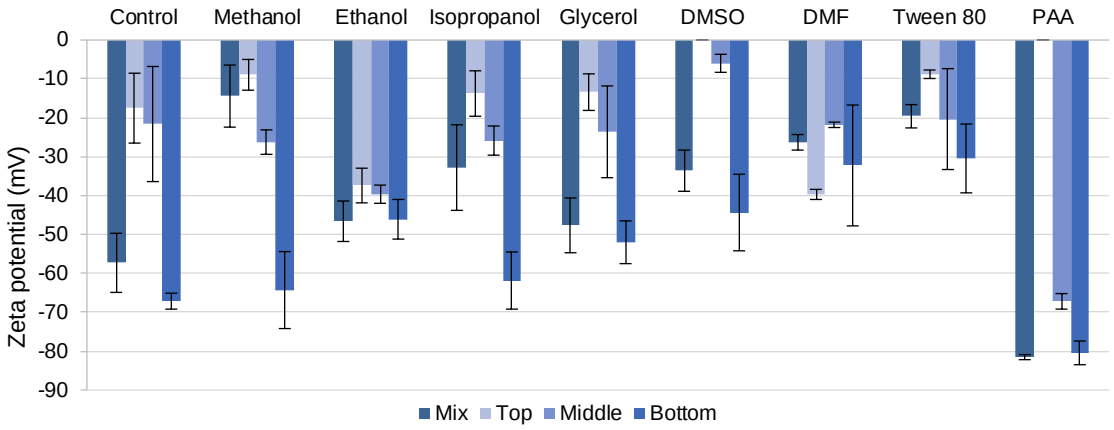

Figure 7 – Zeta potential of deposited cells (Bottom), in suspension (Middle) and of light aggregates (Top) grown on TSB alone (Control) or exposed to 0.25% (v/v) methanol, ethanol, isopropanol, glycerol, DMSO, DMF, Tween 80, or PAA.

The zeta potential is regarded as the potential of the interface that separates the aqueous media and the fluid that is stationary and attached to the surface of a given particle [91]. In this case, the particle is the bacterial cell, and the zeta potential is determined by its electrophoretic mobility. Bacterial cells usually exhibit a negative zeta potential at physiological pH [91]. Also, the higher the zeta potential value, the higher the stability of the cellular dispersion [92].

Nonetheless, *M. smegmatis* exhibited a different behaviour (Figure 7). Cells from the Bottom population normally presented the highest zeta potential value, while cells from the Top population presented the lowest value, followed by Middle population cells. An exception occurred with cells exposed to DMF, with cells at the Top presenting the highest value among the three populations. Among the three solvents that rendered the best results in terms of cell aggregation, the zeta potential was higher for cells at the Bottom population exposed to methanol (-64.3 mV), followed by ethanol (-46.1 mV), and DMSO (-44.4 mV). The Middle population presented the lowest value during exposure to DMSO (-6.0 mV), followed by methanol (-26.3 mV), and ethanol (-39.6 mV). In turn, the zeta potential of the Top population was lower for cells exposed to methanol (-8.9 mV) and highest for ethanol exposure (-37.4 mV). Lastly, the zeta potential for the Mix population was higher for ethanol exposure (-46.6 mV), followed by DMSO (-33.6 mV), and methanol (-14.4 mV). Given that the zeta potential values for each solvent were so different, no conclusions could be drawn regarding the contribution of this parameter to the growth as cell aggregates and/or planktonic cells.

3.1.1. Effect of DMSO concentration on aggregation

Among all the solvents tested, DMSO was the one that rendered the best results for the reduction of cell aggregation. Firstly, the aggregation velocity was drastically reduced, with cells only stabilizing in terms of $OD_{600\ nm}$ after a much longer period (75 minutes), when compared to control conditions (49 minutes). Secondly, no light cell aggregates appeared at the top of the test tube, which constituted a further decrease in cell aggregation. Therefore, it was also important to study the effect of the concentration of DMSO, with concentrations of 0.50% and 1% (v/v) DMSO being tested. As previously done, after 24 hours a cell

aggregation assay was performed (Figure 8), and the aggregation velocities and stabilization times were also determined (Table 3).

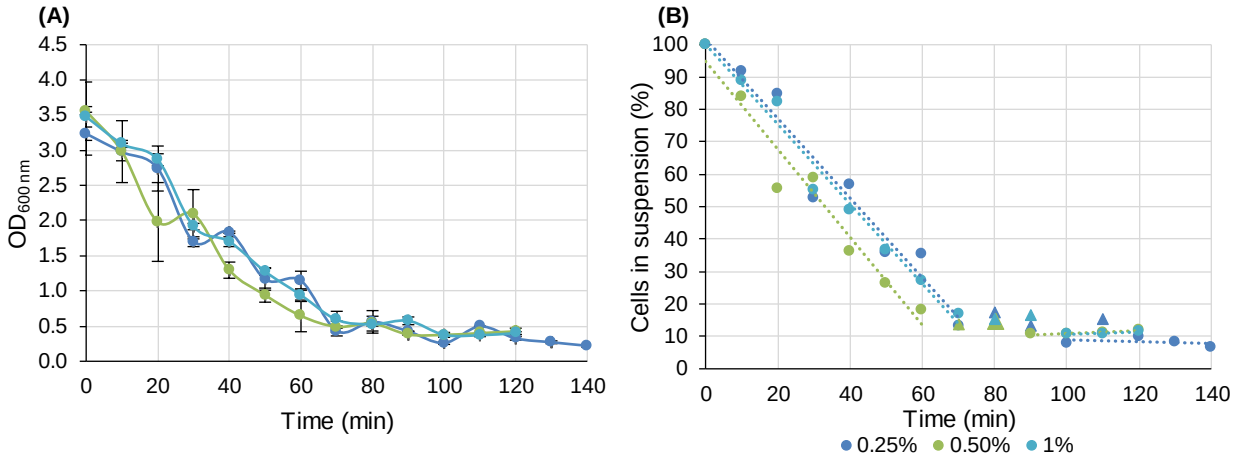

Figure 8 – Optical density ($OD_{600\ nm}$) (A) and percentage of cells in suspension (B) over time of cells exposed for 24 hours to 0.25%, 0.50%, or 1% (v/v) of DMSO. Values considered for the velocity of aggregation and time of stabilization (closed dots); outliers (closed triangles); linear regression (dotted lines).

Table 3 - Parameters obtained in the linear equations for the period of sedimentation of aggregates and stabilization for the different DMSO concentrations tested.

	Aggregation equation parameters		Stabilization equation parameters		Stabilization time (min)
	m (% cells in suspension/min)	b (% cells in suspension)	m (% cells in suspension/min)	b (% cells in suspension)	
0.25%	-1.2282	101.8	-0.0278	11.7	75.06
0.50%	-1.3557	94.9	0.0450	6.4	67.50
1%	-1.2309	100.1	0.0360	7.0	77.89

The cells exposed to increasing concentrations of DMSO presented similar extent of cell aggregation, and so the aggregation velocity did not reduce substantially (Figure 8A, Table 3). Furthermore, no relation could be established between the increase in DMSO concentration and the decrease in aggregation velocity and consequently, the size of aggregates. This indicates that DMSO did not act in a concentration-dependent manner for concentrations up to 1% (v/v).

The fatty acid composition of the phospholipids of the cellular membrane of cells exposed to the different concentrations of DMSO was also assessed, and several alterations were noticed (Figure 9; Figure 10). During exposure to either 0.25%, 0.50%, or 1% DMSO, the Mix population was mainly comprised of SSFAs and MUFAs, followed by 10Me-BFAs (Figure 10). Namely, the Mix population of cells exposed to 0.25% presented a cellular membrane composed by 39.7% of SSFAs, 39.2% of MUFAs, and 18.3% of 10Me-BFAs, while cells exposed to 0.50% DMSO presented a Mix population with a cellular membrane composed by 42.7%, 42.6%, and 18.7% of SSFAs, MUFAs, and 10Me-BFAs, respectively. The Mix population of cells exposed to 1% DMSO presented a cell membrane with 40.7% of SSFAs, 40.4% of MUFAs, and 16.7% of

10Me-BFAs. Therefore, cells of the Mix population responded to the increase in DMSO concentration by increasing the cellular membrane content in SSFAs and in MUFAs. However, the increased content in SSFAs and MUFAs in the cellular membrane was more accentuated during exposure to 0.5% DMSO, with cells exposed to 1% DMSO also presenting a Mix population with a decreased content in 10Me-BFAs, when compared to the Mix population of cells exposed to 0.25% DMSO. Altogether, these alterations could be mainly attributed to the increase in 16:0, 16:1 ω6c, 18:1 ω9c, and to the decrease in 18:0 10-methyl, respectively, when compared to the Mix population of cells exposed to 0.25% DMSO (Figure 9). The Middle population presented more variations in the fatty acid composition of the phospholipids of the cellular membrane, when compared to the Mix and Bottom populations. Even though SSFAs and MUFAs maintained their high prevalence, the membrane of the cells in suspension presented a higher percentage of PUFAs than of 10Me-BFAs. When compared with the Middle population of cells exposed to 0.25% DMSO, the content of the cellular membrane in polyunsaturated fatty acids comprised 18.3% and 26.5% of the membrane of cells exposed to 0.50% or 1% DMSO, respectively, due to an increase in 18:3 ω6c and a concomitant decrease in 18:1 ω9c. It is important to mention that the Mix and Bottom populations presented similarities in terms of the fatty acid composition of the phospholipids of the cellular membrane, which could be associated with the elevated percentage of biomass dry weight belonging to cell aggregates (Figure 11A). The main difference between the Bottom and Mix populations of cells exposed to 0.25% or 1% DMSO was a small increase in the content in MUFAs of 3.0% and 0.82%, respectively, and a decreased content in MUFAs by 1.4% during exposure to 0.50% DMSO. Moreover, when compared to the Mix population of cells exposed to 0.25% DMSO, the cellular membrane of the Mix population of cells exposed to 0.50% or 1% DMSO did not present alterations in the saturation degree. The cellular membrane of the Bottom population exposed to 0.50% or 1% DMSO presented a saturation degree 1.03-fold higher than the one observed in the corresponding population in control conditions. However, the contrary was observed for the Middle population. When compared to the Middle population of cells exposed to 0.25% DMSO, the cells of the Middle population exposed to 1% DMSO presented a 1.04-fold decrease in the saturation degree, being further decreased when exposed to 0.5% DMSO (1.12-fold).

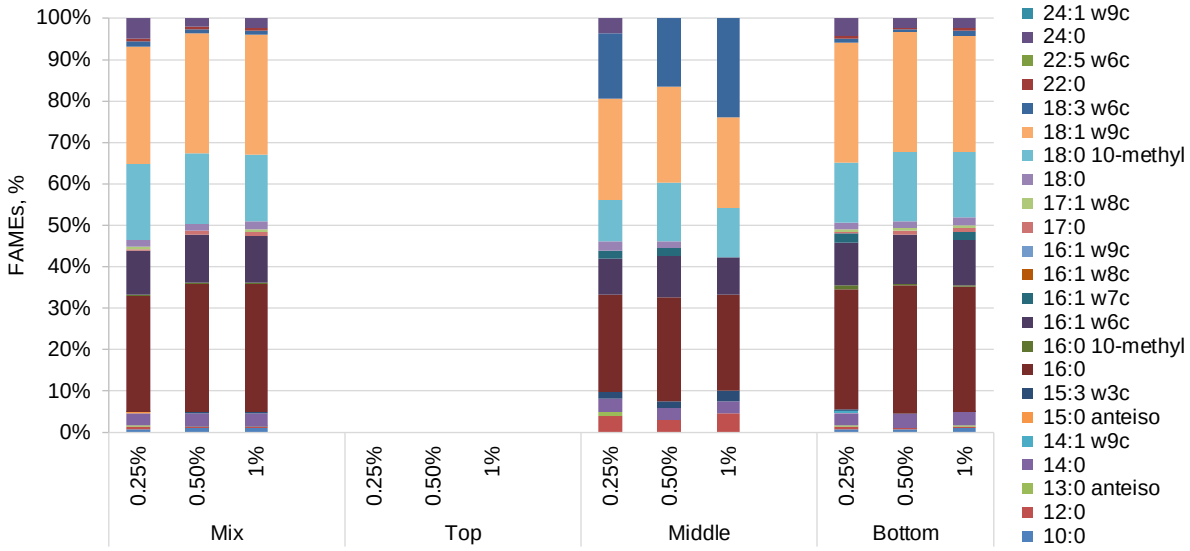

Figure 9 - Fatty acid composition of cells exposed to 0.25%, 0,50%, or 1% (v/v) DMSO before (Mix sample) and after the cell aggregation assay (Top, Middle, and Bottom samples).

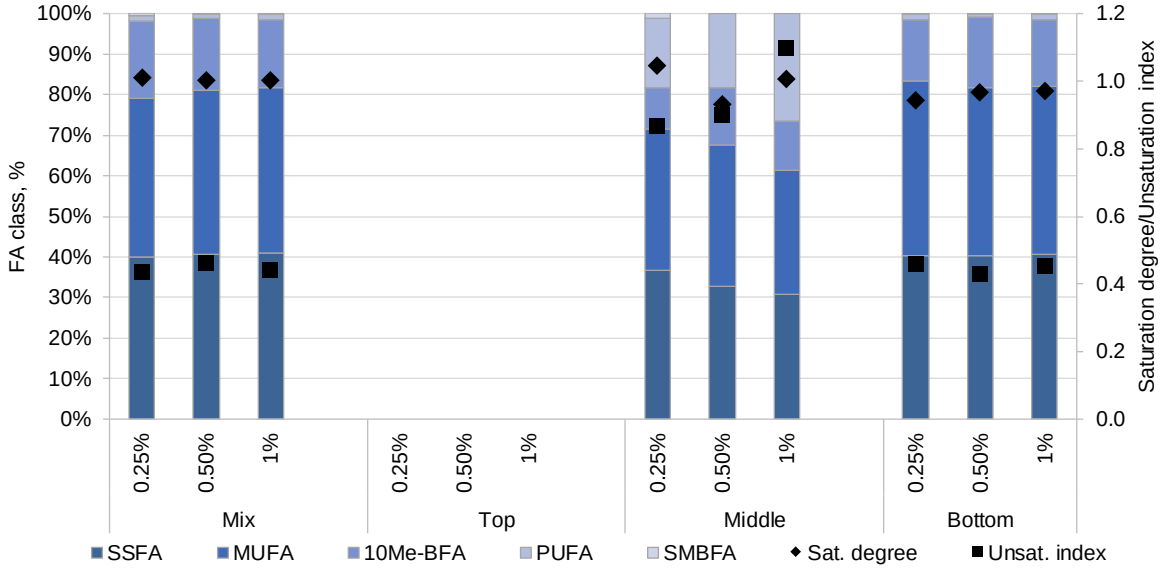

Figure 10 - Fatty acid composition and the corresponding saturation degree and unsaturation index of cells exposed to 0.25%, 0.50%, or 1% (v/v) DMSO before (Mix sample) and after the cell aggregation assay (Top, Middle, and Bottom samples).

In addition to the fatty acid composition of the phospholipids of the cellular membrane, the biomass dry weight and the zeta potential were also assessed (Figure 11).

Regarding the biomass dry weight, and even though there appears to be differences between the conditions, such cannot be stated due to the error bars (Figure 11A). However, what is common is the high prevalence of cells belonging to the Bottom population in the biomass dry weight, corroborating the similar fatty acid composition of the phospholipids of the cellular membrane observed between the cells from the Mix and the Bottom populations. In the zeta potential values, especially for the Middle population, it was

noticeable that its value increased from -5.98 mV to -12.25 mV during exposure to 0.50% DMSO (Figure 11B). During exposure to 1% DMSO, its value increased up to -11.82 mV.

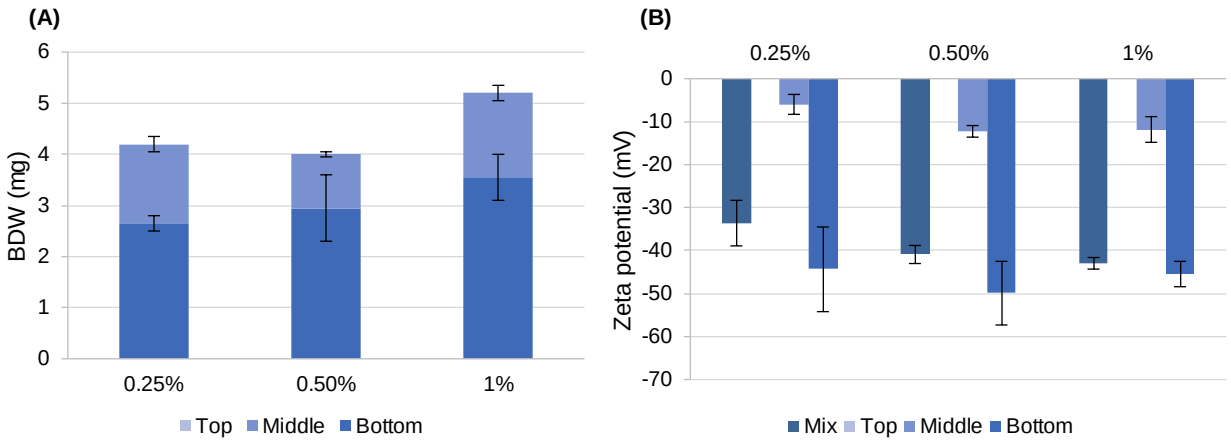

Figure 11 - Biomass dry weight (BDW) (A) and zeta potential (B) of deposited cells (Bottom), in suspension (Middle) and of light aggregates (Top) of cells exposed to 0.25%, 0.50%, or 1% DMSO.

3.2. Temperature effect on aggregation

3.2.1. Growth temperature

In section 3.1 it was observed that the cellular membrane of cells exposed to each solvent presented an increased unsaturation index in the Middle population, when compared to the Bottom population. Besides the exposure to solvents to reduce or even prevent aggregation, the temperature at which the growth occurs may also play an important role. A common adaptation of prokaryotes to temperature decrease is the increase in membrane fluidity [79]. Such mechanism could be achieved through the incorporation of unsaturated fatty acids in the cellular membrane. Moreover, as the exposure to DMSO rendered a decrease in the velocity of aggregation and a longer stabilization period, its effect coupled with the increase and/or decrease in temperature could produce a lesser cell aggregation extent. To assess the effect of growth temperature coupled with the exposure to DMSO on the size and quantity of cell aggregates, *M. smegmatis* cells were grown either on TSB alone or exposed to 0.25% (v/v) DMSO, at room temperature, 30°C, or 37°C, for 24 h. Afterwards, a cell aggregation assay was performed, and the aggregation velocity and time of stabilization were assessed (Figure 12; Table 4).

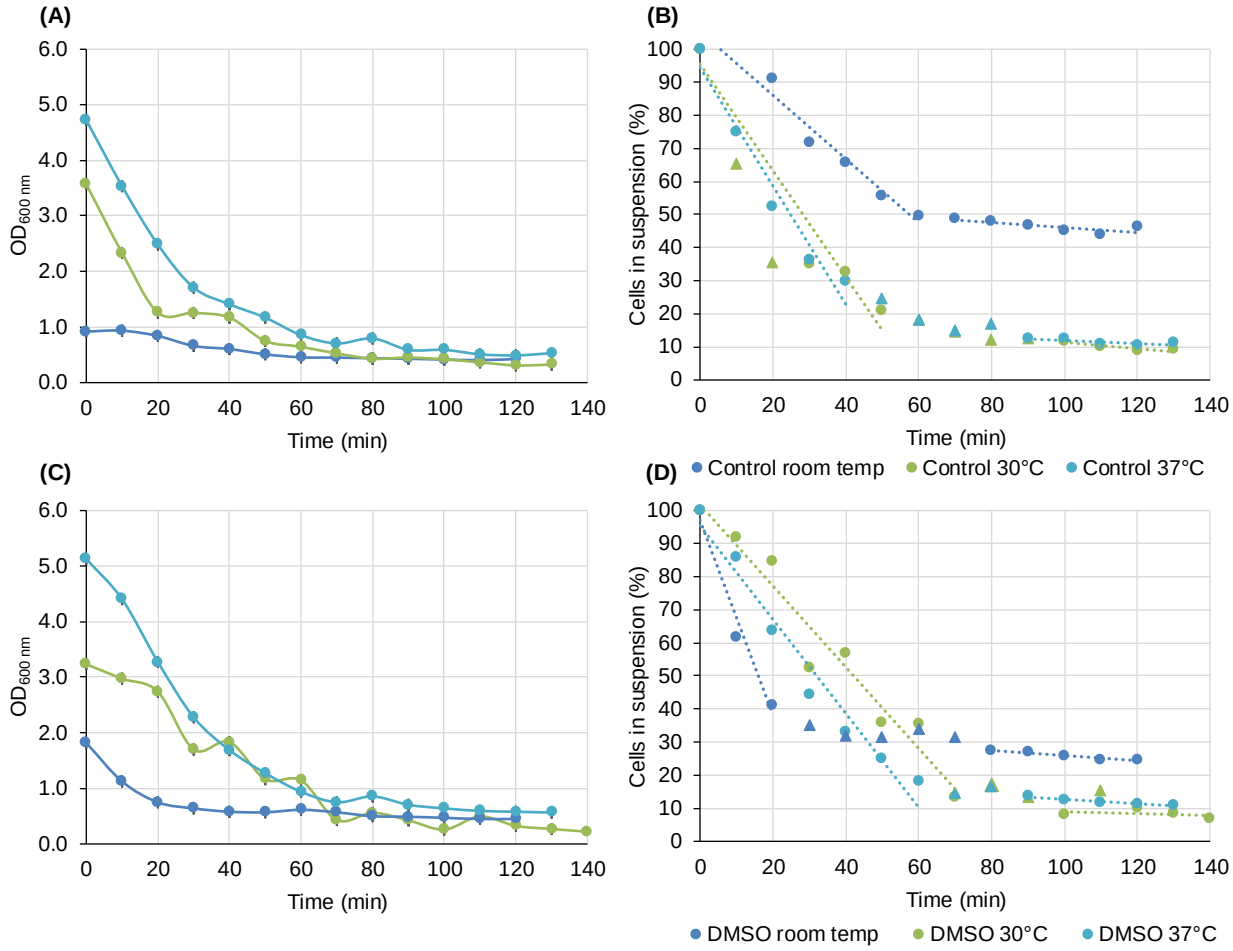

Figure 12 – Optical density ($OD_{600\ nm}$) (A) and percentage of cells in suspension (B) over time of cells grown on TSB alone or exposed for 24 hours to 0.25% (v/v) DMSO, at room temperature 30°C, or 37°C. Values considered for the velocity of aggregation and time of stabilization (closed dots); outliers (closed triangles); linear regression (dotted lines).

Table 4 - Parameters obtained in the linear equations for the period of sedimentation of cell aggregates and stabilization for the temperatures tested.

	T (°C)	Aggregation equation parameters		Stabilization equation parameters		Stabilization time (min)
		m (% cells in suspension/min)	b (% cells in suspension)	m (% cells in suspension/min)	b (% cells in suspension)	
Control	**Room T**	-0.9627	105.4	-0.0761	53.7	58.27
	30	-1.6086	95.5	-0.0952	20.9	49.29
	37	-1.7894	94.5	-0.0466	16.6	44.69
0.25% DMSO	**Room T**	-2.9396	97.1	-0.0769	33.6	22.16
	30	-1.2282	101.8	-0.0278	11.7	75.06
	37	-1.4213	95.5	-0.0663	19.3	56.25

For both the control condition and the DMSO exposure, it was observed that the $OD_{600\ nm}$ value obtained after 24 h was larger in a temperature-dependent manner, being, therefore, the lowest for cells grown at room temperature and the highest for growth at 37°C (Figure 12A). These results could have meant that the

number of planktonic cells was increasing with the increase in temperature, independently of the culture media conditions. However, by observing the slopes for each condition and its corresponding velocity of aggregation, the latter did not decrease with the increase in temperature (Figure 12B; Figure 12D; Table 4). Therefore, the increase in $OD_{600\ nm}$ may not be related to the increase in the number of planktonic cells, and instead with a general growth increase. Moreover, in the control conditions, the higher the temperature, the higher the velocity of aggregation (Figure 12B; Table 4). This result could indicate that an increase in growth temperature, without DMSO exposure, could also promote the growth as cell aggregates. It is important to mention that the low aggregation velocity attributed to growth at room temperature could be due to the low $OD_{600\ nm}$ obtained in the beginning of the cell aggregation assay. Regarding the growth of cells exposed to DMSO, the velocity of aggregation was the highest for growth at room temperature, and lowest for cells grown at 30°C (Figure 12B; Table 4). Therefore, this could indicate that the growth temperature is important to obtain cell aggregation reduction during exposure to DMSO. Nevertheless, DMSO still exerts an effect at 37°C, with the velocity of aggregation being lower and the stabilization taking longer when compared to control conditions at the same temperature. In the case of growth at room temperature, the combination of lower temperature with DMSO might have enhanced the growth of *M. smegmatis* in the form of cell aggregates, with large cell clusters being visible to the naked eye (data not shown).

The fatty acid composition of the phospholipids of the cellular membrane for each cell population after the completion of the cell aggregation assay was analysed, with differences being noticed between temperatures and between the absence or presence of DMSO (Figure 13; Figure 14). Additionally, the biomass dry weight and the zeta potential were also assessed (Figure 15).

As a response to the temperature increase to 30°C or 37°C, all cell populations with or without exposure to DMSO presented an increase in the content of the 18:0 10-methyl and 16:0 fatty acids in the phospholipids of the cellular membrane, with a concomitant decrease in the content of the 18:1 ω9c fatty acid, when compared to its counterparts when grown at room temperature (Figure 13). Moreover, all cell populations grown at 30°C with or without exposure to DMSO presented an increased content in the 24:0 fatty acid, when compared to the remaining temperatures. Consequently, all cell populations presented an increase in the content of the cellular membrane in SSFAs and 10Me-BFAs, and a decreased content in MUFAs and PUFAs as a response to increasing temperatures, when compared to growth at room temperature (Figure 14).

The exposure to DMSO itself also led to alterations in the fatty acids of the phospholipids of the cellular membrane. At room temperature, and in comparison to control conditions at the same temperature, Mix population cells exposed to DMSO exhibited a cellular membrane with decreased content in MUFAs by 3.0% and in PUFAs by 3.4%, with increased composition in SSFAs by 1.1% and 10Me-BFAs by 4.6%. At 30°C, the cellular membrane of the Mix population exposed to DMSO presented a cellular membrane with an increase of 3.4% in 10Me-BFAs and of 0.8% in PUFAs, coupled with a decrease in SSFAs by 2.1% and in MUFAs by 2.3%, when compared to growth at 30°C in control conditions. The Mix population of cells

exposed to DMSO at 37°C responded with minor alterations in the cellular membrane, presenting an increase in SSFAs by 0.8%, MUFAs by 0.3% and in PUFAs by 0.1%, while decreasing the 10Me-BFAs by 1.3%, when compared to control conditions at 37°C. Consequently, the saturation degree of the Mix population of cells exposed to DMSO was 1.09-fold and 1.01-fold higher at room temperature and 37°C, respectively, and maintained constant at 30°C, when compared to its control condition counterparts. Light cell aggregates were only visible for cells grown on TSB alone at 30°C and exposed to DMSO at room temperature. Regarding the Middle population of cells exposed to DMSO at room temperature, and when compared to the Middle population of cells grown at room temperature in control conditions, the cellular membrane was characterized by an increased fluidity due to an increase of 13.3% in PUFAs, with a consequent decrease in SSFAs by 14.9%, in MUFAs by 7.1%, and in 10Me-BFAs by 0.2%. Remarkably, the cellular membrane was composed of 37% of PUFAs. At 30°C, cells from the Middle population responded to the DMSO exposure by increasing the content of the cellular membrane in SSFAs by 2.1% in and MUFAs by 4.4%, while decreasing the content in 10Me-BFAs by 0.7%, PUFAs by 0.6%, and SMBFAs by 5.1%, when compared to the Middle population of cells grown at 30°C in control conditions. Furthermore, growth at 37°C with DMSO resulted in a Middle cell population with increased membrane fluidity, with the cells presenting a cellular membrane with increased content in MUFAs by 0.7% and in PUFAs by 0.9%, with a concomitant decrease in the content of SSFAs by 0.9%, when compared to the Middle population of cells grown at 37°C in control conditions. Consequently, the saturation degree of the Middle population decreased for growth at room temperature, 30°C, and 37°C by 1.34-, 1.08-, and 1.05-fold, respectively, in comparison to the Middle cell populations in the control condition counterparts. The Bottom population of cells exposed to DMSO at room temperature comprised cells with a cellular membrane with increased content in SSFAs by 0.7% and in 10Me-FAs by 2.7%, coupled with a decreased content in MUFAs by 1.5% and in PUFAs by 2.7%, compared with the Bottom population in control conditions grown at room temperature. At 30°C, the opposite occurred, with the Bottom population of cells exposed to DMSO presenting a cellular membrane with an increase in the content of MUFAs by 2.7% and PUFAs by 1.0%, with a decrease in SSFAs by 2.8% and in 10Me-BFAs by 1.5%, when compared to the corresponding Bottom population without DMSO exposure. Cells exposed to DMSO at 37°C presented a Bottom population with an increased cellular membrane content in SSFAs by 0.2% and in MUFAs by 0.4%, with a consequent decrease in 10Me-BFAs by 0.6%, in comparison to control conditions. Moreover, the saturation degree of the cellular membrane of cells in the Bottom population increased 1.05-fold for growth at room temperature, and decreased 1.15-, and 1.01-fold for growth at 30°C and 37°C, respectively, when compared to the Bottom population of cells in control conditions grown at the corresponding temperatures.

The total biomass dry weight obtained after 24 h of growth was also influenced by the different temperatures tested. For both the control and exposure to DMSO, the higher the temperature, the higher the total biomass dry weight (Figure 15A). Consequently, the biomass dry weight of cells in the Bottom population also increased with the increase in temperature, being the type of cells that comprised most of the cultures. Thus, this could be the reason why Mix and Bottom populations presented similar fatty acid

compositions of the phospholipids of the cellular membrane. Surprisingly, the percentage of cells in suspension grown at room temperature in control conditions was of 64.8%. However, this might be due to the low cell density obtained after the 24 h of growth. Regarding the alterations obtained during exposure to DMSO, the one that particularly stood out was the total biomass dry weight at 37°C, with its value being the highest amongst both conditions and growth temperatures. However, the percentage of cells in suspension remained identical to the one obtained in control conditions at 37°C, accounting for 21.7% of the biomass dry weight, compared to 22%, respectively. Moreover, exposure to DMSO at 30°C allowed for a higher percentage of cells grown in a planktonic state, with a consequent reduction in cell aggregates, as already observed in section 3.1. At room temperature, the exposure to DMSO resulted in a decrease of cells in suspension, with the appearance of a Top population.

The zeta potential of the cellular membrane also presented some differences (Figure 15B). Namely, cells exposed to DMSO at room temperature presented lower zeta potential values for all populations, which is consistent with the observation of large cell aggregates visible to the naked eye. Additionally, the same occurred at 30°C, with cells exposed to DMSO presenting zeta potential values of -33.6 mV, -5.98 mV, and -44.35 mV for the Mix, Middle and Bottom populations, respectively, contrasting with the values obtained in the control conditions of -57.3 mV, -21.6 mV, and -67.15 mV. No large alterations were observed during exposure to DMSO at 37°C in terms of zeta potential, with the cells in the Middle population presenting a similar zeta potential to the control (-57.6 mV to -56.85 mV, respectively). Also, the zeta potential in the Bottom population slightly decreased from -71.35 mV to -65.55 mV, and the Mix population suffered an increase in its zeta potential value from -63.65 mV to -72.15 mV, when compared to their control condition counterparts.

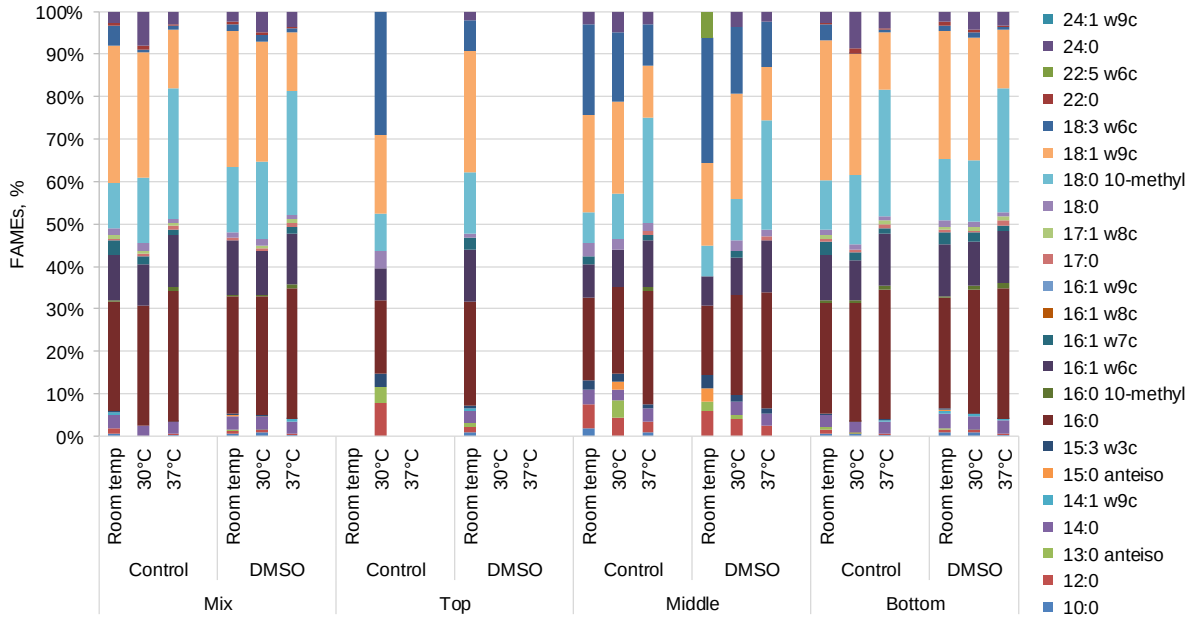

Figure 13 - Fatty acid composition of cells grown on TSB alone or exposed for 24 hours to 0.25% (v/v) DMSO, at room temperature 30°C, or 37°C before (Mix sample) and after the cell aggregation assay (Top, Middle, and Bottom samples).

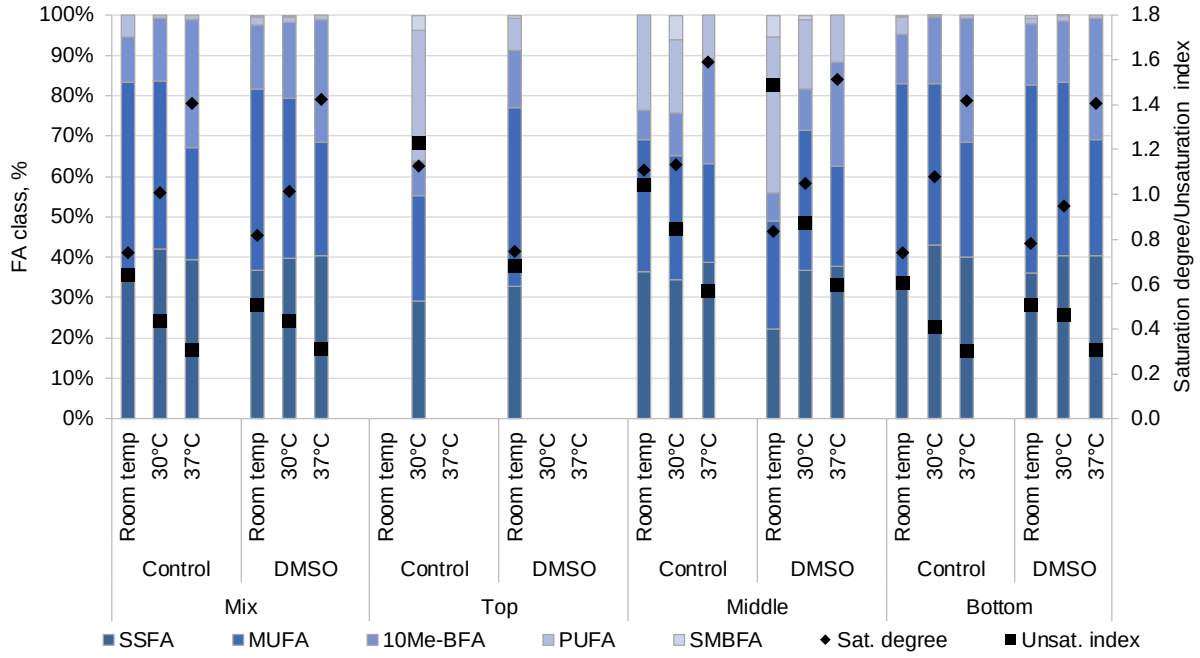

Figure 14 - Fatty acid composition and the corresponding saturation degree and unsaturation index of cells grown on TSB alone or exposed for 24 hours to 0.25% (v/v) DMSO, at room temperature 30°C, or 37°C before (Mix sample) and after the cell aggregation assay (Top, Middle, and Bottom samples).

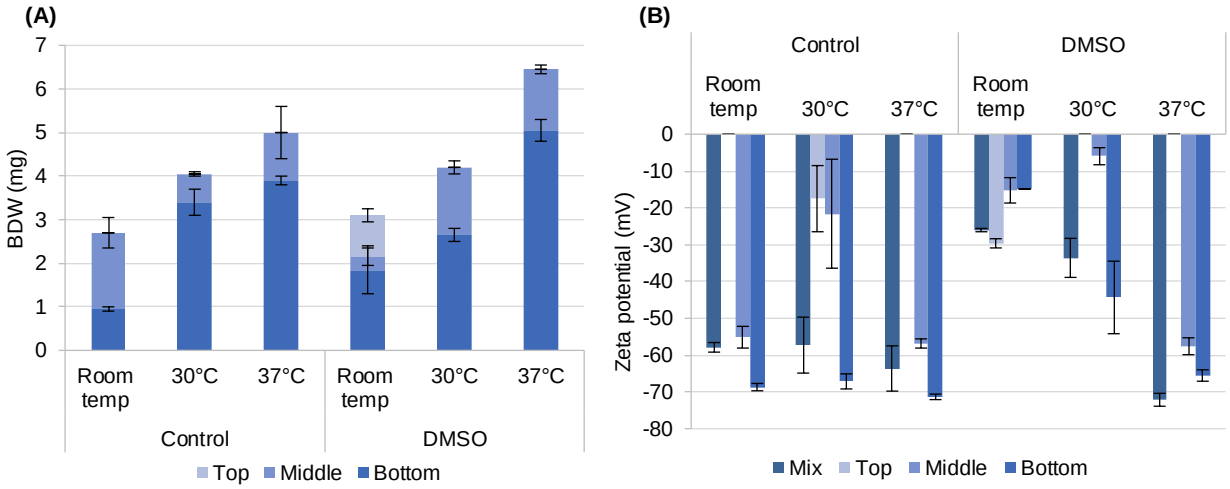

Figure 15 - Biomass dry weight (BDW) (A) and zeta potential (B) of deposited cells (Bottom), in suspension (Middle) and of light aggregates (Top) of cells grown on TSB alone or exposed for 24 hours to 0.25% (v/v) DMSO, at room temperature 30°C, or 37°C.

3.2.2. Cold shocks and oxygen deprivation

The increase in the content of unsaturated fatty acids in the phospholipids of the cellular membrane is closely related to the decrease in temperatures, given that the bacterial cells need to increase the fluidity of their membrane [79]. Also, it was noticeable from the exposure to the different solvents that the increase in

the unsaturation index was associated with the location of the different types of cell populations in the test tube – Top, Middle, or Bottom. However, a 24-hour growth at decreased temperatures was demonstrated to not reduce the velocity of aggregation. Therefore, to further study the effect of temperature decrease in the fatty acid composition of the phospholipids of the cellular membrane and in the cell aggregation extent, *M. smegmatis* was exposed to 0.25% (v/v) DMSO and subjected to cold shocks of either 5 or 15 minutes. In addition to the cold shocks, the effect of oxygen deprivation was also assessed, with the cold shocks being performed with or without agitation, with the nomenclature of TS-S and TS-NS, respectively. Moreover, two other conditions were performed, in which the culture was not stirred for either 5 or 15 min at room temperature or 30°C, NS or 30°C-NS, respectively. The control condition (30°C-S) consisted of normal growth of cells exposed to 0.25% (v/v) DMSO at 30°C without changes in temperature and/or agitation. It is important to mention that the first five shocks were applied in the first eight hours of the culture, while the remaining two shocks were applied between the 22rd and 24th hours of culture, during the exponential phase. After 24 h, a cell aggregation assay was performed (Figure 16), and the velocity of aggregation and the stabilization time were also assessed (Table 5).

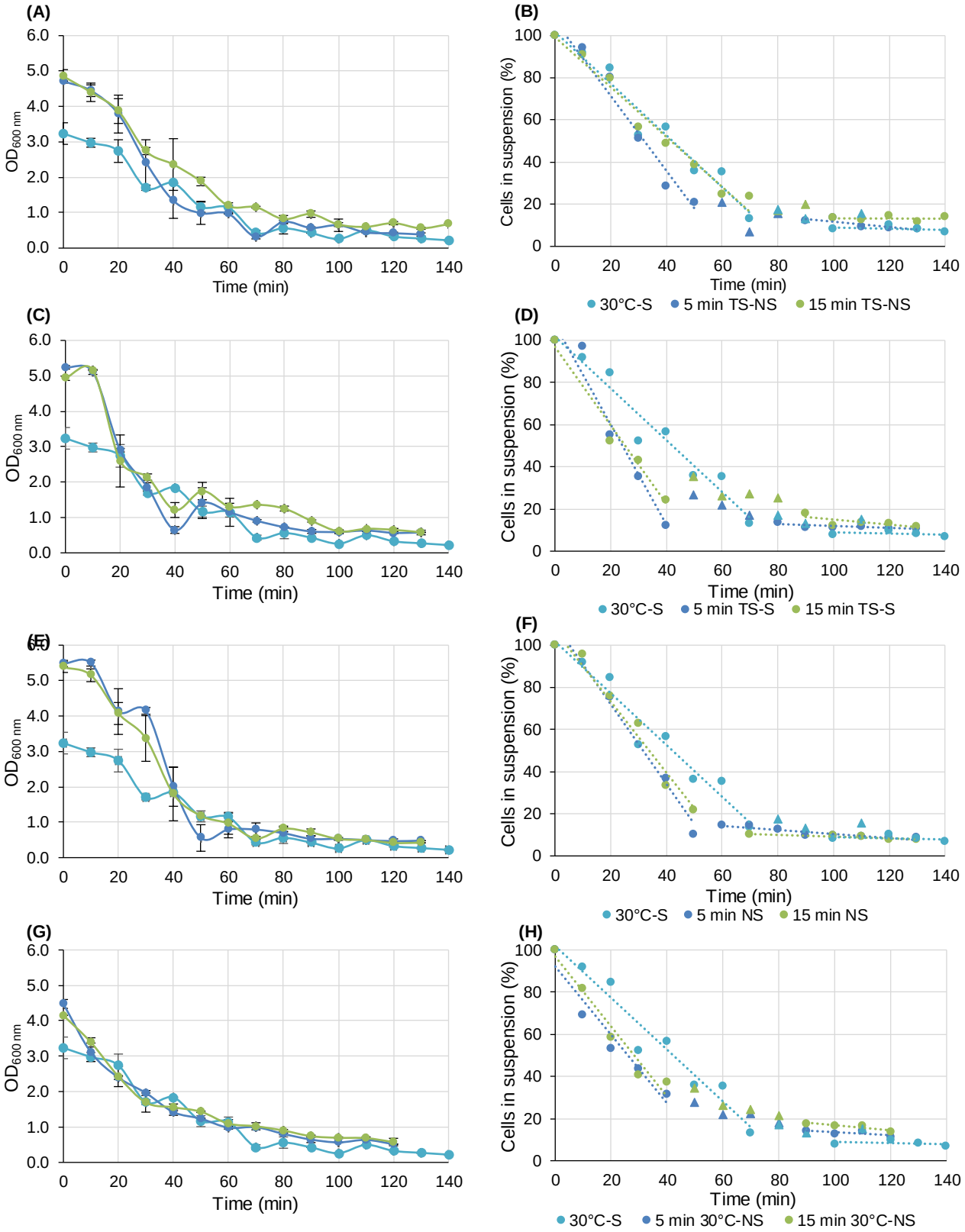

Figure 16 – Optical density ($OD_{600\ nm}$) (A, C, E, G) and percentage of cells in suspension (B, D, F, H) over time of cells exposed to 0.25% (v/v) DMSO grown at 30°C with agitation (30°C-S), or submitted to the thermal and oxygen shocks TS-NS (A, B), TS-S (C, D), NS (E, F), and 30°C-NS (G, H). Values considered for the velocity of aggregation and time of stabilization (closed dots); outliers (closed triangles); linear regression (dotted lines).

Table 5 - Parameters obtained in the linear equations for the period of sedimentation of cell aggregates and stabilization for the thermal shocks tested.

	Time	Aggregation equation parameters		Stabilization equation parameters		Stabilization time (min)
		m (% cells in suspension/min)	b (% cells in suspension)	m (% cells in suspension/min)	b (% cells in suspension)	
30°C-S	-	-1.2282	101.8	-0.0278	11.7	75.06
TS-NS	5 min	-1.7786	107.0	-0.1263	24.3	50.04
TS-S		-2.3740	107.6	-0.1174	24.8	36.68
NS		-1.8931	109.9	-0.0620	16.4	51.06
30°C-NS		-1.6223	92.2	-0.0715	20.7	46.08
TS-NS	15 min	-1.1847	99.3	-0.0041	13.7	72.51
TS-S		-1.8603	96.9	-0.1204	27.1	40.16
NS		-1.6872	107.1	-0.0414	13.3	56.97
30°C-NS		-1.6602	96.9	-0.1217	29.0	44.10

When applying the same shock to the cells, it was observed that the shock length was a relevant parameter (Figure 16; Table 5). Apart from the 30°C-NS shock, all the shocks were more effective in reducing aggregation velocity and delaying the stabilization time when applied for 15 min, rather than 5 min. Comparing the types of shocks performed, a pattern regarding the aggregation velocities was observed for the 15-min shocks. The TS-NS shock resulted in the lowest aggregation velocity (Figure 16A; Figure 16B; Table 5), followed by the 30°C-NS shock (Figure 16G; Figure 16H; Table 5), the NS shock (Figure 16E; Figure 16F; Table 5) and, lastly, the TS-S shock was the one that resulted in the highest aggregation velocity obtained (Figure 16C; Figure 16D; Table 5). However, it is important to mention that, when comparing to the control condition (30°C-S), a better aggregation velocity was only achieved once by applying the TS-NS shock for 15 min. Moreover, the longer stabilization time was also achieved with the culture that suffered the TS-NS shocks of 15 min, even though it was faster than in the control condition. Given that shocks combined with agitation returned higher aggregation velocities than cells that were only not agitated (either NS or 30°C-NS), the reduction in aggregation velocity observed in the TS-NS 15-minute shocks could thus be the result of the combination of both stresses.

Similar to the previous cell aggregation assays performed, samples from the different cell populations were taken and the fatty acid composition of the phospholipids of the cellular membrane was analysed (Figure 17; Figure 18), as well as the biomass dry weight (Figure 19A) and the zeta potential (Figure 19B).

M. smegmatis cells were able to alter their cellular membrane composition when exposed to the different shocks studied, as well as to the two shock lengths applied (Figure 17). Namely, for all the shocks, all cell populations presented a cellular membrane with an increase in the content of 18:0 10-methyl, and a consequent decrease in 18:1 ω9c, when compared to the control condition. Nevertheless, the focus will be on the 15-min TS-NS shocks given that it returned a lower aggregation velocity with a similar stabilization time when compared to the control condition.

In comparison with control conditions, the Mix population that suffered the 15-min TS-NS shocks presented a cellular membrane with an increase in the content in 10Me-BFAs by 8.4% due to the increase in the 18:0 10-methyl fatty acid, and a decrease in SSFAs by 4.2% and MUFAs by 3.9% attributed to the decrease in the 18:1 ω9c and 24:0 fatty acids (Figure 17; Figure 18). The Middle population presented a cellular membrane characterized by a decrease of 2.5% in SSFAs and of 1.9% in MUFAs, which could be mainly attributed to the decrease in the 18:1 ω9c, and 12:0 fatty acids, with the 24:0 fatty acid no longer being produced, when compared to the Middle population in control conditions. Moreover, the content of the cellular membrane of cells belonging to the Middle population in PUFAs was also reduced by 10%, due to a decrease in the 18:3 ω6c fatty acid, with 10Me-BFAs comprising 26% of the cellular membrane. When compared to the Bottom population of control conditions, the cellular membrane of the Bottom population suffering the 15-min TS-NS shocks was characterized by a decrease in SSFAs by 4.0% and in MUFAs by 9.1%, coupled with an increase in 10Me-BFAs by 14%, which may be attributed to a decrease in the 18:1 ω9c and 24:0 fatty acids, and an increase in the 18:0 10-methyl fatty acid. It is noteworthy that the Bottom population presented a similar fatty acid composition of the phospholipids of the cellular membrane to the Mix population.

The saturation degree of the cellular membrane of cells in the Mix and Middle populations exposed to the 15-min TS-NS shocks was similar to the one obtained in control conditions for the corresponding populations and increased in the Bottom population when compared to its control condition counterpart (Figure 18). Given that the saturation degree is given by the quotient between SSFAs and MUFAs, the similar values between the control condition and the Mix or Middle populations could be explained by the joint reduction of both fatty acid classes in the cellular membrane in similar percentages as a response to the different shocks studied. However, in the Bottom population, the cellular membrane presented a decreased content in MUFAs that was larger than the decrease in the content of SSFAs, and so the saturation degree increased. Therefore, cells in the Bottom population presented a saturation degree 1.15-fold higher than the one observed in the Bottom population of the control condition. Regarding the unsaturation index, its values suffered larger alterations in the cellular membrane of cells in suspension, that is, the Middle population. Namely, the unsaturation index of the cellular membrane of the Middle population was 1.60-fold higher when exposed to the 15-minute TS-NS shocks than in control conditions. Nevertheless, the unsaturation index of the cellular membrane of cells belonging to the Mix and Bottom populations that were exposed to the TS-NS shocks was 1.16- and 1.33-fold lower, respectively, than the unsaturation index of the cellular membrane of the corresponding populations in control conditions. Altogether, these results suggest that the cells suffering the 15-min T-NS shocks made little alterations in the fluidity of the cellular membrane despite the decrease in the content in unsaturated fatty acids of the cellular membrane. Nevertheless, an exception was observed for the Bottom population, in which the rigidity of the cellular membrane was increased as a response to the 15-min TS-NS shocks.

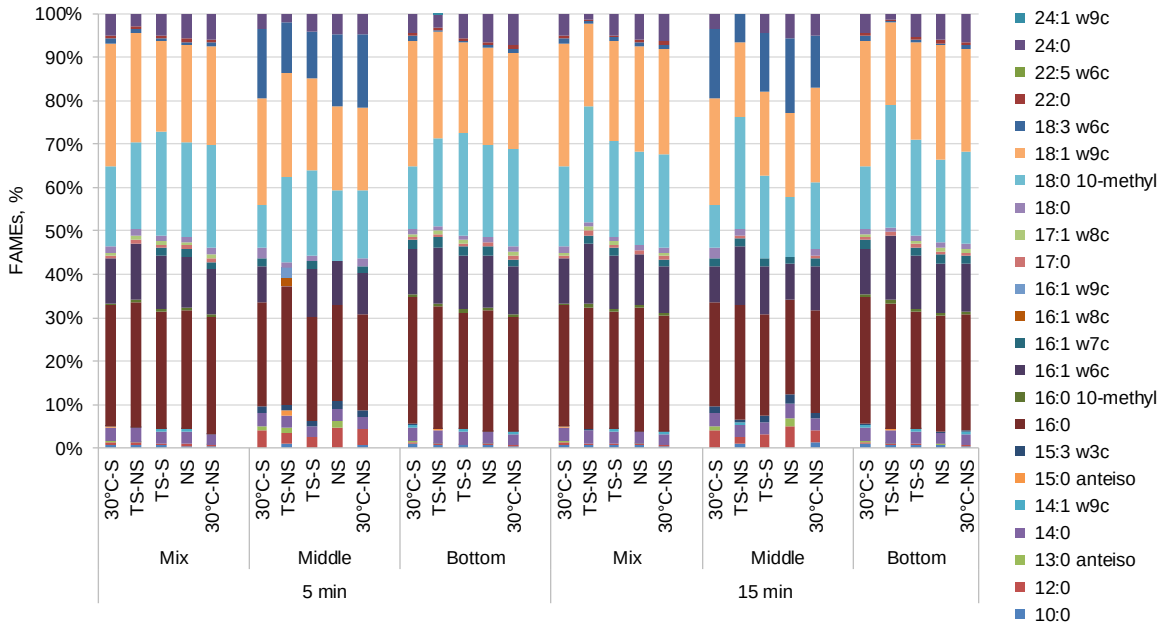

Figure 17 - Fatty acid composition of cells exposed to 0.25% (v/v) DMSO grown at 30°C with agitation (30°C-S), or submitted to the thermal and oxygen shocks (TS-NS, TS-S, NS, 30°C-NS) before (Mix sample) and after the cell aggregation assay (Top, Middle, and Bottom samples).

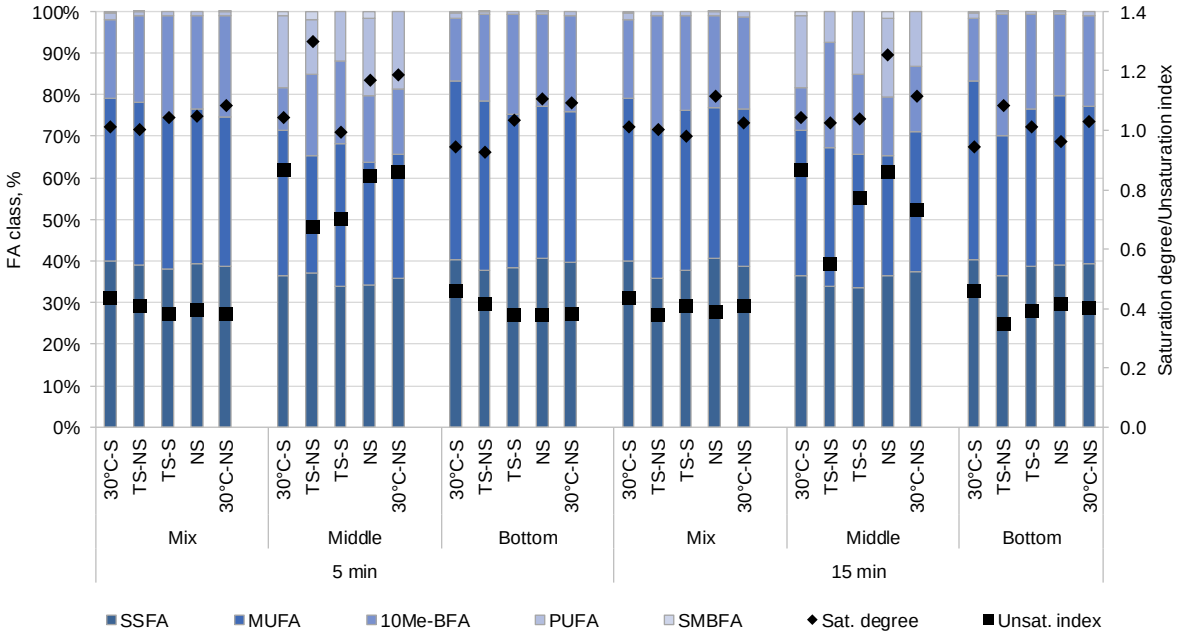

Figure 18 – Fatty acid composition and the corresponding saturation degree and unsaturation index of cells exposed to 0.25% (v/v) DMSO grown at 30°C with agitation (30°C-S), or submitted to the thermal and oxygen shocks (TS-NS, TS-S, NS, 30°C-NS) before (Mix sample) and after the cell aggregation assay (Top, Middle, and Bottom samples).

Regarding the biomass dry weight, it was noticeable that the cells that comprised the cell aggregates were in larger quantities when compared to cells in suspension (Figure 19A). Furthermore, the percentage of cells in the Middle population increased in every type of shock with the increase in shock length, except

for cells exposed to the TS-S shock. The cells in the Bottom population were reduced with the increase in shock length, except for the cells that suffered the NS shock, in which the opposite occurred. However, even though the total biomass dry weight was increased in every condition, when compared to the control condition, the percentage of cells in suspension was reduced. Namely, cells in suspension accounted for 23.2% of the biomass dry weight of cells that suffered the 15-min TS-NS shocks, which contrasts with the 36.9% of cells in suspension obtained in the control condition. Cells exposed to all the different shocks presented higher zeta potential for all populations, when compared to control conditions (Figure 19B). Particularly, the cellular membrane of cells suffering the 15-min TS-NS shocks presented an increase in zeta potential from -33.6 mV to -63.3 mV for the Mix population, from -6.0 mV to -32.5 mV for the Middle population and from -44.4 mV to -77.1 mV for the Bottom population, when compared to control conditions. Moreover, it is important to mention that cells exposed to the 15-min shocks presented a cellular membrane with decreased zeta potential when compared to its 5-min counterparts.

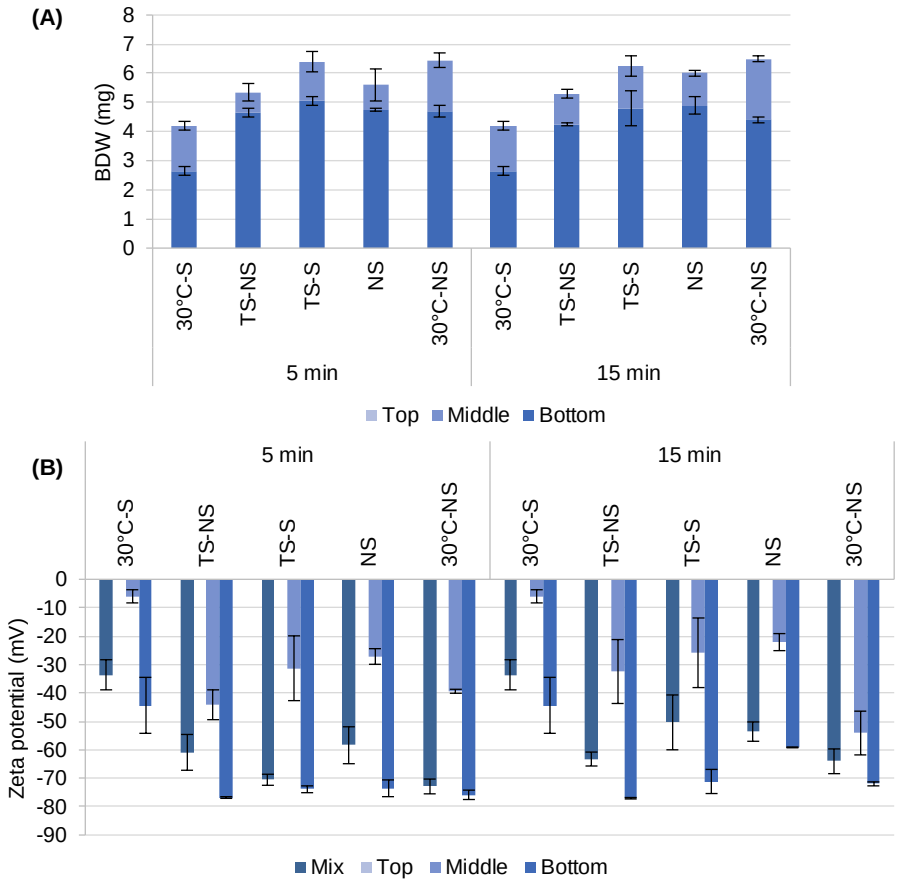

Figure 19 - Biomass dry weight (BDW) (A) and zeta potential (B) of deposited cells (Bottom), in suspension (Middle) and of light aggregates (Top) of cells exposed to 0.25% (v/v) DMSO grown at 30°C with agitation (30°C-S), or submitted to the thermal and oxygen shocks (TS-NS, TS-S, NS, 30°C-NS).

3.2.3. Adaptation to 15 min cold shocks without agitation

The TS-NS 15-min shock, in which cells exposed to 0.25% (v/v) DMSO suffered 15-min temperature shocks without agitation, was the only shock able to reduce the velocity of aggregation when compared to the culture without any stress. Therefore, it was important to understand the modifications that *M. smegmatis* employed at the cellular membrane level to adapt to the constant cold shocks as well as to the oxygen stress. To this end, the same number of shocks was applied and samples were taken before and after each shock to analyse the fatty acid composition of the phospholipids of the cellular membrane and the zeta potential. It is important to mention that the first five shocks were applied in the first eight hours of the culture, while the remaining two shocks were applied between the 22rd and 24th hours of culture, during the exponential phase. After the seven shocks were applied for 24 h, a cell aggregation assay was performed, with samples from each population being taken to analyse the fatty acid composition of the phospholipids of the cellular membrane, biomass dry weight, and zeta potential. Moreover, a control condition was also executed, in which samples were taken at the same time, and for the same purpose, but without the implementation of the 15-min TS-NS shock.

The fatty acid composition of the phospholipids of the cellular membrane during the adaptation to the 15-min TS-NS shocks, as well as the main fatty acid classes, saturation degree and unsaturation index can be consulted in Figure 20.

Cells exposed to 0.25% (v/v) DMSO without any stress applied to them altered the fatty acid composition of the phospholipids of the cellular membrane over time, and up to the fifth check-up, by decreasing the content in 10Me-BFAs and PUFAs, through the decrease in the fatty acids 18:0 10-methyl and 18:3 ω6c, and increasing the content in MUFAs, due to the increase in 18:1 ω9c (Figure 20A; Figure 20C). However, this trend was reversed at the 6th check-up, with the cellular membrane being characterized by a decreasing content in MUFAs while the content in 10Me-BFAs increased in comparison to the previous check-up. In comparison, the cells that suffered the 15-min TS-NS shocks also presented a cellular membrane with a gradually reduced content in PUFAs due to the decrease in the 18:3 ω6c fatty acid over time (Figure 20B; Figure 20D). However, the cellular membrane of cells suffering the 15-min TS-NS shocks presented a different pattern from control conditions, regarding the content in MUFas and 10Me-BFAs, mainly attributed to the fatty acids 18:1 ω9c and 18:0 10-methyl. Namely, the cellular membrane of cells suffering the 15-min TS-NS shocks presented a gradually increasing content in MUFAs and a decreasing content in 10Me-BFAs, that were up to 16.3% higher and 14.9% lower, respectively, than the observed content in the cellular membrane of cells in control conditions at the end of the assay.

The saturation degree in the control condition decreased up until the 5th check-up, being then increased at the 6th check-up and constant thereafter (Figure 20C). The unsaturation index followed the symmetric pattern of the saturation degree, suffering a slight increase between the 2nd and 3rd check-ups, followed by a decrease until the 6th and stabilization at the 7th check-up. Regarding the cells that suffered the 15-min

TS-NS shocks, its saturation degree decreased immediately as a response to the 1st shock, followed by a slight increase after the 2nd, 3rd, and 4th shocks, decreasing again from the 5th to the 7th shocks. The unsaturation index increased after the 1st and 2nd shocks, followed by a decrease after the 3rd shock and an increase at the 4th and 5th shocks, decreasing before the 6th shock, followed by a stabilization after the 7th shock. By comparing with the control condition, the saturation degree at the end of the 15-min TS-NS shocks was 1.22-fold lower and the unsaturation index was 1.19-fold higher, which corresponds to an increase in membrane fluidity.

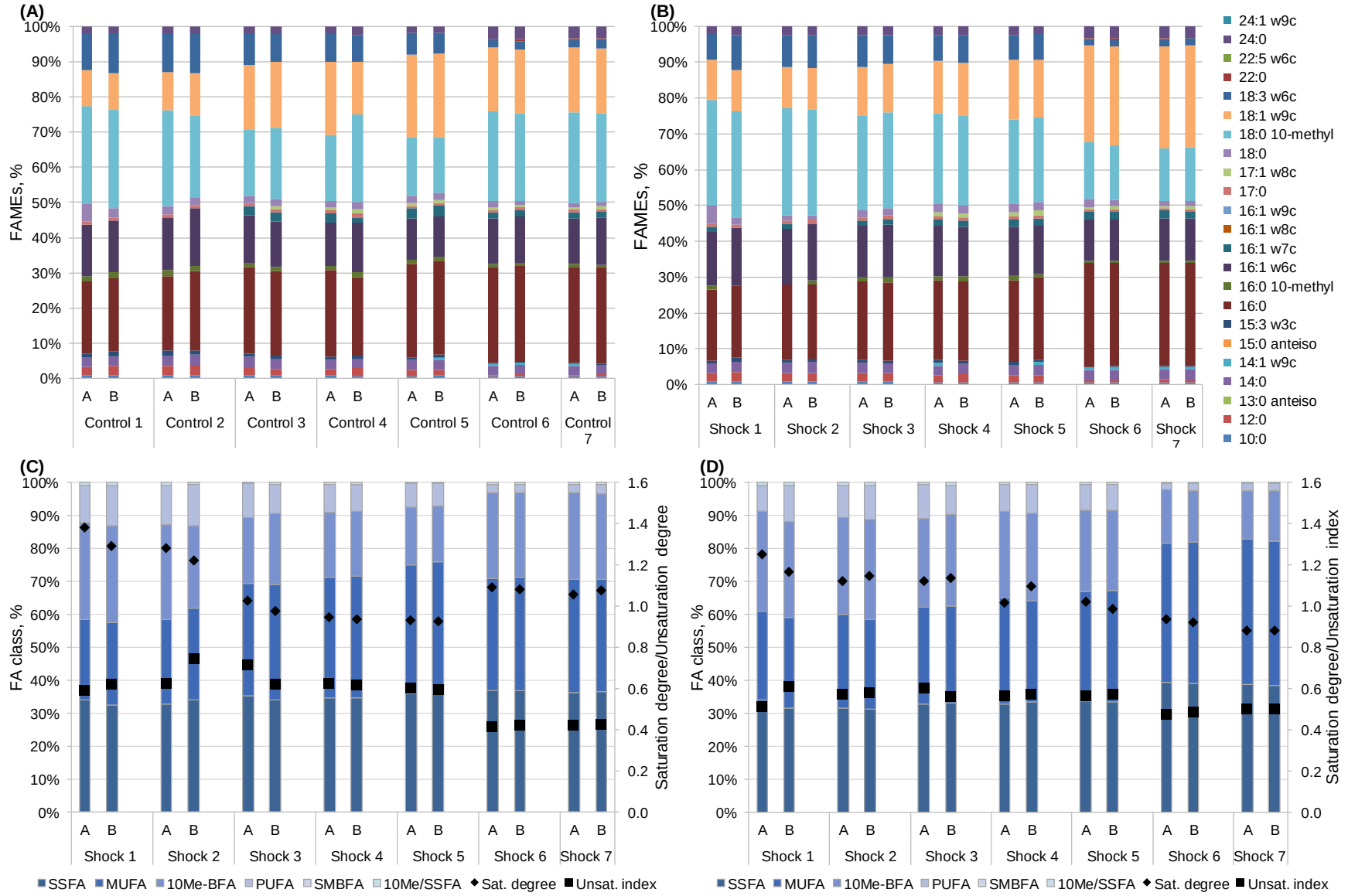

Figure 20 – Fatty acid composition (A, B) and its corresponding fatty acid classes, saturation degree, and unsaturation index (C, D) of cells exposed to 0.25% (v/v) DMSO and grown with agitation at 30°C (A, C) or with the application of 15-minute TS-NS shocks (B, D).

The zeta potential before and after each shock was also measured (Figure 21).

By comparing the zeta potential pattern over time between the control condition and the 15-min TS-NS shock, it is observable that both did not largely differ (Figure 21). Furthermore, the zeta potential obtained after the completion of the seven 15-min TS-NS shocks was equal to the one obtained in control conditions (-68.9 mV). This result suggests that the cells did not need to alter the net surface charge of the cellular membrane in response to the cold shocks.

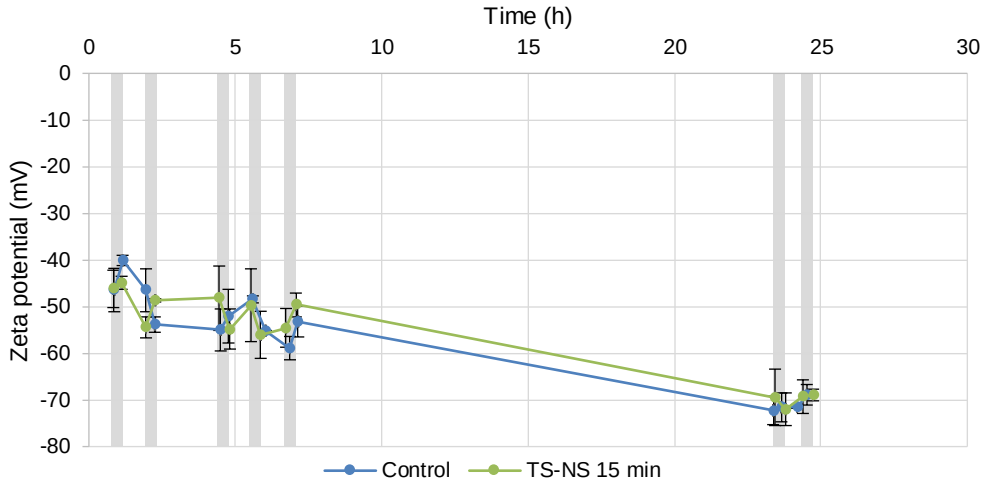

Figure 21 – Zeta potential of cells exposed to 0.25% (v/v) DMSO with (TS-NS 15 min) or without (Control) the application of 15-minute TS-NS shocks. The grey area represents the time and duration of the shocks applied.

After the application of the seven 15-min TS-NS shocks, a cell aggregation assay was performed, and the aggregation velocities and stabilization times were determined (Figure 22; Table 6).

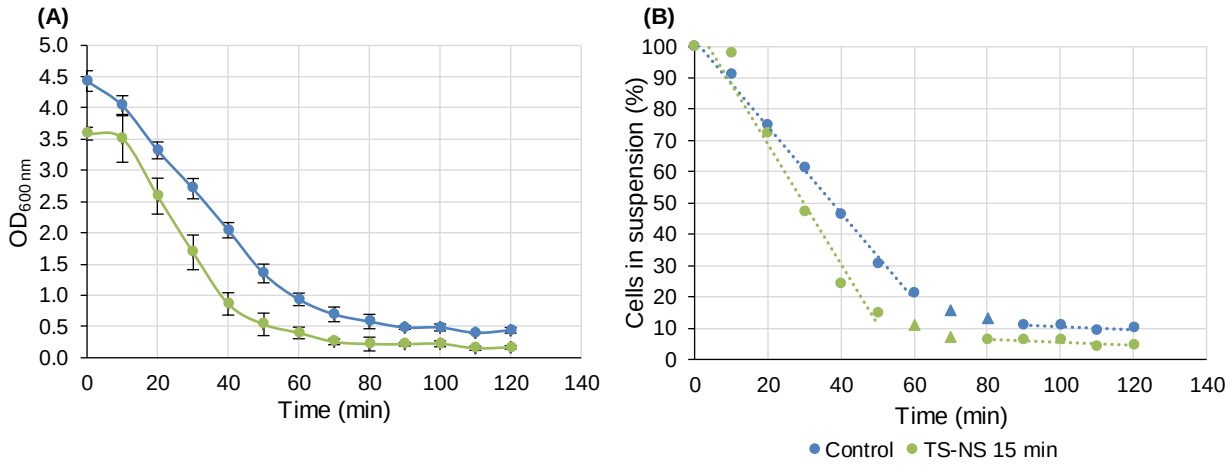

Figure 22 – Optical density ($OD_{600\,nm}$) (A) and percentage of cells in suspension (B) over time of cells exposed to 0.25% (v/v) DMSO grown with agitation at 30°C (Control) or submitted to the 15-minute TS-NS thermal and oxygen shock. Values considered for the velocity of aggregation and time of stabilization (closed dots); outliers (closed triangles); linear regression (dotted lines).

Table 6 - Parameters obtained in the linear equations for the period of sedimentation of cell aggregates and stabilization for the cold shock tested.

	Time	Aggregation equation parameters		Stabilization equation parameters		Stabilization time (min)
		m (% cells in suspension/min)	b (% cells in suspension)	m (% cells in suspension/min)	b (% cells in suspension)	
Control	-	-1.3812	102.13	-0.0497	15.429	65.12
TS-NS	15 min	-1.9204	107.35	-0.0474	10.216	51.86

Contrary to what was previously observed, the aggregation velocity of cells exposed to the TS-NS 15-min shock was far superior to the one obtained for the control condition (Figure 22; Table 6). Also, its interception time was much quicker. This could probably be attributed to the withdrawal of several samples during the growth period.

With the completion of the aggregation assay, the cell populations obtained were studied in terms of the fatty acid composition of the phospholipids of the cellular membrane (Figure 23), biomass dry weight (Figure 24A), and zeta potential (Figure 24B).

The fatty acid composition of the phospholipids of the cellular membrane of cells exposed to 15-min TS-NS in this experiment was different to the one obtained previously that can be consulted in Figure 17. The difference could also be due to the withdrawal of several samples, which could have disturbed the culture. In the present experiment, and regarding the Mix population, the cells presented a cellular membrane with a decreased content in 10Me-BFAs by 9.3% as a consequence of the decrease in the 18:10 10-methyl fatty acid, and an increased content in SSFAs by 1.0% and in MUFAs by 8.7% through the increase in the 16:0 and 18:1 ω9c fatty acids, in comparison to the control condition (Figure 23). In the Middle population, the cells presented a cellular membrane also characterized by an increased content in SSFAs by 1.2% and in MUFAs by 8.8%, while decreasing the content in 10Me-BFAs by 7.9% and PUFAs by 2.1%, when compared to the cellular membrane of the Middle population in control conditions. This was mostly achieved through the increase in the 16:0 and 18:1 ω9c fatty acids, and the decrease in the 18:0 10-methyl and 18:3 ω6c fatty acids. In comparison to the Bottom population in control conditions, the cellular membrane of cells belonging to the Bottom population that suffered the 15-min TS-NS shocks presented an increased content in SSFAs by 0.4% and in MUFAs by 8.6%, through the increase in the 16:0 and 18:1 ω9c fatty acids, and a decrease in 10Me-BFAs by 8.6%, achieved with the decrease in the 18:0 10-methyl fatty acid. Due to the decreased content of the cellular membrane in 18:0 10-methyl with a consequent increase in 18:1 ω9c for all the observed populations, it was expected that the cellular membrane would be mainly composed of MUFAs (Figure 23B). Therefore, the saturation degree of the cellular membrane of the Mix, Middle and Bottom populations was 1.22-, 1.24-, and 1.24-fold lower, respectively, when compared to the values obtained for the three corresponding cell populations in control conditions. Regarding the unsaturation index, the opposite occurred, with its values increasing in all the populations.

Additionally, the Mix population contained a fatty acid composition of the phospholipids of the cellular membrane similar to the Bottom population. By analysing the biomass dry weight obtained for the Middle and Bottom populations, it is noticeable that the latter had a larger influence on the total biomass content (Figure 24A). Therefore, the Mix population was mainly comprised of cells belonging to the Bottom population, which explains the similar fatty acid compositions of the phospholipids of the cellular membrane. However, and despite the unexpected increase in velocity of aggregation, cells suffering the 15-min TS-NS shocks presented an increase of 0.375 mg in the amount of cells in suspension, comprising 37.6% of the culture. This represents an increase of 5.8% in comparison to control conditions. Such increase in Middle population resulted in a consequent decrease of cells in the Bottom population of around 0.2 mg.

After the cell aggregation assay, the zeta potential of the Mix population was -66.25 mV, with the Middle population presenting a less negative value (-62.35 mV) (Figure 24B). The Bottom population had the highest zeta potential value of -69.4 mV. By comparing with the control, the cells that suffered the 15-min TS-NS shocks presented lower zeta potentials values overall, except for the Middle population.

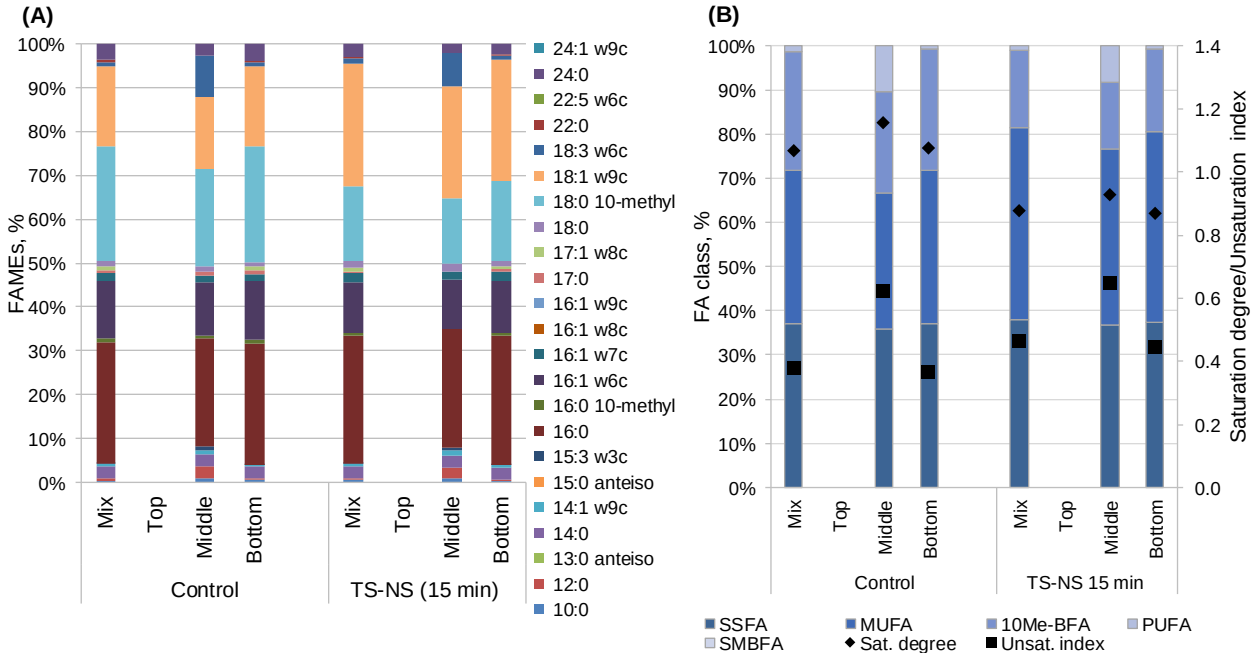

Figure 23 – Fatty acid composition (A), its fatty acid classes and the corresponding saturation degree and unsaturation index (B) of cells exposed to 0.25% (v/v) DMSO grown at 30°C with agitation (Control), or submitted to the 15-minute thermal and oxygen shock TS-NS before (Mix sample) and after the cell aggregation assay (Top, Middle, and Bottom samples).

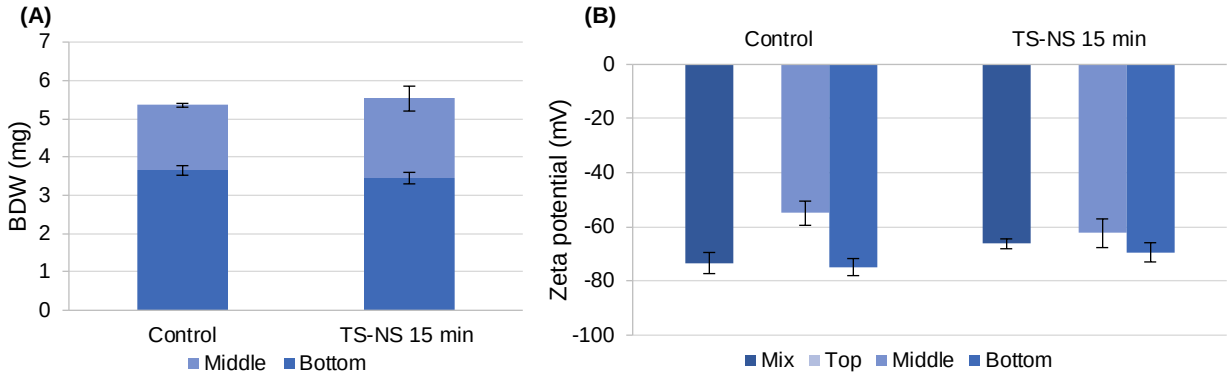

Figure 24 – Biomass dry weight (BDW) (A) and zeta potential (B) of cells exposed to 0.25% (v/v) DMSO grown at 30°C with agitation (Control) or submitted to the 15-minute thermal and oxygen shock TS-NS before (Mix sample) and/or after the aggregation assay (Top, Middle, and Bottom samples).

3.3. Cell aggregation under carbon-starvation conditions

Previous studies with *M. smegmatis* MC^2 155 have shown that carbon starvation induces a dispersion of cell aggregates, with an increase in planktonic cells [76]. Furthermore, cells resuspended in a carbon-depleted medium presented a decrease in aggregated cells. Therefore, to test whether carbon depletion would promote growth as planktonic cells, a culture of cells in exponential phase was resuspended in a 3-day old culture supernatant. To this end, both cultures were centrifuged, with the supernatant of the exponential phase cells being replaced by the supernatant from the stationary phase culture. Afterwards, the exponentially growing cells were resuspended and left to grow for further 16 h, with samples being taken before the exchange, immediately after, 1 h later, and 16 h later. The fatty acid composition of the phospholipids of the cellular membrane and zeta potential were analysed.

The growth was monitored before and after the media exchange by measuring the optical density at 600 nm ($OD_{600\ nm}$) and as expected, the cells resuspended in the spent medium were not able to grow due to the unavailability of carbon source (Figure 25).

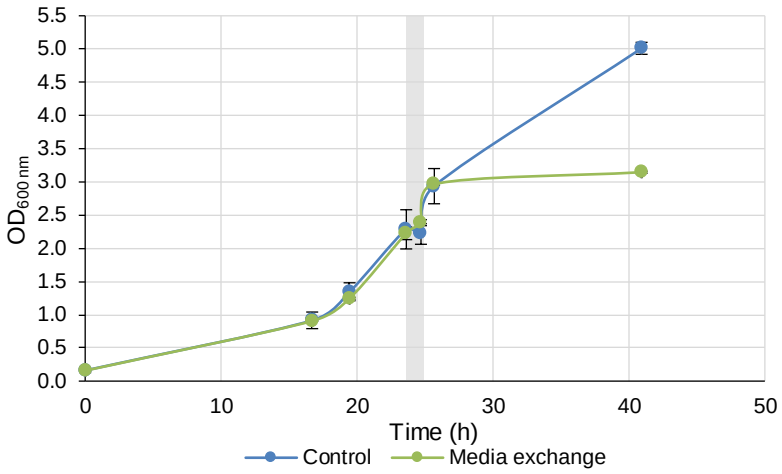

Figure 25 – Optical density ($OD_{600\,nm}$) over time of cells grown in fresh TSB (control) or resuspended in carbon-depleted medium. The dashed area represents the period of culture medium exchange.

After a 16-hour incubation period, both the control (Figure 26) and the cells resuspended in a carbon-depleted medium were observed by fluorescence microscopy (Figure 27).

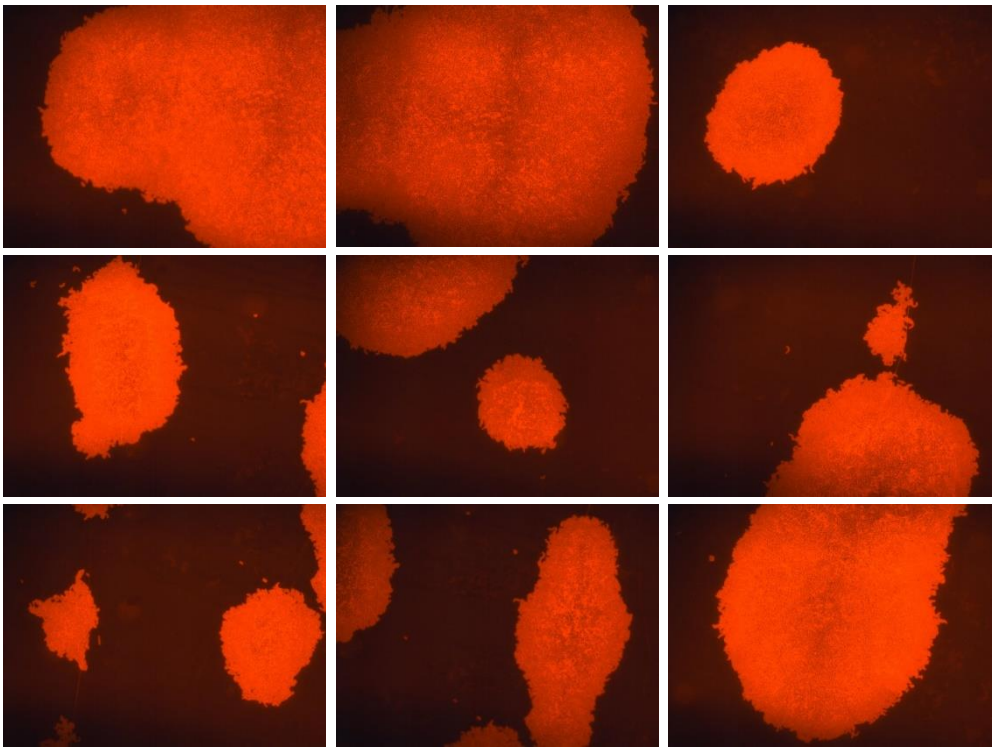

Figure 26 – Cells grown on TSB for 41 h stained with Rhodamine B. Horizontal and vertical field widths of 8.0 µm and 6.0 µm, respectively.

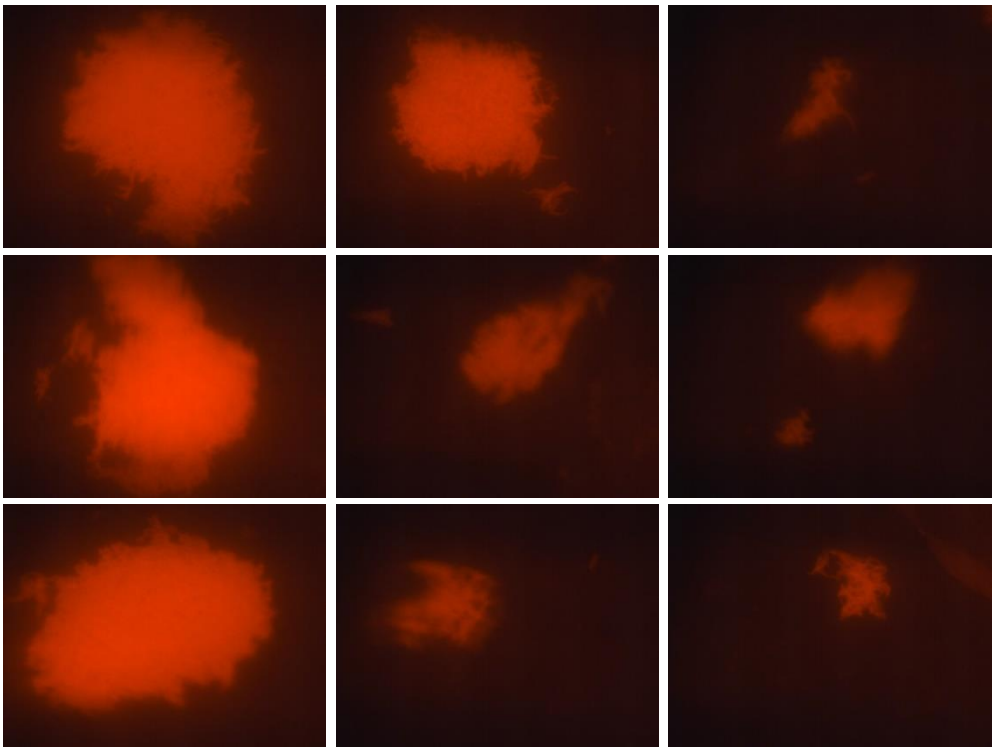

Figure 27 – Cells grown for 41 h after being grown during the last 16 h in carbon-depleted TSB stained with Rhodamine B. Horizontal and vertical field widths of 8.0 µm and 6.0 µm, respectively.

The culture grown on TSB for 41 h presented large cell aggregates that occupied on average 28% of the photographed area (Figure 26). Cells resuspended on spent medium produced smaller cell aggregates, occupying an average area of 11.5% (Figure 27). Moreover, the morphology of individual cells could not be observed due to a blurry appearance, which could be due to the production of a biosurfactant in response to the lack of carbon source.

The fatty acid composition of the phospholipids of the cellular membrane of cells in control condition or resuspended in carbon-depleted medium was also assessed (Figure 28; Figure 29). Before the media exchange, both conditions were similar in terms of the fatty acid composition of the phospholipids of the cellular membrane (Figure 28). After cells had been resuspended in carbon-depleted medium for 1 h, no changes were observed at the cellular membrane level, given that the cells did not have enough time to adapt to the new conditions. At the 41st h of growth (equivalent to the 16th h of media exchange), the cells in control conditions had reached the stationary phase, and so, the cells with exchanged media presented a similar fatty acid composition of the phospholipids of the cellular membrane because they entered the stationary phase earlier due to the absence of carbon source. Nevertheless, the cellular membrane of cells resuspended in carbon-depleted medium presented a minor increase in 18:3 ω6c of 1.45% and in 16:1 ω6c of 0.85% when compared to control conditions. Altogether, the membrane of cells with exchanged media presented an increased content in PUFAs by 1.6% and MUFAs by 0.2%, with a decrease in SSFAs by 2.1%. Moreover, the saturation degree and the unsaturation index of the cellular membrane of cells with

exchanged media presented alterations, with the saturation degree being 1.07-fold lower and the unsaturation index being 1.13-fold higher than the one obtained for the control condition (Figure 29).

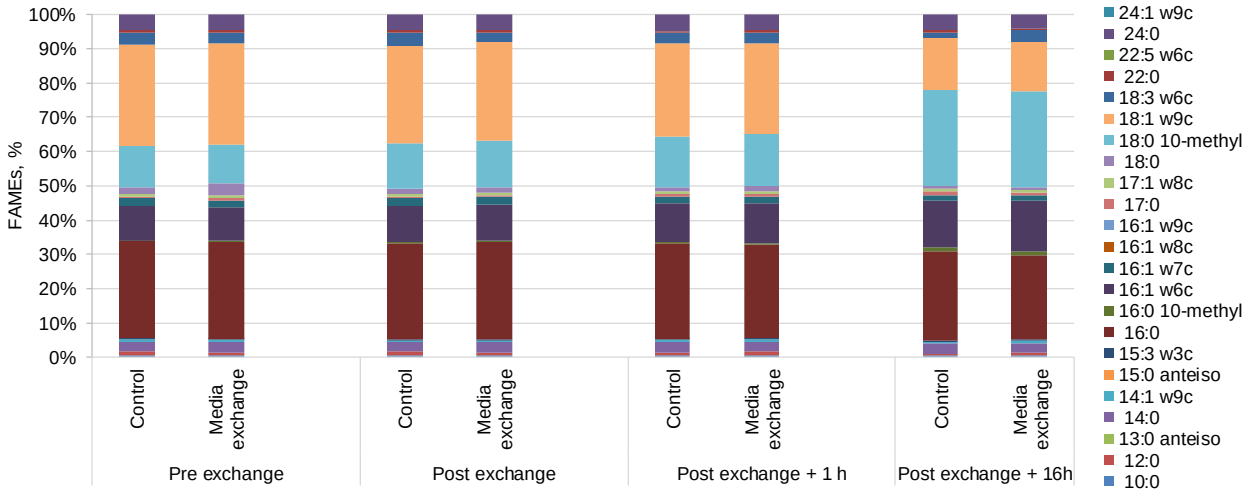

Figure 28 - Fatty acid composition of cells grown for 41 h uninterruptedly in TSB (Control) or resuspended for 16 h in carbon depleted medium pre-exchange, immediately after the exchange, 1 h, and 16 h later.

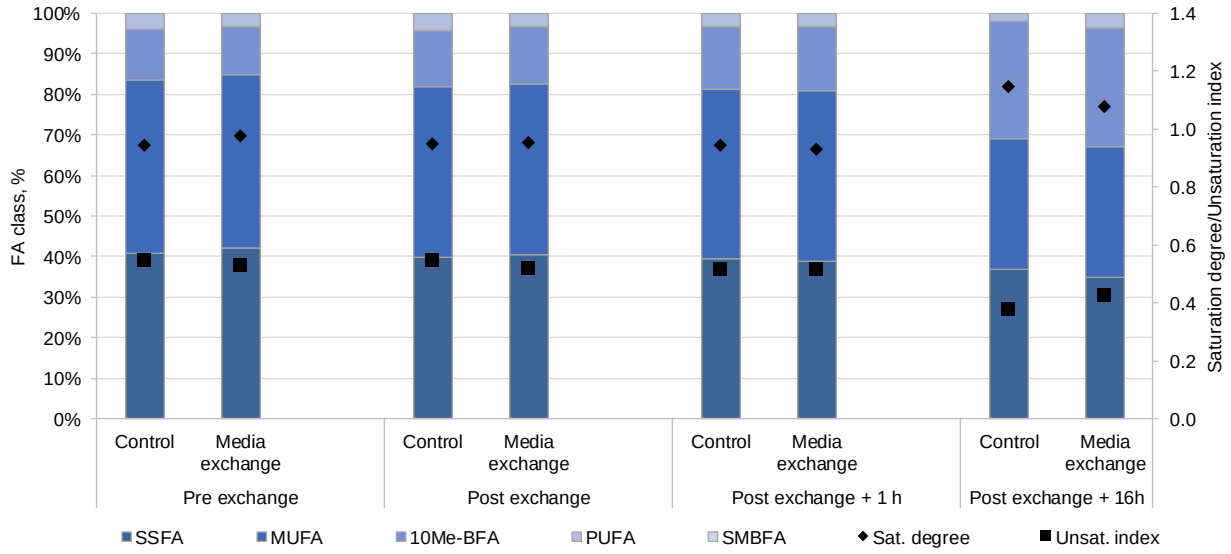

Figure 29 – Fatty acid composition and the corresponding saturation degree and unsaturation index of cells grown for 41 h uninterruptedly in TSB (Control) or resuspended for 16 h in carbon depleted medium pre-exchange, immediately after the exchange, 1 h, and 16 later.

Moreover, the zeta potential of the cells was measured (Figure 30). Until the 16th h of media exchange, both conditions presented similar zeta potentials (Figure 30). However, at that stage, and compared to the zeta potential of -55.2 mV for the control condition, the cells resuspended in a carbon-depleted medium presented a more negative zeta potential of -69.2 mV, which was also similar to the one obtained 1 h after the exchange (-70.65 mV). This suggests that the cells did not need to change this parameter to adapt to

carbon starvation. In turn, cells grown in fresh medium for the whole 41 h required alterations in their zeta potential to a less negative value.

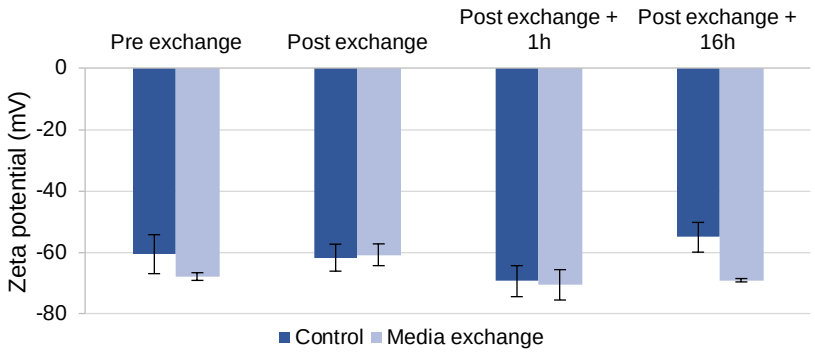

Figure 30 – Zeta potential of cells grown for 41 h uninterruptedly in TSB (Control) or resuspended for 16 h in carbon depleted medium pre-exchange, immediately after the exchange, 1 h, and 16 h later.

3.4. Ammonium-containing compounds as nitrogen source supplements

From the same study with *M. smegmatis* MC^2 155, it was also found that the addition of excess ammonium (NH_4^+) to the culture resulted in cell aggregation being severely impaired [76]. Ammonium chloride was the compound tested at concentrations of 25 mM and 75 mM, and it was observed that the higher the concentration, the higher the prevention of cell aggregation. To test this hypothesis in the present study, several ammonium-containing compounds were studied, including ammonium acetate, ammonium chloride, ammonium nitrate, ammonium sulphate, and ammonium bicarbonate. Cultures were grown for 42 h on TSB supplemented with either 50 mM, 75 mM, or 100 mM of each ammonium-containing compound, with samples being taken at 24 and 42 h to analyse the fatty acid composition of the phospholipids of the cellular membrane and the zeta potential. Furthermore, when growth was stopped, the cells were observed by fluorescence microscopy (Figure 31). It is noteworthy that, besides the supplementation with ammonium-containing compounds, the effect of amino acid supplementation (tyrosine, tryptophan, arginine, asparagine, or leucine) in cell aggregation was also studied. However, cultures did not reach high optical density ($OD_{600\ nm}$) values after a 5-day incubation, with large cell aggregates visible to the naked eye being present in every culture (data not shown).

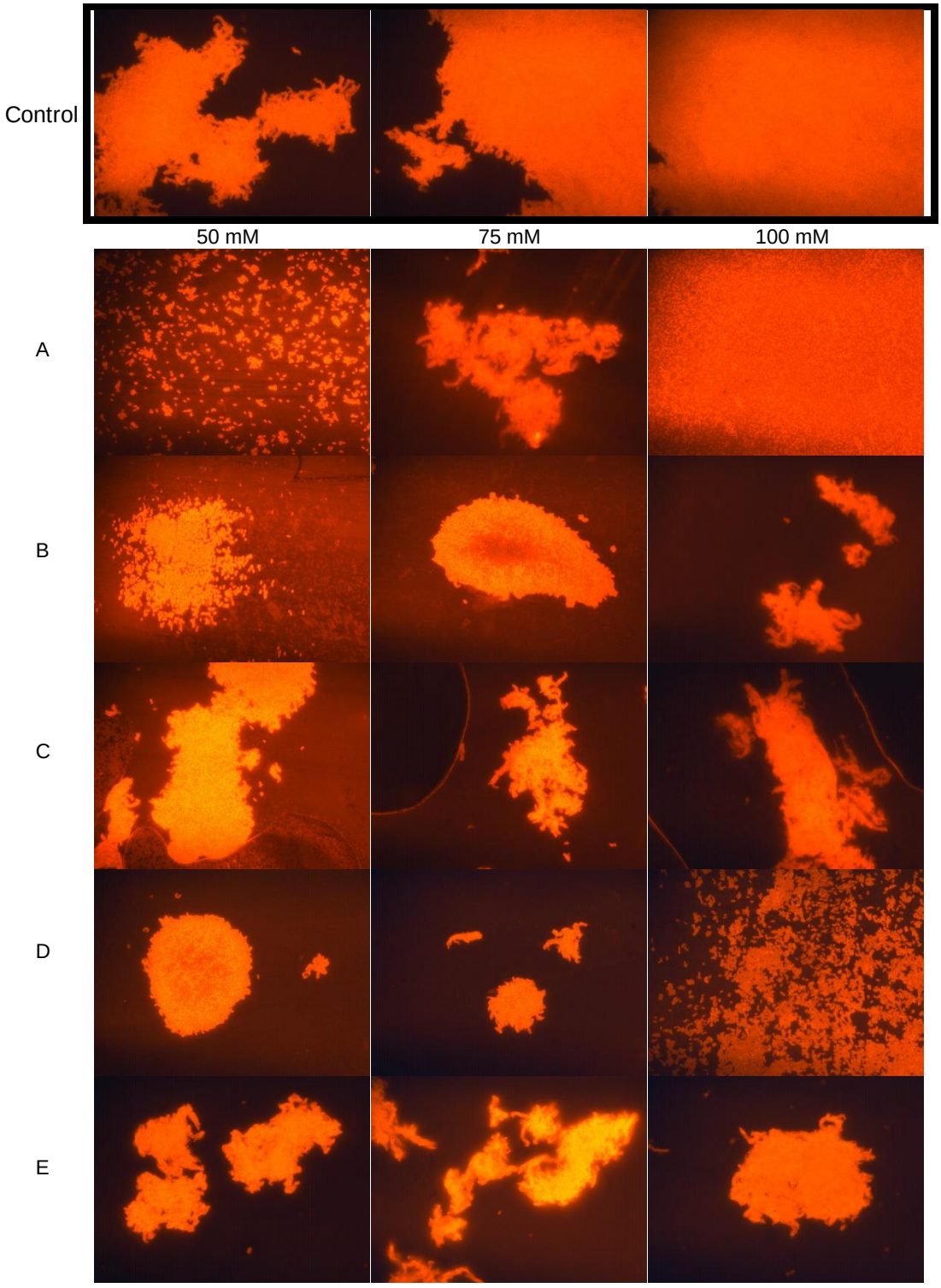

Figure 31 – Cells grown for 42 h either on TSB alone (Control) or supplemented with 50 mM, 75 mM, or 100 mM of ammonium acetate (A), ammonium chloride (B), ammonium nitrate (C), ammonium sulphate (D), or ammonium bicarbonate (E) stained with Nile Red. Horizontal and vertical field widths of 8.0 µm and 6.0 µm, respectively.

Cells in planktonic state were observed during exposure to 50 mM ammonium acetate, 50 mM ammonium chloride, or 100 mM ammonium sulphate (Figure 31). The number of objects per image was calculated, with the control condition presenting an average number of 4.6 objects per image with 52.1% of area. Growth supplementation with 50 mM ammonium acetate presented 556.3 objects per image in 42.3% of area, while supplementation with 50 mM ammonium chloride rendered on average 305.2 objects per image in 44.8% of the area. Moreover, an average of 283.1 objects per image in 35.3% of the area were obtained for supplementation with 100 mM ammonium sulphate. These results suggest that supplementation with the three ammonium-containing compounds allowed for an increased growth of cells in a planktonic state, with the cell aggregates obtained being smaller.

It was also expected that supplementation with 75 mM ammonium chloride would lead to a decrease in aggregated cells. However, this did not occur, with the cells being clustered. Also, cells supplemented with 100 mM ammonium acetate presented large aggregates that were visible to the naked eye (data not shown). Moreover, it is important to mention that the morphology of the cell appeared to be altered according to its growth state – planktonic or aggregated – and to the ammonium-containing compound supplemented. For example, cells exposed to ammonium bicarbonate at every concentration presented a more elongated morphology, while cells that were grown in a planktonic state or supplemented with 50 mM ammonium nitrate presented a smaller bacillus morphology.

At the 24th and 42nd h of growth, the fatty acid composition of the phospholipids of the membrane was assessed (Figure 32; Figure 33). Despite the differences observed at the cellular membrane level as a response to the ammonium-containing compound supplemented, differences were also noticed between the 24th and 42nd h of growth for all conditions (Figure 32A). Namely, the cellular membrane of cells in every condition presented an increase in the content of the 18:0 10-methyl and 16:1 ω6c fatty acids, with a consequent decrease in the content of the 18:3 ω6c and 16:0 fatty acids, from the 24th to the 42nd h of growth. However, there was an exception for cells supplemented with ammonium sulphate or bicarbonate, which presented a cellular membrane with no decrease in the 16:0 fatty acid, while the increase in the 16:1 ω6c fatty acid was more accentuated, and the content in the 24:0 fatty acid was decreased, from the 24th to the 42nd h of growth. Consequently, the cellular membrane of the cells supplemented with the various ammonium-containing compounds presented an increased content in 10Me-BFAs from the 24th to the 42nd h of growth (Figure 33A). Furthermore, with the increase in growth time, the cellular membrane was characterized by an increase in the saturation degree coupled with a decrease in the unsaturation index (Figure 33A). However, as opposed to the remaining conditions, the cellular membrane of cells supplemented with every concentration of ammonium sulphate presented a smaller increase in saturation degree as a response to the increase in growth time, being even smaller in the cellular membrane of cells supplemented with ammonium bicarbonate. Moreover, cells supplemented with 100 mM ammonium acetate presented a cellular membrane with decreased saturation degree as the growth time increased.

The cells supplemented with 100 mM ammonium acetate formed large cell aggregates. The fatty acid composition of the phospholipids of the cellular membrane had striking differences. Namely, when compared to control conditions, the cellular membrane presented an increase in PUFAs by 12% and 3.9% mainly attributed to an increase of the 18:3 ω6c fatty acid by 11% and 3.4% at 24 and 42 h of growth, respectively (Figure 32A; Figure 33A). Such increase in PUFAs was larger than what was observed for the remaining conditions. Consequently, cells supplemented with 100 mM ammonium acetate at both 24 and 42 h of growth presented a cellular membrane with a larger unsaturation index than what was observed for the control and the remaining conditions (Figure 33A).

As observed by fluorescence microscopy, cells in planktonic state were observed during supplementation with either 50 mM ammonium acetate, 50 mM ammonium chloride, or 100 mM ammonium sulphate (Figure 31). After 42 h of growth, and by comparing with control conditions, cells supplemented with 50 mM ammonium acetate presented a cellular membrane with an increase in the content of SSFAs and 10Me-BFAs due to the increase in the content of 18:0 10-methyl by 2.7% and of 16:0 by 0.7% (Figure 32B; Figure 33B). Moreover, the cellular membrane was characterized by a decrease in the production of MUFAs which could be mainly due to the decrease in 18:1 ω9c by 2.2% and in 16:1 ω6c by 0.5%. Growth supplemented with 50 mM ammonium chloride after 42 h of growth also resulted in cells with a cellular membrane with reduced composition in MUFAs again through the decrease in 18:1 ω9c by 2% and in 16:1 ω6c by 0.84%, coupled with an increase in the content of 18:0 10-methyl by 3.5% and of 16:0 by 0.5%, when compared to control conditions (Figure 32B). Therefore, by comparing growth at 42 h supplemented with both ammonium-containing compounds at a concentration of 50 mM, cells presented a cellular membrane with a higher increase in 18:0 10-methyl and a higher decrease in 16:1 ω6c during exposure to ammonium chloride. In contrast, the cellular membrane of cells supplemented with ammonium acetate presented a larger increase in 16:0 and decrease in 18:1 ω9c. Consequently, cells supplemented with either 50 mM ammonium acetate or 50 mM ammonium chloride at 42 h presented a cellular membrane with a saturation degree that was 1.12- and 1.10-fold higher and an unsaturation index 1.13- and 1.10-fold lower, respectively, in comparison to control conditions (Figure 33B). Cells supplemented with 100 mM ammonium sulphate after 42 h of growth were characterized by a cellular membrane with a decrease in SSFAs and MUFAs through a decrease of 3% in 24:0 and of 1% in 18:1 ω9c, and an increase in 10Me-BFAs due to a 1.5% increase in 18:0 10-methyl (Figure 32B). Therefore, the saturation degree and unsaturation index of the cellular membrane of cells supplemented with 100 mM ammonium sulphate after 42 h of growth were 1.03- and 1.02-fold lower, respectively, in comparison to control conditions (Figure 33B).

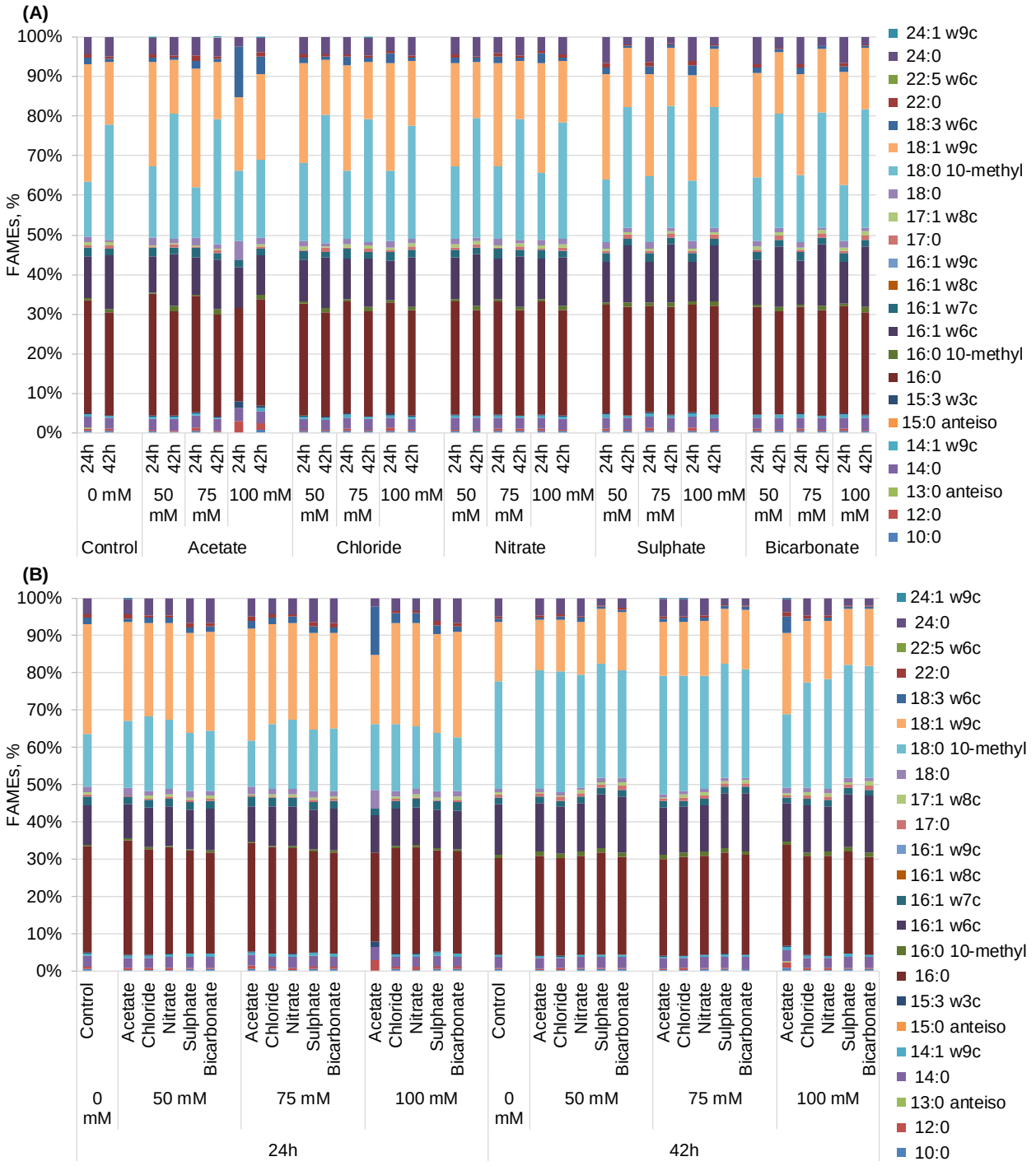

Figure 32 – Fatty acid composition at 24 and 42 hours of cells grown on TSB alone (Control) or supplemented with 50, 75, or 100 mM of ammonium acetate, ammonium chloride, ammonium nitrate, ammonium sulphate, or ammonium bicarbonate organized by ammonium-containing compound (A) or by concentration (B).

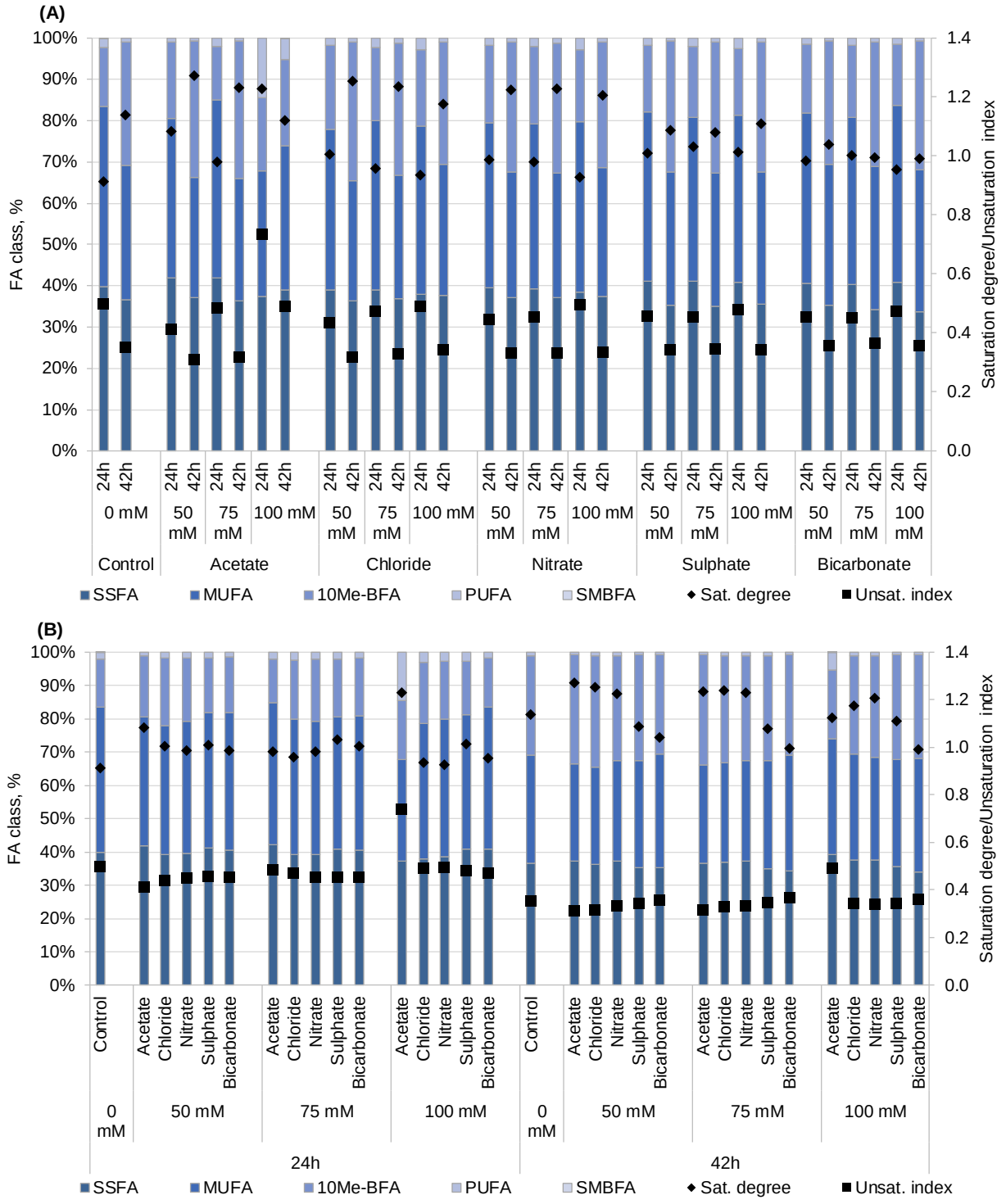

Figure 33 - Fatty acid composition and the corresponding saturation degree and unsaturation index of cells grown on TSB alone (Control) or supplemented with 50, 75, or 100 mM of ammonium acetate, ammonium chloride, ammonium nitrate, ammonium sulphate, or ammonium bicarbonate organized by ammonium-containing compound (A) or by concentration (B).

Cells were also able to alter the zeta potential of the cellular membrane according to the different ammonium-containing compound supplemented (Figure 34). Similar to what occurred with the fatty acid composition of the phospholipids of the cellular membrane, the zeta potential followed a pattern from the 24th to the 42nd h. Namely, with the increase in culture time, the zeta potential became more negative (Figure 34A). However, three exceptions were registered, with cells supplemented with 50 mM ammonium acetate, ammonium chloride, or ammonium bicarbonate presenting a less negative zeta potential at the 42nd h of growth (Figure 34A). Furthermore, cells supplemented with 100 mM ammonium acetate presented the lowest absolute zeta potential value at both growth hours assessed, which could be due to the large cell aggregates formed in this culture. At 24 h of growth, the cells with fewer cell aggregates formed - supplemented with 50 mM ammonium acetate, 50 mM ammonium chloride, or 100 mM ammonium sulphate - suffered an increase in the zeta potential of 0.84% in the first condition mentioned, while in the remaining two a decrease in its zeta potential value of 1.24% and 18.7%, respectively, was registered, when compared to the zeta potential of control conditions at 24 h of growth. Furthermore, at 42 h of growth, the three conditions presented a decrease in its zeta potential value by 6.3%, 6.4%, and 2.6%, respectively, when compared to the zeta potential of cells in control conditions after 42 h of growth. (Figure 34B).

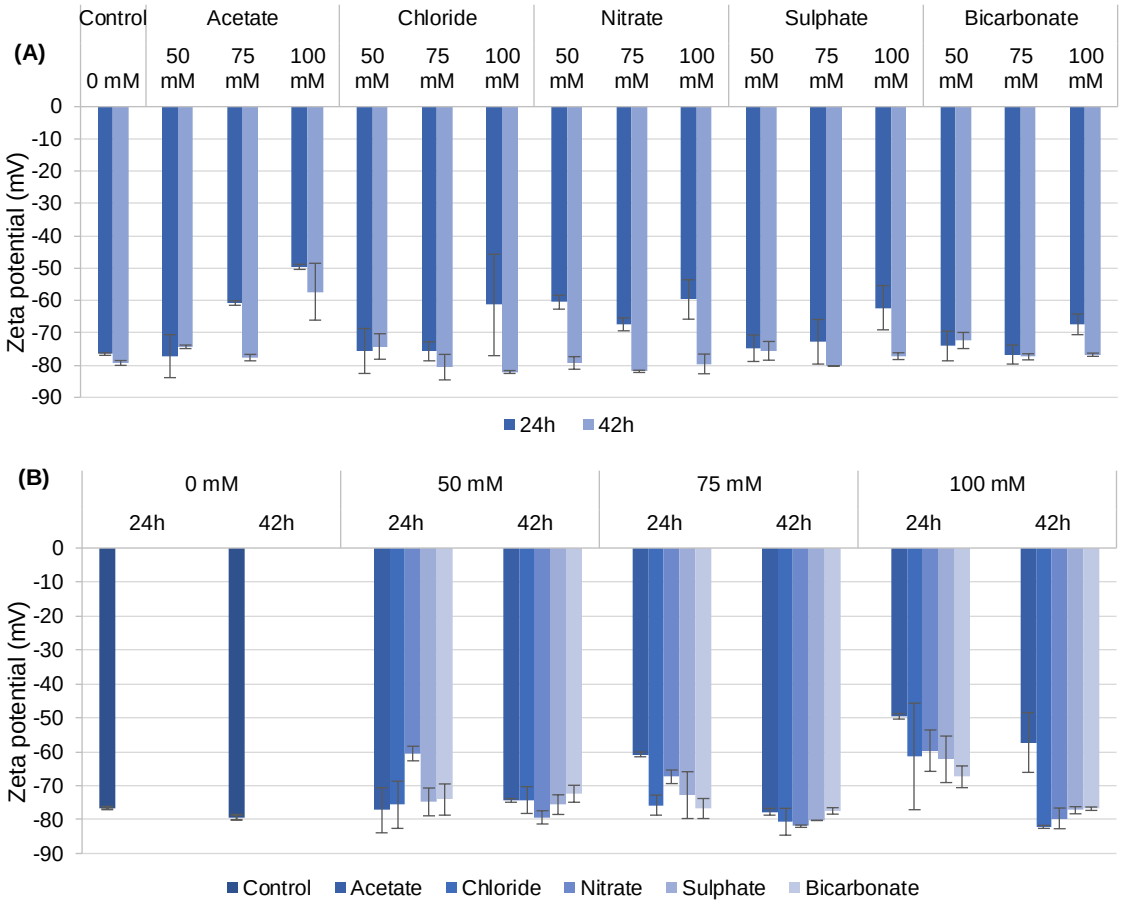

Figure 34 – Zeta potential of cells grown on TSB alone (Control) or supplemented with 50, 75, or 100 mM of ammonium acetate, ammonium chloride, ammonium nitrate, ammonium sulphate, or ammonium bicarbonate at 24 and 42 hours organized by ammonium-containing compound (A) or by concentration (B).

4. Discussion

Tuberculosis is an infectious disease caused by *Mycobacterium tuberculosis*, being considered by the WHO as the leading cause of death by a single infectious agent in 2020 [1]. In fact, in 2019 it was estimated that 10 million people contracted the disease and 1.4 million died [1]. Unfortunately, the unequal access to adequate health care throughout the world, coupled with lack of treatment adherence has led to the appearance of multidrug and extensively drug-resistance strains [6]. MDR and XDR tuberculosis strains require more extensive treatments with the success rate being drastically reduced. Therefore, to prevent the spread of resistant strains, effective vaccination is of extreme importance. The BCG vaccine, which derives from a live attenuated strain of *M. bovis*, is the only approved vaccine for the prevention of tuberculosis [10]. However, its ability to protect adults from pulmonary TB ranges from 0% to 80%, with one of the main reasons being the lack of production standardization [20]. This is mostly due to the formation of aggregates, which then leads to nonviable portions of the harvested bacteria, rendering the quality control of the vaccine difficult [20]. Therefore, the aim of the present study was to search for a reproducible fermentation method that allowed for planktonic cell growth, using the NTM species *M. smegmatis* as a model organism. However, this was not achieved. Still, the present study provides useful insights into the aggregative behaviour of *M. smegmatis* when exposed to different solvents, with the effect of the growth temperature being also assessed. Furthermore, the effect of carbon starvation and nitrogen source supplementation were studied.

Exposure of *M. smegmatis* to 0.25% (v/v) methanol, ethanol, or DMSO led to slower sedimentation of cell aggregates, noticed by the lower absolute value of the velocity of aggregation. Moreover, the time at which all the aggregates were deposited also increased. Both results are an indication that the cells were able to reduce the size of aggregates in response to the exposure of the three mentioned solvents. Cells exposed to methanol did not reach optical densities (at 600 nm) comparable to the ones obtained in during exposure to ethanol or DMSO. In a previous study, *M. smegmatis* was shown to be able to grow with methanol as the sole carbon source, through the production of a methanol dehydrogenase [93]. Nevertheless, the low optical densities obtained could be attributed to a growth inhibition by methanol. The cellular membrane of cells exposed to methanol suffered a decrease in its saturation degree, which is consistent with what was previously observed in *Rhodococcus erythropolis*, given that short-chain alcohols, such as methanol and ethanol, remain in the hydrophilic portion of the phospholipid bilayer, penetrating only slightly into the hydrophobic portion [94, 95]. Therefore, to counterbalance the gaps in the membrane caused by the presence of the alcohol, cells respond by increasing the content of unsaturated fatty acids in the phospholipids of the cellular membrane [94, 96]. Furthermore, *M. vaccae* exposed to 1% ethanol also presented an increased saturation degree of the cellular membrane [97]. However, in the case of *M. smegmatis*, the cellular membrane of cells exposed to ethanol presented a higher saturation degree of the fatty acids than the cells without any solvent exposure. Exposure to DMSO rendered the best overall result, with cells presenting the slowest velocities of aggregation, coupled with a longer stabilization time.

Furthermore, no cell aggregates at the air-liquid interface were observed. Given that the objective was to reduce cell aggregation, the fatty acid composition of the phospholipids of the membrane could play an important role in determining the growth as planktonic cells or cell aggregates. The phospholipids of the cellular membrane of cells exposed to DMSO presented an increase in unsaturated fatty acids when compared to non-exposed cells, with the unsaturation index consequently increasing and the saturation degree decreasing. This behaviour was also observed in *E. coli* as a response to the presence of DMSO in the culture medium [94]. The biomass dry weight of each population was also an important way to assess the impact of each population on the whole culture. Cells exposed to either methanol, ethanol, or DMSO had increased percentages of cells in suspension by more than 18%, when compared to no addition of solvents. Altogether, these results show that cells exposed to either methanol, ethanol, or DMSO reduced their cell aggregation extent, and an increase in the fluidity of the cellular membrane was required during exposure to either methanol or DMSO, while cells exposed to ethanol responded through an increase in cellular membrane rigidity.

Since DMSO was found to be the solvent that returned the best results in terms of reduction of cell aggregation, it was tested whether the decrease in cell aggregation was concentration-dependent. To this end, cells were exposed to either 0.50% or 1% (v/v) DMSO, and growth was not affected. The same was observed for *M. tuberculosis* H37Rv, which could withstand up to 1.3% of DMSO without it affecting its growth capabilities [98]. Even though no significant alterations in terms of cell aggregation were observed, cells from the Middle population increased the content of the phospholipids of the cellular membrane in unsaturated fatty acids in response to the increasing DMSO concentrations, thus increasing the fluidity of the cellular membrane. Surprisingly, this was mainly achieved by the increase in the content of PUFAs with a consequent decrease in MUFAs. *R. erythropolis* DSM 1069 has also resorted to this mechanism when exposed to increasing concentrations of NaCl [99]. This adaptation mechanism could be attributed to expressed fatty acid desaturases that modified the monounsaturated fatty acids [99].

Cells in all the experiments contained a Middle population with a cellular membrane containing a higher unsaturation index than the one observed for the cellular membrane of the Bottom population. Moreover, the composition of the phospholipids of the cellular membrane in unsaturated fatty acids is increased as a response to decreasing growth temperatures [79]. So, the growth and the cell aggregation of *M. smegmatis* were assessed at different temperatures with or without exposure to DMSO. As a response to decreasing temperatures, the main alteration observed at the cellular membrane level was the decrease in the 18:0 10-methyl fatty acid, which has been previously reported for *M. smegmatis* [100], with a consequent increase in the 18:1 ω9c fatty acid. Moreover, the cellular membrane presented a decreased saturation degree in response to decreasing temperatures. This is the common response mechanism of most prokaryotes. However, *R. erythropolis* does the opposite and increases its saturation degree with the decrease in temperatures [101]. Nevertheless, despite the increased content in unsaturated fatty acids observed in the cellular membrane of cells grown at decreased temperatures, cell aggregation was not reduced, and so the aggregation velocity was increased.

Another approach was taken to achieve a higher percentage of cells in planktonic state, which included cold shocks and oxygen stress. After seven 15-min TS-NS shocks applied for 24 h, cells belonging to the Mix and Middle populations presented a cellular membrane with a decreased unsaturation index for all populations, which could be due to the increase observed in 18:0 10-methyl with a concomitant decrease in 18:1 ω9c. However, the saturation degree was unaltered due to the simultaneous decrease in saturated straight fatty acids. Cells from the Bottom population increased their saturation degree, with the cellular membrane becoming more rigid. The 15-min TS-NS shock returned the lowest aggregation velocity, which might mean that the extent of cell aggregation was reduced. However, the percentage of cells in suspension was decreased when compared to unchallenged cells.

The mechanisms employed at the cellular membrane level to adapt to the 15-min TS-NS shocks were assessed, by analysing the fatty acid composition of the cellular membrane before and after each shock. As a response to the stress employed, *M. smegmatis* presented a cellular membrane with decreased saturation degree over time, mainly through the increase in monounsaturated fatty acids. Therefore, and similar to the behaviour in response to lower growth temperatures, the cells decreased their membrane fluidity as time passed, through the increase in 18:1 ω9c. Moreover, the cellular membrane content in PUFAs decreased over time, suggesting that these fatty acids were not required for the cellular membrane fluidity increase. However, after a cell aggregation assay, the cells presented a higher aggregation velocity than what was previously observed. Moreover, in this case, the saturation degree was decreased, due to a higher percentage of monounsaturated fatty acids. The difference could be due to the several withdrawal of samples before and after each shock, thus disturbing the culture and decreasing its total volume.

It was previously reported for *M. smegmatis* that carbon starvation would lead to cell aggregate decrease [76]. Therefore, to test if this was applied to the strain under study, cells in exponential phase were resuspended in a 3-day old culture supernatant. The extent of cell aggregation was analysed by fluorescence microscopy, and the size of the cell aggregates was reduced. In the mentioned study, the effect on the fatty acid composition of the phospholipids of the membrane and electrophoretic mobility was not observed. However, in the present work cells responded to the carbon depletion by decreasing the saturation degree of the cellular membrane through the increase in PUFAs, thus increasing its fluidity. Furthermore, cells in carbon starvation conditions presented a more negative zeta potential. While carbon-depleted medium led to a decrease in the size of cell aggregates, it has also been found that ammonium supplementation favours growth as planktonic cells [76]. Therefore, five ammonium-containing compounds were tested, with a decrease in cell aggregation being observed with either 50 mM ammonium acetate, ammonium chloride, or 100 mM ammonium sulphate. In fact, planktonic cells were observed. Only supplementation with ammonium chloride in cultures of *M. smegmatis* had already been tested, with 75 mM leading to accumulation of planktonic cells [76]. In the present study, the response at the membrane level was assessed, with cells increasing the rigidity of the cellular membrane during exposure to either 50 mM ammonium acetate or ammonium chloride and rendering the cellular membrane more fluid during exposure to 100 mM ammonium sulphate.

5. Conclusion and Future Perspectives

In the present study, the effect of culture media composition and growth temperature on cell aggregation, which is characteristic of mycobacteria, were studied. The extent of cell aggregation was reduced when *M. smegmatis* cells were exposed to either methanol, ethanol, or DMSO, with cells exposed to DMSO presenting the lowest aggregation velocity obtained. Furthermore, the carbon and nitrogen sources of the culture media were found to play an important role in cell aggregation. Namely, cell aggregates were reduced in carbon-starvation conditions, while cells in a planktonic state were able to be obtained during growth supplemented with ammonium-containing compounds.

The mechanisms by which cell aggregation is reduced are still unknown. Therefore, further studies need to be conducted to better understand mycobacterial aggregation. One of the main reasons for the characteristic high surface hydrophobicity of mycobacteria is the presence of long-chain mycolic acids in the cell wall. However, previous studies in *M. smegmatis* have shown that the mycolic acid chain length can be regulated in response to external factors, thus rendering the cell surface hydrophobicity manageable. In future work, it would be of interest to further explore the dispersive ability of DMSO at the cell wall level to understand if the chain length of the mycolic acids is in fact regulated. Moreover, the supplementation with the ammonium-containing compounds that resulted in planktonic growth could be further exploited.

This study constitutes an important contribution regarding the reduction of mycobacterial cell aggregation by changing the composition of the culture media. Namely, exposure to DMSO or supplementation with ammonium-containing compounds was shown to reduce cell aggregation. Tuberculosis is still a deadly disease, especially in under-developed countries, and with mycobacterial cell aggregation being such an impairment in vaccine efficacy, the observations made in this study constitute an important step in the right direction.

6. References

[1] World Health Organization, “Global tuberculosis report,” 2020. https://www.who.int/publications/i/item/9789240013131.

[2] M. J. Kim *et al.*, “Caseation of human tuberculosis granulomas correlates with elevated host lipid metabolism,” *EMBO Mol. Med.*, vol. 2, no. 7, pp. 258–274, 2010, doi: 10.1002/emmm.201000079.

[3] M. J. Marakalala *et al.*, “Inflammatory signaling in human tuberculosis granulomas is spatially organized,” *Nat. Med.*, vol. 22, no. 5, pp. 531–538, 2016, doi: 10.1038/nm.4073.

[4] M. G. Harisinghani, T. C. McLoud, J. A. O. Shepard, J. P. Ko, M. M. Shroff, and P. R. Mueller, “Tuberculosis from head to toe,” *Radiographics*, vol. 20, no. 2, pp. 449–470, 2000, doi: 10.1148/radiographics.20.2.g00mc12449.

[5] A. O’Garra, P. S. Redford, F. W. McNab, C. I. Bloom, R. J. Wilkinson, and M. P. R. Berry, “The immune response in tuberculosis,” *Annu. Rev. Immunol.*, vol. 31, pp. 475–527, 2013, doi: 10.1146/annurev-immunol-032712-095939.

[6] S. M. Gygli, S. Borrell, A. Trauner, and S. Gagneux, “Antimicrobial resistance in *Mycobacterium tuberculosis*: Mechanistic and evolutionary perspectives,” *FEMS Microbiol. Rev.*, vol. 41, no. 3, pp. 354–373, 2017, doi: 10.1093/femsre/fux011.

[7] V. Dartois, “The path of anti-tuberculosis drugs: From blood to lesions to mycobacterial cells,” *Nat. Rev. Microbiol.*, vol. 12, no. 3, pp. 159–167, 2014, doi: 10.1038/nrmicro3200.

[8] D. G. Russell, C. E. Barry 3rd, and J. L. Flynn, “Tuberculosis: What we don’t know can, and does, hurt us,” *Science (New York, N.Y.).*, vol. 328, no. 5980, pp. 852–856, 2010, [Online]. Available: http://science.sciencemag.org/content/328/5980/852.full.

[9] G. V. Bloemberg, S. Gagneux, and E. C. Böttger, “Acquired resistance to bedaquiline and delamanic in therapy for tuberculosis,” *N. Engl. J. Med.*, vol. 373, no. 20, pp. 1986–1988, 2015, doi: 10.1016/j.physbeh.2017.03.040.

[10] L. K. Schrager, J. Vekemens, N. Drager, D. M. Lewinsohn, and O. F. Olesen, “The status of tuberculosis vaccine development,” *Lancet Infect. Dis.*, vol. 20, no. 3, pp. e28–e37, 2020, doi: 10.1016/S1473-3099(19)30625-5.

[11] T. Oettinger, M. Jørgensen, A. Ladefoged, K. Hasløv, and P. Andersen, “Development of the *Mycobacterium bovis* BCG vaccine: Review of the historical and biochemical evidence for a genealogical tree,” *Tuber. Lung Dis.*, vol. 79, no. 4, pp. 243–250, 1999.

[12] *Despacho nº 8264/2016 do Gabinete do Secretário de Estado Adjunto e da Saúde*. 2016, pp. 19694–19694.

[13] D. G. da Saúde, “Programa Nacional de Vacinação 2017,” 2017. doi: 10.1016/j.ajog.2008.08.049.

[14] N. Ritz and N. Curtis, “Mapping the global use of different BCG vaccine strains,” *Tuberculosis*, vol. 89, no. 4, pp. 248–251, 2009, doi: 10.1016/j.tube.2009.03.002.

[15] A. Angelidou *et al.*, “Licensed Bacille Calmette-Guérin (BCG) formulations differ markedly in bacterial viability, RNA content and innate immune activation,” *Vaccine*, vol. 38, pp. 2229–2240, 2020, doi: 10.1016/j.vaccine.2019.11.060.

[16] S. Luca and T. Mihaescu, “History of BCG Vaccine,” *Maedica (Buchar).*, vol. 8, no. 1, pp. 53–58, 2013, [Online]. Available: http://www.ncbi.nlm.nih.gov/pubmed/24023600%0Ahttp://www.pubmedcentral.nih.gov/articlerender.fcgi?artid=PMC3749764.

[17] T. Cernuschi, S. Malvolti, E. Nickels, and M. Friede, “Bacillus Calmette-Guérin (BCG) vaccine: A global assessment of demand and supply balance,” *Vaccine*, vol. 36, no. 4, pp. 498–506, 2018, doi: 10.1016/j.vaccine.2017.12.010.

[18] O. Narvskaya *et al.*, “First insight into the whole-genome sequence variations in *Mycobacterium bovis* BCG-1 (Russia) vaccine seed lots and their progeny clinical isolates from children with BCG-induced adverse events,” *BMC Genomics*, vol. 21, no. 567, pp. 1–12, 2020.

[19] S. Panaiotov, Y. Hodzhev, V. Tolchkov, B. Tsafarova, A. Mihailov, and T. Stefanova, “Complete genome sequence, genome stability and phylogeny of the vaccine strain *Mycobacterium bovis* BCG SL222 Sofia,” *Vaccines*, vol. 9, no. 237, 2021, doi: 10.3390/vaccines9030237.

[20] G. Dietrich *et al.*, “Cultivation of *Mycobacterium bovis* BCG in bioreactors,” *J. Biotechnol.*, vol. 96, pp. 259–270, 2002, doi: 10.1016/S0168-1656(02)00046-9.

[21] L. C. Rodrigues, V. K. Diwan, and J. G. Wheeler, “Protective effect of BCG against tuberculous meningitis and miliary tuberculosis: A meta-analysis,” *Int. J. Epidemiol.*, vol. 22, no. 6, pp. 1154–1158, 1993, doi: https://doi.org/10.1093/ije/22.6.1154.

[22] G. A. Colditz *et al.*, “Efficacy of BCG vaccine in the prevention of tuberculosis. Meta-analysis of the published literature,” *JAMA*, vol. 271, no. 9, pp. 698–702, 1994.

[23] M. M. Venkataswamy, M. F. Goldberg, A. Baena, J. Chan, W. R. Jacobs, and S. A. Porcelli, “In vitro culture medium influences the vaccine efficacy of *Mycobacterium bovis* BCG,” *Vaccine*, vol. 30, no. 6, pp. 1038–1049, 2012, doi: 10.1016/j.vaccine.2011.12.044.

[24] T. C. Eickhoff, “The current status of BCG immunization against tuberculosis,” *Annu. Rev. Med.*, vol. 28, pp. 411–423, 1977, doi: 10.1146/annurev.me.28.020177.002211.

[25] J. Pascoe, C. L. Hendon-Dunn, C. P. D. Birch, G. A. Williams, M. A. Chambers, and J. Bacon,

"Optimisation of *Mycobacterium bovis* BCG fermentation and storage survival," *Pharmaceutics*, vol. 12, no. 900, 2020, doi: 10.3390/pharmaceutics12090900.

[26] E. Whitlow, A. S. Mustafa, and S. N. M. Hanif, "An overview of the development of new vaccines for tuberculosis," *Vaccines*, vol. 8, no. 586, pp. 1–13, 2020, doi: 10.3390/vaccines8040586.

[27] S. Afkhami, A. D. Villela, M. R. D'Agostino, M. Jeyanathan, A. Gillgrass, and Z. Xing, "Advancing immunotherapeutic vaccine strategies against pulmonary tuberculosis," *Front. Immunol.*, vol. 11, no. September, pp. 1–10, 2020, doi: 10.3389/fimmu.2020.557809.

[28] D. Marinova, J. Gonzalo-Asensio, N. Aguilo, and C. Martin, "MTBVAC from discovery to clinical trials in tuberculosis-endemic countries," *Expert Rev. Vaccines*, vol. 16, no. 6, pp. 565–576, 2017, doi: 10.1080/14760584.2017.1324303.

[29] J. Gonzalo-Asensio, D. Marinova, C. Martin, and N. Aguilo, "MTBVAC: Attenuating the human pathogen of tuberculosis (TB) toward a promising vaccine against the TB epidemic," *Front. Immunol.*, vol. 8, pp. 1–8, 2017, doi: 10.3389/fimmu.2017.01803.

[30] N. Fritschi, N. Curtis, and N. Ritz, "Bacille Calmette Guérin (BCG) and new TB vaccines: Specific, cross-mycobacterial and off-target effects," *Paediatr. Respir. Rev.*, vol. 36, pp. 57–64, 2020, doi: 10.1016/j.prrv.2020.08.004.

[31] S. H. E. Kaufmann *et al.*, "The BCG replacement vaccine VPM1002: From drawing board to clinical trial," *Expert Rev. Vaccines*, vol. 13, no. 5, pp. 619–630, 2014, doi: 10.1586/14760584.2014.905746.

[32] N. E. Nieuwenhuizen *et al.*, "The recombinant Bacille Calmette-Guérin vaccine VPM1002: Ready for clinical efficacy testing," *Front. Immunol.*, vol. 8, no. 1147, pp. 1–9, 2017, doi: 10.3389/fimmu.2017.01147.

[33] L. Grode *et al.*, "Increased vaccine efficacy against tuberculosis of recombinant *Mycobacterium bovis* Bacille Calmette-Guérin mutants that secrete listeriolysin," *J. Clin. Invest.*, vol. 115, no. 9, pp. 2472–2479, 2005, doi: 10.1172/JCI24617.

[34] C. Huang and W. Hsieh, "Efficacy of *Mycobacterium vaccae* immunotherapy for patients with tuberculosis: A systematic review and meta-analysis," *Hum. Vaccin. Immunother.*, vol. 13, no. 9, pp. 1960–1971, 2017, doi: 10.1080/21645515.2017.1335374.

[35] M. I. Gröschel, S. A. Prabowo, P. Cardona, J. L. Stanford, and T. S. Van Der Werf, "Therapeutic vaccines for tuberculosis - A systematic review," *Vaccine*, vol. 32, pp. 3162–3168, 2014, doi: 10.1016/j.vaccine.2014.03.047.

[36] M. Saqib, R. Khatri, B. Singh, A. Gupta, A. Kumar, and S. Bhaskar, "*Mycobacterium indicus pranii* as a booster vaccine enhances BCG induced immunity and confers higher protection in animal

models of tuberculosis," *Tuberculosis*, vol. 101, pp. 164–173, 2016, doi: 10.1016/j.tube.2016.10.002.

[37] C. F. Von Reyn *et al.*, "Safety and immunogenicity of an inactivated whole cell tuberculosis vaccine booster in adults primed with BCG: A randomized, controlled trial of DAR-901," *PLoS One*, vol. 12, no. 5, pp. 1–16, 2017, doi: 10.1371/journal.pone.0175215.

[38] T. Masonou *et al.*, "CD4+ T cell cytokine responses to the DAR-901 booster vaccine in BCG-primed adults: A randomized, placebo-controlled trial," *PLoS One*, vol. 14, no. 5, pp. 1–17, 2019, doi: 10.1371/journal.pone.0217091.

[39] P. J. Cardona, "RUTI: A new chance to shorten the treatment of latent tuberculosis infection," *Tuberculosis*, vol. 86, pp. 273–289, 2006, doi: 10.1016/j.tube.2006.01.024.

[40] O. Van Der Meeren *et al.*, "Phase 2b controlled trial of M72/AS01E vaccine to prevent tuberculosis," *N. Engl. J. Med.*, vol. 379, no. 17, pp. 1621–1634, 2018, doi: 10.1056/nejmoa1803484.

[41] A. Luabeya *et al.*, "First-in-human trial of the post-exposure tuberculosis vaccine H56:IC31 in *Mycobacterium tuberculosis* infected and non-infected healthy adults," vol. 33, pp. 4130–4140, 2015, doi: 10.1016/j.vaccine.2015.06.051.

[42] R. N. Coler *et al.*, "The TLR-4 agonist adjuvant, GLA-SE, improves magnitude and quality of immune responses elicited by the ID93 tuberculosis vaccine: First-in-human trial," *npj Vaccines*, vol. 3, no. 34, pp. 1–9, 2018, doi: 10.1038/s41541-018-0057-5.

[43] D. V Vasina *et al.*, "First-in-human trials of GamTBvac, a recombinant subunit tuberculosis vaccine candidate: Safety and immunogenicity assessment," *Vaccines*, vol. 7, no. 166, pp. 1–15, 2019.

[44] V. Vetter, G. Denizer, L. R. Friedland, J. Krishnan, and M. Shapiro, "Understanding modern-day vaccines: What you need to know," *Ann. Med.*, vol. 50, no. 2, pp. 110–120, 2018, doi: 10.1080/07853890.2017.1407035.

[45] F. Smaill and Z. Xing, "Human type 5 adenovirus-based tuberculosis vaccine: Is the respiratory route of delivery the future?," *Expert Rev. Vaccines*, vol. 13, no. 8, pp. 927–930, 2014, doi: 10.1586/14760584.2014.929947.

[46] Z. Xing, C. T. McFarland, J. M. Sallenave, A. Izzo, J. Wang, and D. N. McMurray, "Intranasal mucosal boosting with an adenovirus-vectored vaccine markedly enhances the protection of BCG-primed guinea pigs against pulmonary tuberculosis," *PLoS One*, vol. 4, no. 6, p. e5856, 2009, doi: 10.1371/journal.pone.0005856.

[47] B. Pérez De Val *et al.*, "Goats primed with *Mycobacterium bovis* BCG and boosted with a recombinant adenovirus expressing Ag85A show enhanced protection against tuberculosis," *Clin. Vaccine Immunol.*, vol. 19, no. 9, pp. 1339–1347, 2012, doi: 10.1128/CVI.00275-12.

[48] H. M. Vordermeier, K. Huygen, M. Singh, R. G. Hewinson, and Z. Xing, “Immune responses induced in cattle by vaccination with a recombinant adenovirus expressing mycobacterial antigen 85A and *Mycobacterium bovis* BCG,” *Infect. Immun.*, vol. 74, no. 2, pp. 1416–1418, 2006, doi: 10.1128/IAI.74.2.1416-1418.2006.

[49] F. Smaill *et al.*, “A human type 5 adenovirus-based tuberculosis vaccine induces robust T cell responses in humans despite preexisting anti-adenovirus immunity,” *Sci. Transl. Med.*, vol. 5, no. 205, pp. 1–11, 2013, doi: 10.1126/scitranslmed.3006843.

[50] E. Stylianou *et al.*, “Improvement of BCG protective efficacy with a novel chimpanzee adenovirus and a modified vaccinia Ankara virus both expressing Ag85A,” *Vaccine*, vol. 33, no. 48, pp. 6800–6808, 2015, doi: 10.1016/j.vaccine.2015.10.017.

[51] M. D. Tameris *et al.*, “Safety and efficacy of MVA85A, a new tuberculosis vaccine, in infants previously vaccinated with BCG: A randomised, placebo-controlled phase 2b trial,” *Lancet*, vol. 381, no. 9871, pp. 1021–1028, 2013, doi: 10.1016/S0140-6736(13)60177-4.

[52] M. Wilkie *et al.*, “A phase I trial evaluating the safety and immunogenicity of a candidate tuberculosis vaccination regimen, ChAdOx1 85A prime – MVA85A boost in healthy UK adults,” *Vaccine*, vol. 38, pp. 779–789, 2020, doi: 10.1016/j.vaccine.2019.10.102.

[53] S. Khoshnood *et al.*, “Novel vaccine candidates against *Mycobacterium tuberculosis*,” *Int. J. Biol. Macromol.*, vol. 120, pp. 180–188, 2018, doi: 10.1016/j.ijbiomac.2018.08.037.

[54] R. S. Gupta, B. Lo, and J. Son, “Phylogenomics and comparative genomic studies robustly support division of the genus *Mycobacterium* into an emended genus *Mycobacterium* and four novel genera,” *Front. Microbiol.*, vol. 9, no. 67, pp. 1–41, 2018, doi: 10.3389/fmicb.2018.00067.

[55] A. C. Pereira, B. Ramos, A. C. Reis, and M. V. Cunha, “Non-tuberculous mycobacteria: Molecular and physiological bases of virulence and adaptation to ecological niches,” *Microorganisms*, vol. 8, pp. 1–49, 2020, doi: 10.3390/microorganisms8091380.

[56] T. M. Shinnick and R. C. Good, “Mycobacterial taxonomy,” *Eur. J. Clin. Microbiol. Infect. Dis.*, vol. 13, no. 11, pp. 884–901, 1994, doi: 10.1007/BF02111489.

[57] S. Guallar-Garrido, V. Campo-Pérez, A. Sánchez-Chardi, M. Luquin, and E. Julián, “Each mycobacterium requires a specific culture medium composition for triggering an optimized immunomodulatory and antitumoral effect,” *Microorganisms*, vol. 8, no. 734, pp. 1–16, 2020.

[58] A. Arbues *et al.*, “Construction, characterization and preclinical evaluation of MTBVAC, the first live-attenuated *M. tuberculosis*-based vaccine to enter clinical trials,” *Vaccine*, vol. 31, pp. 4867–4873, 2013, doi: 10.1016/j.vaccine.2013.07.051.

[59] C. Desel, S. H. E. Kaufmann, S. Bandermann, and L. Grode, “Recombinant mycobacterium as a vaccine,” 2013.

[60] R. Hernandez-Pando, L. Pavon, E. H. Orozco, J. Rangel, and G. A. W. Rook, “Interactions between hormone-mediated and vaccine-mediated immunotherapy for pulmonary tuberculosis in BALBc mice,” *Immunology*, vol. 100, pp. 391–398, 2000, doi: 10.1046/j.1365-2567.2000.00054.x.

[61] P. J. Cardona *et al.*, “Immunotherapy with fragmented *Mycobacterium tuberculosis* cells increases the effectiveness of chemotherapy against a chronical infection in a murine model of tuberculosis,” *Vaccine*, vol. 23, pp. 1393–1398, 2005, doi: 10.1016/j.vaccine.2004.09.008.

[62] R. K. Angara, S. Yousuf, S. K. Gupta, and A. Ranjan, “An IclR like protein from mycobacteria regulates leuCD operon and induces dormancy-like growth arrest in *Mycobacterium smegmatis*,” *Tuberculosis*, vol. 108, pp. 83–92, 2018, doi: 10.1016/j.tube.2017.10.009.

[63] S. Lesellier *et al.*, “Bioreactor-grown Bacillus of Calmette and Guérin (BCG) vaccine protects badgers against virulent *Mycobacterium bovis* when administered orally: Identifying limitations in baited vaccine delivery,” *Pharmaceutics*, vol. 12, no. 782, pp. 1–22, 2020, doi: 10.3390/pharmaceutics12080782.

[64] S. K. Parker, K. M. Curtin, and M. L. Vasil, “Purification and characterization of mycobacterial phospholipase A: An activity associated with mycobacterial cutinase,” *J. Bacteriol.*, vol. 189, no. 11, pp. 4153–4160, 2007, doi: 10.1128/JB.01909-06.

[65] Y. J. Tang, W. Shui, S. Myers, X. Feng, C. Bertozzi, and J. D. Keasling, “Central metabolism in *Mycobacterium smegmatis* during the transition from O2-rich to O2-poor conditions as studied by isotopomer-assisted metabolite analysis,” *Biotechnol. Lett.*, vol. 31, pp. 1233–1240, 2009, doi: 10.1007/s10529-009-9991-7.

[66] R. D. Pietersen *et al.*, “Tween 80 induces a carbon flux rerouting in *Mycobacterium tuberculosis*,” *J. Microbiol. Methods*, vol. 170, pp. 1–7, 2020, doi: 10.1016/j.mimet.2019.105795.

[67] A. E. Grzegorzewicz *et al.*, “Assembling of the *Mycobacterium tuberculosis* cell wall core,” *J. Biol. Chem.*, vol. 291, no. 36, pp. 18867–18879, 2016, doi: 10.1074/jbc.M116.739227.

[68] C. E. Barry *et al.*, “Mycolic acids: Structure, biosynthesis and physiological functions,” *Prog. Lipid Res.*, vol. 37, no. 2–3, pp. 143–179, 1998, doi: 10.1016/S0163-7827(98)00008-3.

[69] K. A. Abrahams and G. S. Besra, “Mycobacterial cell wall biosynthesis: A multifaceted antibiotic target,” *Parasitology*, vol. 145, pp. 116–133, 2018, doi: 10.1017/S0031182016002377.

[70] M. Jankute, J. A. G. Cox, J. Harrison, and G. S. Besra, “Assembly of the mycobacterial cell wall,” *Annu. Rev. Microbiol.*, vol. 69, pp. 405–423, 2015, doi: 10.1146/annurev-micro-091014-104121.

[71] J. Liu, C. E. Barry III, G. S. Besra, and H. Nikaido, “Mycolic acid structure determines the fluidity of the mycobacterial cell wall,” *J. Biol. Chem.*, vol. 271, no. 47, pp. 29545–29551, 1996, doi: 10.1074/jbc.271.47.29545.

[72] P. E. Kolattukudy, N. D. Fernandes, A. K. Azad, A. M. Fitzmaurice, and T. D. Sirakova, “Biochemistry and molecular genetics of cell-wall lipid biosynthesis in mycobacteria,” *Mol. Microbiol.*, vol. 24, no. 2, pp. 263–270, 1997, doi: 10.1046/j.1365-2958.1997.3361705.x.

[73] N. Caceres *et al.*, “Evolution and role of corded cell aggregation in *Mycobacterium tuberculosis* cultures,” *Tuberculosis*, vol. 93, pp. 690–698, 2013, doi: 10.1016/j.tube.2013.08.003.

[74] S. Borrego, E. Niubó, O. Ancheta, and M. E. Espinosa, “Study of the microbial aggregation in *Mycobacterium* using image analysis and electron microscopy,” *Tissue Cell*, vol. 32, no. 6, pp. 494–500, 2000, doi: 10.1016/S0040-8166(00)80005-1.

[75] P. Chakraborty and A. Kumar, “The extracellular matrix of mycobacterial biofilms: Could we shorten the treatment of mycobacterial infections?,” *Microb. Cell*, vol. 6, no. 2, pp. 105–122, 2019, doi: 10.15698/mic2019.02.667.

[76] W. H. DePas, M. Bergkessel, and D. K. Newman, “Aggregation of nontuberculous mycobacteria is regulated by carbon-nitrogen balance,” *mBio*, vol. 10, no. 4, e01715-19, 2019, https://doi.org/10.1128/mBio.01715-19.

[77] A. K. Ojha, X. Trivelli, Y. Guerardel, L. Kremer, and G. F. Hatfull, “Enzymatic hydrolysis of trehalose dimycolate releases free mycolic acids during mycobacterial growth in biofilms,” *J. Biol. Chem.*, vol. 285, no. 23, pp. 17380–17389, 2010, doi: 10.1074/jbc.M110.112813.

[78] D. Sambandan *et al.*, “Keto-mycolic acid-dependent pellicle formation confers tolerance to drug-sensitive *Mycobacterium tuberculosis*,” *MBio*, vol. 4, no. 3, pp. 1–10, 2013, doi: 10.1128/mBio.00222-13.

[79] C. C. C. R. de Carvalho and M. J. Caramujo, “The various roles of fatty acids,” *Molecules*, vol. 23, no. 2583, pp. 1–36, 2018, doi: 10.3390/molecules23102583.

[80] M. Sinensky, “Homeoviscous adaptation - A homeostatic process that regulates the viscosity of membrane lipids in *Escherichia coli*,” *Proc. Natl. Acad. Sci. U. S. A.*, vol. 71, no. 2, pp. 522–525, 1974, doi: 10.1073/pnas.71.2.522.

[81] C. E. Barry and K. Mdluli, “Drug sensitivity and environmental adaptation of mycobacterial cell wall components,” *Trends Microbiol.*, vol. 4, no. 7, pp. 275–281, 1996, doi: 10.1016/0966-842X(96)10031-7.

[82] D. Poger, B. Caron, and A. E. Mark, “Effect of methyl-branched fatty acids on the structure of lipid

bilayers," *J. Phys. Chem. B*, vol. 118, no. 48, pp. 13838–13848, 2014, doi: 10.1021/jp503910r.

[83] L. Alibaud *et al.*, "Temperature-dependent regulation of mycolic acid cyclopropanation in saprophytic mycobacteria: Role of the *Mycobacterium smegmatis* 1351 gene (MSMEG-1351) in cis-cyclopropanation of α-mycolates," *J. Biol. Chem.*, vol. 285, no. 28, pp. 21698–21707, 2010, doi: 10.1074/jbc.M110.125724.

[84] A. Gouzy *et al.*, "*Mycobacterium tuberculosis* exploits asparagine to assimilate nitrogen and resist acid stress during infection," *PLoS Pathog.*, vol. 10, no. 2, pp. 1–14, 2014, doi: 10.1371/journal.ppat.1003928.

[85] Z. He and J. De Buck, "Cell wall proteome analysis of *Mycobacterium smegmatis* strain MC2 155," *BMC Microbiol.*, vol. 10, no. 121, pp. 1–10, 2010, doi: 10.1186/1471-2180-10-121.

[86] J. M. Reyrat and D. Kahn, "*Mycobacterium smegmatis*: An absurd model for tuberculosis?," *TRENDS Microbiol.*, vol. 9, no. 10, pp. 472–473, 2001.

[87] A. Ojha, M. Anand, A. Bhatt, L. Kremer, W. R. Jacobs, and G. F. Hatfull, "GroEL1: A dedicated chaperone involved in mycolic acid biosynthesis during biofilm formation in mycobacteria," *Cell*, vol. 123, pp. 861–873, 2005, doi: 10.1016/j.cell.2005.09.012.

[88] M. A. L. R. M. Cortes and C. C. C. R. de Carvalho, "Effect of carbon sources on lipid accumulation in *Rhodococcus* cells," *Biochem. Eng. J.*, vol. 94, pp. 100–105, 2015, doi: 10.1016/j.bej.2014.11.017.

[89] F. D. A. Gonçalves and C. C. C. R. de Carvalho, "Phenotypic modifications in *Staphylococcus aureus* cells exposed to high concentrations of vancomycin and teicoplanin," *Front. Microbiol.*, vol. 7, no. 13, pp. 1–15, 2016, doi: 10.3389/fmicb.2016.00013.

[90] P. Kaszycki, T. Walski, N. Hachicho, and H. J. Heipieper, "Biostimulation by methanol enables the methylotrophic yeasts *Hansenula polymorpha* and *Trichosporon* sp. to reveal high formaldehyde biodegradation potential as well as to adapt to this toxic pollutant," *Appl. Microbiol. Biotechnol.*, vol. 97, no. 12, pp. 5555–5564, 2013, doi: 10.1007/s00253-013-4796-y.

[91] E. Kłodzińska *et al.*, "Effect of zeta potential value on bacterial behavior during electrophoretic separation," *Electrophoresis*, vol. 31, no. 9, pp. 1590–1596, 2010, doi: 10.1002/elps.200900559.

[92] C. Ayala-Torres, N. Hernández, A. Galeano, L. Novoa-Aponte, and C. Y. Soto, "Zeta potential as a measure of the surface charge of mycobacterial cells," *Ann. Microbiol.*, vol. 64, no. 3, pp. 1189–1195, 2014, doi: 10.1007/s13213-013-0758-y.

[93] A. A. Dubey, S. R. Wani, and V. Jain, "Methylotrophy in mycobacteria: Dissection of the methanol metabolism pathway in *Mycobacterium smegmatis*," *J. Bacteriol.*, vol. 200, no. 17, pp. 1–12, 2018, doi: 10.1128/JB.00288-18.

[94] F. J. Weber and J. A. M. De Bont, “Adaptation mechanisms of microorganisms to the toxic effects of organic solvents on membranes,” *Biochim. Biophys. Acta - Rev. Biomembr.*, vol. 1286, no. 3, pp. 225–245, 1996, doi: 10.1016/S0304-4157(96)00010-X.

[95] C. C. C. R. de Carvalho, B. Parreño-Marchante, G. Neumann, M. M. R. Da Fonseca, and H. J. Heipieper, “Adaptation of *Rhodococcus erythropolis* DCL14 to growth on n-alkanes, alcohols and terpenes,” *Appl. Microbiol. Biotechnol.*, vol. 67, no. 3, pp. 383–388, 2005, doi: 10.1007/s00253-004-1750-z.

[96] N. Kabelitz, P. M. Santos, and H. J. Heipieper, “Effect of aliphatic alcohols on growth and degree of saturation of membrane lipids in *Acinetobacter calcoaceticus*,” *FEMS Microbiol. Lett.*, vol. 220, no. 2, pp. 223–227, 2003, doi: 10.1016/S0378-1097(03)00103-4.

[97] C. Pacífico, P. Fernandes, and C. C. C. R. de Carvalho, “Mycobacterial response to organic solvents and possible implications on cross-resistance with antimicrobial agents,” *Front. Microbiol.*, vol. 9, no. MAY, pp. 1–12, 2018, doi: 10.3389/fmicb.2018.00961.

[98] J. Ollinger *et al.*, “A dual read-out assay to evaluate the potency of compounds active against *Mycobacterium tuberculosis*,” *PLoS One*, vol. 8, no. 4, 2013, doi: 10.1371/journal.pone.0060531.

[99] C. C. C. R. de Carvalho, M. P. C. Marques, N. Hachicho, and H. J. Heipieper, “Rapid adaptation of *Rhodococcus erythropolis* cells to salt stress by synthesizing polyunsaturated fatty acids,” *Appl. Microbiol. Biotechnol.*, vol. 98, no. 12, pp. 5599–5606, 2014, doi: 10.1007/s00253-014-5549-2.

[100] R. Taneja, U. Malik, and G. K. Khuller, “Effect of growth temperature on the lipid composition of *Mycobacterium smegmatis* ATCC 607,” *J. Gen. Microbiol.*, vol. 113, pp. 413–416, 1979.

[101] C. C. C. R. de Carvalho, “Adaptation of *Rhodococcus erythropolis* cells for growth and bioremediation under extreme conditions,” *Res. Microbiol.*, vol. 163, no. 2, pp. 125–136, 2012, doi: 10.1016/j.resmic.2011.11.003.